University of Alberta

Polymeric micelles for the solubilization and selective delivery of cyclosporine A as a model P-glycoprotein inhibitor

By
Hamidreza Montazeri Aliabadi

©

A THESIS SUBMITTED TO THE FACULTY OF GRADUATE STUDIES AND RESEARCH IN PARTIAL FULLFILMENT OF THE REQUIREMENTS FOR THE DEGREE OF DOCTOR OF PHILOSOPHY IN PHARMACEUTICAL SCIENCES

Faculty of Pharmacy and Pharmaceutical Sciences

Edmonton, Alberta

Fall 2007

Library and Archives Canada

Published Heritage Branch

395 Wellington Street
Ottawa ON K1A 0N4
Canada

Bibliothèque et Archives Canada

Direction du Patrimoine de l'édition

395, rue Wellington
Ottawa ON K1A 0N4
Canada

Your file Votre référence
ISBN: 978-0-494-33033-3
Our file Notre référence
ISBN: 978-0-494-33033-3

NOTICE:
The author has granted a non-exclusive license allowing Library and Archives Canada to reproduce, publish, archive, preserve, conserve, communicate to the public by telecommunication or on the Internet, loan, distribute and sell theses worldwide, for commercial or non-commercial purposes, in microform, paper, electronic and/or any other formats.

The author retains copyright ownership and moral rights in this thesis. Neither the thesis nor substantial extracts from it may be printed or otherwise reproduced without the author's permission.

AVIS:
L'auteur a accordé une licence non exclusive permettant à la Bibliothèque et Archives Canada de reproduire, publier, archiver, sauvegarder, conserver, transmettre au public par télécommunication ou par l'Internet, prêter, distribuer et vendre des thèses partout dans le monde, à des fins commerciales ou autres, sur support microforme, papier, électronique et/ou autres formats.

L'auteur conserve la propriété du droit d'auteur et des droits moraux qui protège cette thèse. Ni la thèse ni des extraits substantiels de celle-ci ne doivent être imprimés ou autrement reproduits sans son autorisation.

In compliance with the Canadian Privacy Act some supporting forms may have been removed from this thesis.

While these forms may be included in the document page count, their removal does not represent any loss of content from the thesis.

Conformément à la loi canadienne sur la protection de la vie privée, quelques formulaires secondaires ont été enlevés de cette thèse.

Bien que ces formulaires aient inclus dans la pagination, il n'y aura aucun contenu manquant.

Canada

Dedications

This manuscript is dedicated to

My loving and understanding wife, who has been by my side in all the rainy days;

My parents, who have always been the main motivation for all my studies;

And

My daughter, ***Sara****, who truly is "the wind below my wings".*

Abstract

One of the major causes of failure in cancer treatment is multi-drug resistance (MDR), where cancer cells simultaneously become resistant to different anticancer drugs. Over-expression of membrane efflux pumps like P-glycoprotein (P-gp) that recognizes different chemotherapeutic agents and transports them out of the cell, plays a major role in MDR. P-gp inhibitors have shown little benefit in overcoming drug resistance in clinic because systemic administration of P-gp inhibitors will reduce the elimination of P-gp substrates (e.g., anticancer drugs) from healthy cells that overexpress P-gp leading to intolerable toxicities by anticancer drugs. The objective of this research is to develop a tumor targeted carrier that permits specific delivery of P-gp inhibitors to tumorogenic P-gp. Polymeric micelles have shown promise in tumor targeted delivery of hydrophobic drugs. Although P-gp inhibitors are structurally diverse, they share the physicochemical property of lipophilicity necessary for plasma membrane penetration. This makes them ideal candidates for incorporation in polymeric micelles.

In this thesis we have focused on self-associating poly(ethylene oxide)-*b*-poly(ε-caprolactone) (PEO-*b*-PCL) block copolymers as biodegradable polymeric nanocarriers for tumor targeted delivery of cyclosporine A (CyA) as a model P-gp inhibitor. We hypothesized that poly (ethylene oxide)-*block*-poly (ε-caprolactone) (PEO-b-PCL) micelles may efficiently encapsulate resistance modulators like cyclosporine A (CyA) and therefore provide a sustained release formulation that is capable of changing the normal distribution of the drug, minimizing its toxicities, and redirecting it towards solid tumor, without loosing the MDR modulatory effect. PEO-*b*-PCL copolymers were

assembled to carriers of 80-100 nm, caused a 100 fold increase in the aqueous solubility of CyA and retained 94 % of their drug content after 24 h. In healthy rats, a 6.1 fold increase in the blood AUC was observed for polymeric micellar CyA compared to commercial formulation of CyA. PEO-*b*-PCL micelles reduced uptake of encapsulated CyA by kidney and caused a reduction in the nephrotoxicity of CyA. The creatinine clearance was lowered (1.9 fold) by the commercial formulation but did not change when polymeric micellar CyA was injected for 7 days. Polymeric micelles caused 1.7 and 2.5 fold increases in the blood and tumor concentrations of CyA, respectively, in Lewis Lung Carcinoma (LLC1) bearing mice, while maintaining the in vitro efficacy of CyA as an MDR modulator after co-administration with doxorubicin. Overall, our results points to a great potential for PEO-*b*-PCL micelles for the solubilization and selective delivery of CyA as a model P-gp inhibitors. The polymeric micellar formulation may prove to be a safer alternative to Sandimmune® for intravenous administration of CyA as an immunosuppressant, as well.

Acknowledgments

This research project has been fulfilled because of collaboration of a group and organization. Hereby, I would like to thank some of them in particular:

- My supervisor, Dr. A. Lavasanifar, for her continuous support, guidance, and insight, without which I sure would have been lost. Her caring attitude and kind approach towards many problems in a routine research work is what carried me through this though journey.
- Dr. D. Brocks, who was just as kind and caring as I was his own student. His guidance, passionate approach to research, and kindness made me feel welcome in his laboratory like a second home.
- Dr. F. Jamali, who has been a huge supporter of me and all graduate students and a true inspiration to everybody who works in this field.
- Dr. Mike Doschak, who agreed to be in my supervision committee on such a short notice, and helped me a great deal with the final steps.
- Dr. H. Uludag, for his guidance regarding studying material and preparing for the oral exams.
- Dr. Xiao-bing Xiong, who taught me a great deal about working in the lab, and doing research in general.
- Abdullah Mahmud, Sara Elhasi, Kamyar Sarkhosh, Ziyad Binkhathlan, and Mostafa Shahin, who were like a second family to me, for all their help and support.
- Faculty staff, in particular, Jeff Turchinsky, Don White, Gordon McRae, Shirley Swift, personnel of the faculty office, Joyce Johnson, Dr. Ali Aghazadeh and Dr. Somayaji.
- All the graduate students in Faculty of Pharmacy and Pharmaceutical Sciences, specially Samar Hamdy, Aws Alshamsan, Anooshiravan Shayganpoor, Reem Elbekai, ... with special thanks to Dr. Saeed Sattari who helped me enormously with the first steps.
- RX & D HRF/CIHR, Novartis Pharmaceuticals Canada Inc., and Biochem Pharma for the scholarships and U of A for Walter H. Johns, Marie Arnold Cancer Research, Queen Elizabeth II Graduate Scholarships that enabled me to complete this program.
- Everybody else in the great organization that we call "Faculty of Pharmacy and Pharmaceutical Sciences, U of A".

- **And last but not least, in memory of Dr. J. Samuel, who would never be forgotten**.

Table of contents

Chapter 1: **INTRODUCTION**.....1
1.1. Polymeric micelles: An overview.....2
1.1.1 Design of polymeric micelles for drug delivery applications....3
1.1.1.1 Micelle forming polymer-drug conjugations.....5
1.1.1.2 Polyion complex micelles.....5
1.1.1.3 Polymeric micellar nano-containers.....6
1.1.2 Methods of physical encapsulation in polymeric micelles.....6
1.1.2.1 Direct addition.....6
1.1.2.2 Dialysis.....6
1.1.2.3 Oil/water emulsion.....7
1.1.2.4 Solvent evaporation method.....7
1.1.2.5 Co-solvent evaporation method.....7
1.1.2.6 Freeze-drying method.....7
1.1.3 Applications of polymeric micelles in drug delivery.....10
1.1.3.1 Polymeric micelles as solubilizing agents.....10
1.1.3.2 Polymeric micelles as controlled release delivery systems.....12
1.1.3.3 Polymeric micelles as carriers for drug targeting.....17
1.1.3.3.1 Enhanced Permeation and Retention (EPR) Effect...18
1.1.3.3.2 Characteristics of ideal carriers for passive drug targeting by EPR effect.....25
1.1.3.3.3 Polymeric micelles for active or stimuli responsive targeting.....26
1.1.4 Polymeric micellar delivery systems in clinical trials.....27
1.1.5 Poly(ethylene oxide)-*block*-poly(ε-caprolactone) (PEO-*b*-PCL) micelles for drug solubilization and delivery.....31
1.2 Multidrug resistance.....33
1.2.1. Responsible mechanisms for MDR.....34
1.2.1.1 Reduced uptake or enhanced efflux of anticancer drugs..34
1.2.1.2 Overexpression of detoxifying enzymes.....35
1.2.1.3 Underexpression or mutation of anticancer drug targets..36
1.2.1.4 Inhibition of apoptotic pathways.....36
1.2.2 P-glycoprotein (P-gp).....37
1.2.2.1 Structure.....38
1.2.2.2. Distribution and role in normal tissue.....42
1.2.2.2.1 Gastrointestinal (GI) tract.....42
1.2.2.2.2 Liver.....43
1.2.2.2.3 Kidney.....44

1.2.2.2.4 Blood brain barrier (BBB).....44
1.2.2.2.5 Hematologic cells.....45
1.2.3 Role of P-gp in MDR.....45
1.2.4 P-gp inhibitors for chemosensitization of MDR tumors.....47
1.2.4.1 First generation.....49
1.2.4.2 Second generation.....49
1.2.4.3 Third generation.....50
1.2.5 Clinical trials on the use of P-gp inhibitors in MDR.....50
1.3 Cyclosporine A (CyA).....52
1.3.1. Pharmacokinetic of CyA.....54
1.3.1.1 Absorption and distribution.....54
1.3.1.2 Metabolism.....55
1.3.1.3 Elimination.....55
1.3.1.4 Protein binding.....55
1.3.2. The immunosuppressant activity of CyA.....56
1.3.3. CyA as an MDR modulator.....58
1.3.4. Side effects associated with CyA administration.....59
1.4 Thesis Proposal.....60
1.4.1 Objective.....60
1.4.2 Rationale and significance.....60
1.4.3 Hypotheses.....62
1.4.4 Specific aims.....63

Chapter 2: **EXPERIMENTAL PROCEDURES.....64**
2.1 Materials.....65
2.2 Methods.....66
2.2.1 Synthesis of MPEO-*b*-PCL block copolymers 66
2.2.2 Characterization of the block copolymers.....66
2.2.3 Preparation of MPEO-*b*-PCL micelles.....67
2.2.4 Encapsulation of CyA in MPEO-*b*-PCL micelles 67
2.2.5 Characterization of MPEO-*b*-PCL micelles.....68
2.2.6 In vitro release study.....69
2.2.7 Optimization of CyA encapsulation.....70
2.2.8 Determination of unbound fraction of CyA in rat blood.....71
2.2.8.1 Sample preparation.....71
2.2.8.2 Determination of CyA levels.....72
2.2.8.3 Measurement of unbound fraction.....73
2.2.9 Pharmacokinetic studies.....73
2.2.9.1 Animals.....73
2.2.9.2 Procedure.....74

2.2.9.3 Pharmacokinetic data analysis.....75
2.2.10 Biodistribution.....76
2.2.11 Nephrotoxicity experiments.....76
2.2.11.1 Animals.....76
2.2.11.2 Treatments.....77
2.2.11.3 Determination of CyA levels in blood and kidney after treatment period.....78
2.2.11.4 Assessment of renal function.....78
2.2.11.5 Histological studies.....79
2.2.12 Biodistribution of CyA loaded micelles in tumor bearing animals.....79
2.2.12.1 Animal model.....80
2.2.12.2 Treatment.....80
2.2.13 Assessment of *in vitro* cytotoxicity of DOX in co - administration with CyA.....80
2.2.14 Statistical analysis.....82

Chapter 3: **RESULTS.....84**
3.1. Polymer synthesis and characterization.....85
3.2. Preparation and characterization of MPEO-*b*-PCL micelles.....85
3.3. Encapsulation of CyA in MPEO-*b*-PCL micelles.....86
3.4. *In vitro* release.....88
3.5. Pharmacokinetic of CyA as Sandimmune® and polymeric micellar formulation.....90
3.6. Biodistribution.....92
3.7. Modification of the characteristics of CyA loaded MPEO-*b*-PCL micelles.....96
3.8. Novel use of an *in vitro* method to assess the *in vivo* stability of CyA polymeric micellar formulations.....99
3.8.1 The effect of CyA loaded levels on the *in vitro* release for different polymeric micellar formulations of CyA.....99
3.8.2 Determination of unbound fraction (*fu*).....102
3.8.3 Pharmacokinetics of different micellar formulations.....102
3.9 Nephrotoxicity of PM-CyA (H) in comparison to Sandimmune® 107
3.10 Assessing the in vitro efficacy of PM-CyA (H) in reversal of drug resistance to DOX.....113
3.11 Tumor accumulation.....119

Chapter 4: **GENERAL DISCUSSION AND CONCLUSION.....121**

4.1. Discussion.....122
4.1.1 Polymer synthesis and characterization.....123
4.1.2 Micelle preparation and characterization.....124
4.1.3 Optimization of micellar characterization for CyA delivery 126
4.1.3.1 The effect of loading conditions on micellar characteristics and CyA encapsulation.....127
4.1.3.2 The effect of molecular weight of PCL on micellar characteristics and level of CyA encapsulation.....127
4.1.3.3 The effect of solvent/co-solvent composition.....128
4.1.4 *In vitro* release of CyA from polymeric micelles.....131
4.1.5 Determining the unbound fraction of CyA in blood *in vitro* as a measure of *in vivo* stability of PM-CyA.....134
4.1.6 Pharmacokinetic and Biodistribution of PM-CyA.....136
4.1.7 Nephrotoxicity.....141
4.1.8 Tumor accumulation.....147
4.1.9 Assessing the *in vitro* efficacy of CyA formulations in sensitizing resistant breast tumor cells to DOX.....149
4.2. Conclusions.....152
4.3. Future Perspectives.....154
4.4. References.....157

List of Tables

Table 1.1 – The result of preclinical studies for tumor targeted micellar delivery systems. 28

Table 1.2 – Polymeric micellar delivery systems in clinical trials.....29

Table 1.3 – Drug solubilization by PEO-*b*-PCL polymeric micelles.....33

Table 1.4 – ABC transporters involved in drug resistance.....35

Table 1.5 – Clinical trials with P-gp inhibitors.....52

Table 3.1 – Characteristics of the prepared MPEO-*b*-PCL block copolymers.....86

Table 3.2 – Average size and polydispersity of unloaded MPEO-*b*-PCL micelles with different molecular weights.....86

Table 3.3 – The effect of PCL molecular weight on CyA encapsulation in MPEO-*b*-PCL micelles (using water as the aqueous phase and 2 mg CyA initial level).....87

Table 3.4 – The effect of initial CyA level and ionic strength of the aqueous phase on the CyA encapsulation in MPEO-*b*-PCL micelles.....88

Table 3.5 – Non-compartmental pharmacokinetic parameters (±SD) of CyA after i.v. administration of polymeric micellar CyA in comparison to Sandimmune®..91

Table 3.6 – Area under the blood, plasma, and tissue concentrations versus time curve (±SD) for CyA after i.v. administration of Sandimmune® and polymeric micellar CyA to rats.....95

Table 3.7 – The effect of solvent/co-solvent composition on the average diameter and polydispersity index of unloaded MPEO-*b*-PCL micelles of different PCL molecular weights.....97

Table 3.8 – The effect of solvent/co-solvent composition on the encapsulation efficiency of CyA in MPEO-*b*-PCL micelles of different MPEO and PCL molecular weights.....98

Table 3.9 – Characteristics of different PEO-*b*-PCL based nanocarriers prepared for this project. Values are recorded as mean ± standard deviation.....100

Table 3.10 – Pharmacokinetic parameters (mean±SD) for the different formulations of CyA under study in rat.....104

Table 3.11 – Indices of renal function in rats before (day 0) and after (day 8) treatment.....109

Table 3.12 – IC_{50} and sensitivity factor for DOX alone and in combination with CyA formulations and controls against MDA-MB-435/LLC6^{WT} cells.....115

Table 3.13 – IC_{50} and sensitivity factor for DOX alone and in combination with CyA formulations and controls in the resistant cell line.....119

List of Figures

Figure 1.1 – The process of self-assembly for amphiphilic diblock copolymers.....3

Figure 1.2 – Chemical structure of most commonly used core-forming blocks in block copolymer micelles.....4

Figure 1.3 – Physical methods of drug encapsulation in polymeric micelles: A) dialysis; B) O/W emulsion; C) solvent evaporation; C) co-solvent evaporation; and D) Freeze-drying methods.....8,9

Figure 1.4 – Modes of drug release from: A) block copolymer-drug conjugate micelles; B) micellar nanocontainers; C) polyion complex micelles.....15

Figure 1.5 – Structural differences between normal and tumor tissue; a) Normal tissue containing linear blood vessels lined by a smooth layer of endothelial cells and lymph vessels; b) Tumor tissue with defective blood vessels that are leaky and irregularly shaped, usually without lymphatic drainage.....19

Figure 1.6 – The role of progenitor cells: Angiogenic factors that are released by tumor induce mobilization of VEGFR1-expressing hematopoietic stem cells ($VEGFR1^+$ myeloid cells) and VEGFR2-expressing circulating endothelial precursors ($VEGFR2^+$ CEPs) from the bone marrow.....21

Figure 1.7 – The classic 'angiogenic switch', has to occur to ensure exponential tumor growth. The switch begins with perivascular detachment and vessel dilation, followed by angiogenic sprouting, new vessel formation and maturation, and the recruitment of perivascular cells. Blood-vessel formation will continue as long as the tumor grows, and the blood vessels specifically feed hypoxic and necrotic areas of the tumor to provide it with essential nutrients and oxygen.....22

Figure 1.8 – Topological map and domain organization of P-gp.....38

Figure 1.9 – P-gp structure; A) Cartoon based on electron microscopic images (courtesy of Kevin Hannavy); B) Projection map of P-gp from above the extracellular face of membrane.....41

Figure 1.10 – Proposed mechanisms of P-gp function in drug efflux: (1) passive drug uptake; (2a) hydrophobic channel between intracellular and extracellular space; (2b) "flip" mechanism; (2c) "vacuum cleaner model".....46

Figure 1.11 – Regulation of apoptosis by P-gp : A) increase in pH and caspase 8 inhibition; B) movement of SM and decrease in ceramide production.....48

Figure 1.12 – Chemical structure of CyA.....53

Figure 1.13 – T-cell activation and the mechanism of action of calcineurin inhibitors...57

Figure 3.1 – The effect of solubilizing vehicle on the *in vitro* rate of CyA release; Data is presented as mean ± SD (n =3). Inset depicts an enlargement of the release profile of the micellar formulations involved in this experiment.....89

Figure 3.2 – CyA concentration – time profile in whole blood after i.v injection of Sandimmune® and polymeric micellar CyA. Data for polymeric micellar CyA is normalized to injected dose of CyA in Sandimmune® and presented as mean ± SD.....91

Figure 3.3 – CyA concentration vs. time profiles in (A) blood, (B) plasma, (C) kidney, (D) liver, (E) spleen and (F) heart following i.v administration of polymeric micellar CyA in comparison to CyA in Cremophor EL (Sandimmune®) formulation in rats. Micellar data is normalized to injected dose of Cremophor EL and presented as mean ± SD.....94

Figure 3.4 – kp vs. time profiles for CyA after i.v administration of polymeric micellar CyA and Sandimmune®. The data presents A) kidney, B) liver, C) spleen, and D) heart to plasma ratios. The data for polymeric micelles is normalized to injected dose of CyA in Sandimmune® and presented as mean ± SD.....95

Figure 3.5 – The effect of solvent/co-solvent composition on molar CyA loading in MPEO-*b*-PCL micelles of different MPEO/PCL molecular weights. Data presented as mean +SD.....99

Figure 3.6 – *In vitro* rate of CyA release from Cremophor EL and micellar formulations at 37°C; the inset depicts an enlargement of the release rate data for the micellar formulations only on linear y-axis scale. Each point represents average release ± SD.....101

Figure 3.7 – The concentrations versus time profile in whole blood after i.v. injection of different CyA formulations. Data for PM-CyA (L) and PM-CyA (I) is normalized to injected dose of Sandimmune® and PM-CyA .All data are presented as mean ± SD.....103

Figure 3.8 – Ranking of *fu* and pharmacokinetic parameters for CyA formulations. Continuous lines over the symbol of groups indicate lack of significance between groups encompassed by the lines; groups not encompassed within lines are significantly different (one way ANOVA and post-hoc Dunnett T3 test, $p<0.05$). Data presented as mean + SD.....105

Figure 3.9 – Relationships between *fu* and drug loading content, micellar size, and pharmacokinetic parameters for different CyA formulations.....106

Figure 3.10 – Average weight gain ± SD (%) in rats treated with saline, 20 mg/kg/day of CyA as part of Sandimmune® and PM-CyA (H), corresponding concentrations of Cremophor EL and empty MPEO-*b*-PCL micelles as appeared in the Sandimmune® and PM-CyA.....109

Figure 3.11 – Changes in A) body weight, B) plasma potassium level, C) CLur, and D) CLcr for animals treated with saline, Cremophor EL, unloaded polymeric micelles, Sandimmune® and PM-CyA expressed as a percent of variable measured in the same treatment group on day zero (one way ANOVA followed by a post-hoc Duncan's Multiple Range test, $p<0.05$). Each bar represents the mean + SD for the group.....110

Figure 3.12 – A) Average CyA levels + SD (μg/g or mL) in rat blood and kidneys after 7 day treatment with Sandimmune® and PM-CyA at 20 mg/Kg/day of CyA; B) Kidney/Blood levels ratios for after 7 day treatment with Sandimmune® and PM-CyA at 20 mg/Kg/day of CyA (asterisks indicate a significant difference [$p < 0.05$]).....111

Figure 3.13 – Stained kidney sections of rats given saline, PM-CyA and Sandimmune® (n=3; optical magnification is × 400): A) a representative H&E stained kidney tissue from saline treated rats; B) a representative PAS stained kidney tissue from saline treated rat; C) a representative H&E stained kidney tissue from rats treated with PM-CyA. The cell structures are within the normal limits and cannot be distinguished from the saline treated control group; D) a representative PAS stained kidney tissue from rats treated with PM-CyA. There are no unusual PAS positive structures in the tubules, and again, not distinguished from the saline treated control group (Figure 3B); E) a representative H&E stained kidney tissue from rats treated with Sandimmune®. The fine perinuclear vacuolation of tubular epithelial cells, shown by arrows, was present throughout the cortex in the kidney sections obtained from this group; F) a representative PAS stained kidney tissue from rats treated with Sandimmune®. The tubular epithelium shows occasional PAS positive intracytoplasmic droplets, but most of the vacuoles were PAS negative.....112

Figure 3.14 – Cell survival for the wild type cell line in the presence of different formulations of CyA and controls. Data presented as mean ± SD.....113

Figure 3.15 – Cytotoxicity profile of DOX alone and DOX in the presence of unloaded micelles and Cremophor EL at identical concentrations to what are present in Sandimmune® and PM-CYA (H) formulations, respectively, against MDA-MB-435/LLC6^{WT} cells. Data presented as mean ± SD.....114

Figure 3.16 – Cytotoxicity profile of DOX alone and DOX in the presence of 5 and 10 μg/mL CyA as Sandimmune® and PM-CyA (H) against MDA-MB-435/LLC6^{WT} cells (n=4). Data presented as mean ± SD.....115

Figure 3.17 – Cytotoxicity of CyA formulations and the carriers present in each formulation against MDA-MB-435/LCC6^{MDR} cells. Each point represents mean cell viability ± SD.....116

Figure 3.18 – Cytotoxicity profile of DOX alone and DOX in the presence of unloaded micelles and Cremophor EL at identical concentrations to what are present in Sandimmune® and PM-CYA (H) formulations, respectively against MDA-MB-435/LLC6^{MDR} cells. Data presented as mean ± SD.....117

Figure 3.19 – Cytotoxicity profile of DOX alone and DOX in the presence of 5 and 10 μg/mL CyA as Sandimmune® and PM-CyA (H) against MDA-MB-435/LLC6^{MDR} cells.....118

Figure 3.20 – Cytotoxicity profile of DOX in the presence of 5 and 10 μg/mL CyA as free drug, and 10 μg/mL as Sandimmune® and PM-CyA (H) against MDA-MB-435/LLC6^{MDR} cells. Data presented as mean ± SD.....118

Figure 3.21 – Tissue distribution (6 h post-dose concentrations) of CyA after a single i.v dose of 10 mg/kg as Sandimmune and PM-CyA (H) to tumor (Lewis lung carcinoma) bearing mice. Data is presented as mean + SD.....120

List of Abbreviations

ABC	ATP-binding cassette
ASP	Aspartic acid
AUC	Area under the curve
BBB	Blood brain barrier
BSA	Bovine serum albumin
CDDP	Circulating endothelial progenitor cells
CEP	Cisplatin
CL	Clearance
CLcr	Creatinine clearance
CLur	Urea clearance
CMC	Critical micellar concentration
CNS	Central nervous system
CyA	Cyclosporine A
CYP	Cytochrome P450
DACHPt	Dichloro(1,2-diaminocyclohexane) platinum(II)
DLS	Dynamic light scattering
DMF	N,N-Dimethylformamide
DNA	Deoxyribonucleic acid
DOX	Doxorubicin
DSC	Differential scanning calorimetery
DLT	Dose limiting toxicity
eNOS	Endothelial nitric oxide synthase

EPR	Enhanced permeation and retention
fu	Unbound fraction
GI	Gastrointestinal
GST	Glutathione S-transferase
h	Hour
HDL	High-density lipoprotein
HIF	Hypoxia-inducible transcription factor
HL	Hyperlipidemic
HRE	Hypoxia-response elements
IL	Interleukin
IP	Intraperitoneal
kb	Tissue to blood concentration ratio
kp	Tissue to plasma concentration ratio
LDL	Low-density lipoprotein
LLC	Lewis Lung Carcinoma
LRP	Lung resistance protein
MDR	Multidrug resistance
M_n	Number average molecular weight
µL	Microlitre
mL	Milliliter
MMP	Matrix metalloproteinase
MRP	Multidrug resistance associated protein
MTX	Methotrexate

MW	Molecular weight
NBD	Nucleotide-binding domain
MTD	Maximum tolerable dose
NFAT	Nuclear factor of activated T-cell
NL	Normolipidemic
nm	Nanometer
NO	Nitric oxide
P407	Poloxamer 407
P(ASP)	Poly(L-aspartic acid)
PBLA	poly(β-benzyl-L-aspartate)
PBLG	Poly(β-benzyl-L-glutamate)
PCL	Poly(ε-caprolactone)
PDLLA	Poly(D,L-lactide)
PEO	Poly(ethylene oxide)
P(Glu)	Poly(glutamic acid)
P-gp	P-glycoprotein
PHSA	poly(N- hexyl stearate L-aspartamide)
PLA	Poly(lactic acid)
PLH	Poly(L-histidine)
PLGA	Poly(lactic-*co*-glycolic acid)
PMN	Polymorphonuclear leukocytes
PM-CyA	Polymeric micellar CyA

PM-CyA (L)	Polymeric micellar CyA-low level of loading
PM-CyA (I)	PM-CyA-intermediate level of loading
PM-CyA (H)	PM-CyA-high level of loading
PVP	Poly(N-vinylpyrrolidone)
PXT	Paclitaxel
RAS	Renin-Angiotensin System
RBC	Red blood cells
RES	Reticuloendothelial System
ROS	Reactive oxygen species
TGF	Transforming growth factor
THF	Tetrahydrofuran
TX	Thromboxane
Vc	Volume of central compartment
Vd	Volume of distribution
VEGF	Vascular endothelial growth factor
VEGFR	VEGF receptor
VLDL	Very low density lipoprotein

CHAPTER 1: INTRODUCTION

1.1. Polymeric Micelles: an overview

The goal of drug delivery is to enhance drug performance. However, finding the optimal delivery technology for a given drug is often a matter of serendipity. In recent years, polymeric micelles have been the focus of much interest as novel colloidal delivery systems that can fulfill the requirements of an ideal and versatile drug carrier [1-18]. Polymeric micelles are core/shell structures formed through self assembly of amphiphilic block copolymers (Figure 1.1). They have a nanoscopic, usually spherical, core/shell structure where the hydrophobic core acts as a microreservoir for the encapsulation of hydrophobic drugs, proteins or DNA; and the hydrophilic shell interfaces the biological media.

The unique feature that has made polymeric micelles superior to other colloidal delivery systems is the versatility of the core/shell structure. Chemical flexibility of the polymeric micellar structure allows for the development of "custom made" carriers that may be designed with respect to the physicochemical properties of the incorporated drug, pathophysiology of the disease, site of drug action, and proposed route of administration. Variations in the chemical structure of the core-forming block in polymeric micelles may be used to improve drug encapsulation, enhance micellar stability and control the rate of drug release from the carrier. The chemical structure of the micelle-forming block copolymer may also be modified to change the biological destination of the polymeric micellar carrier, enhance their specificity for an organ or tissue or make them responsive to an external stimulus thereby enhancing the targeting efficiency of the drug carrier.

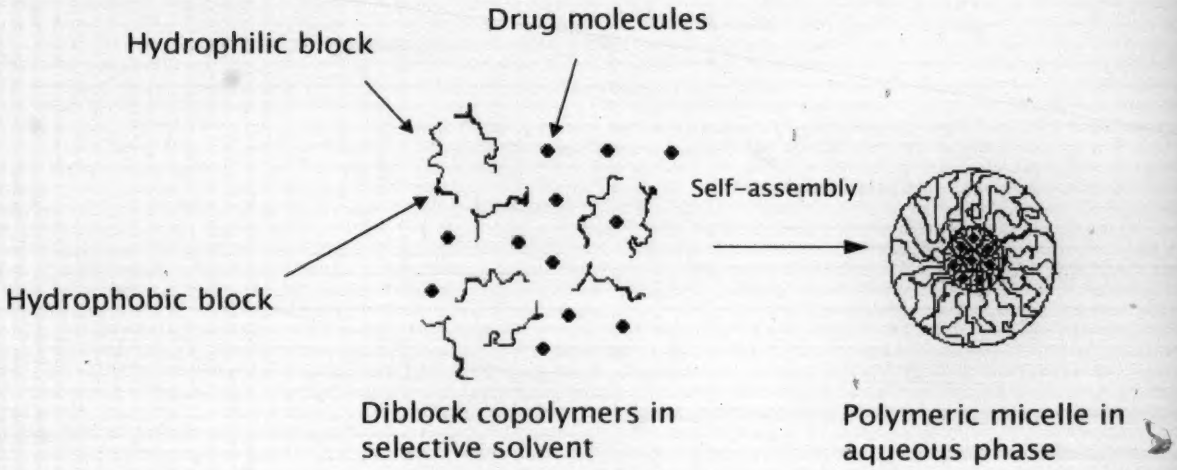

Figure 1.1 – The process of self-assembly for amphiphilic diblock copolymers

1.1.1. Design of polymeric micelles for drug delivery applications

Polymeric micellar carriers investigated for the purpose of drug delivery to date may be categorized under three distinct designs: polymer-drug conjugates, polyion complex, and micellar nano-containers. Each design creates different characteristics that may offer greater opportunities for a specific purpose or therapeutic approach. In most cases, the shell forming block consists of a poly(ethylene oxide) (MPEO) chain. The chemical structure of most commonly used core forming blocks is shown in Figure 1.2.

Polyesters:

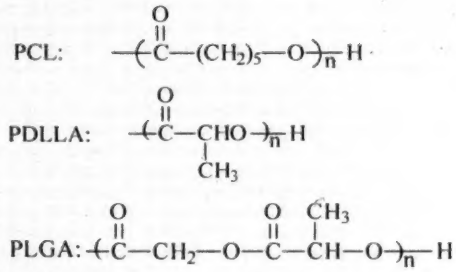

Poly(amino acid)s:

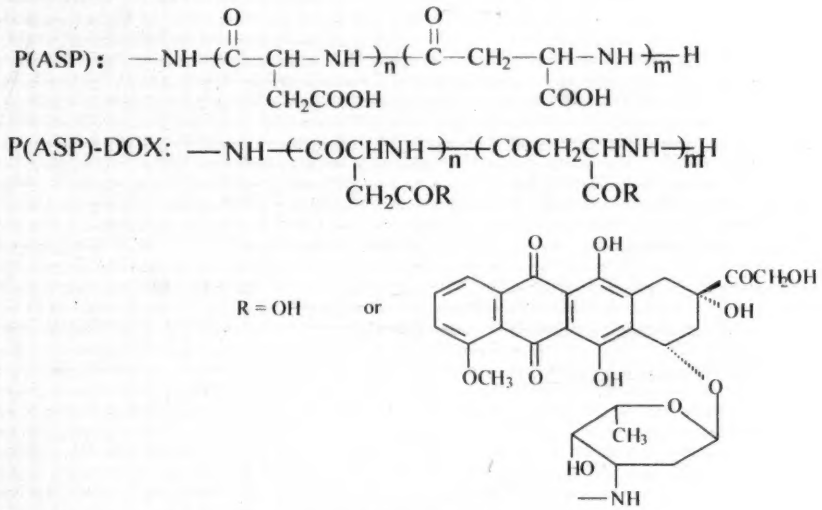

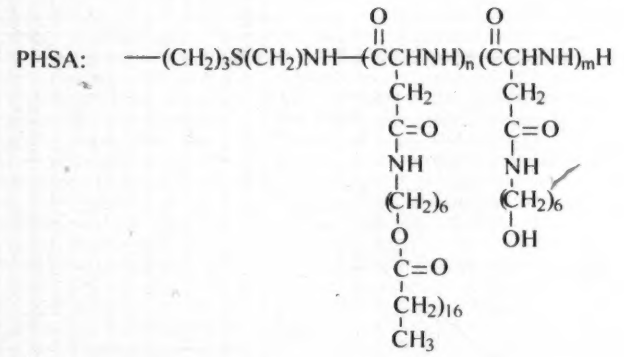

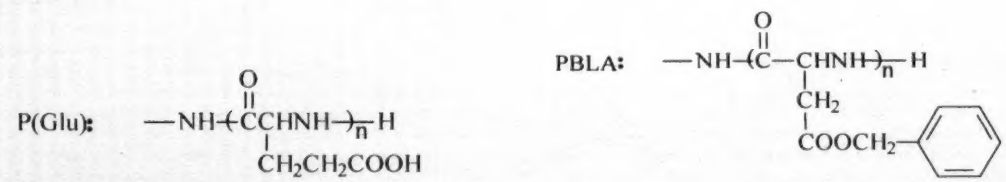

Figure 1.2 – Chemical structure of most commonly used core-forming blocks in micelle-forming block copolymers.

1.1.1.1. Micelle forming polymer-drug conjugates – The stability of incorporated drug inside the carrier is one of the most important concerns if polymeric micelles are intended for controlled release or targeted drug delivery. On the other hand, the incorporation of relatively hydrophilic drugs inside the hydrophobic core of polymeric micelles through hydrophobic interaction is unlikely. This problem may be answered through formation of hydrolysable chemical bonds between the functional group(s) of the polymeric backbone and the drug and further stabilization of the hydrolysable bond within the hydrophobic core of polymeric micelle. Development of different micelle-forming drug conjugates based on poly(ethylene oxide)-*block*-poly(ester) and poly(ethylene oxide)-*block*-poly(amino acid) block copolymers have been the subject of several studies [19-27]. Drug conjugation to MPEO-*block*-poly(ester)s is mostly carried out through formation of covalent bonds between the activated terminal hydroxyl group of the polyester section (Figure 1.2) and reactive groups on the drug molecule [28-30]. The poly(amino acid) block has clear advantages over poly(ester) block for drug conjugation, however, due to the presence of several functional groups (Figure 1.2), which provide multiple sites for the conjugation of drug molecules to one polymeric chain (Figure 1.3B-D). This may lead to a lower dose of administration for the polymeric drug. On the other hand, the diversity of functional groups in a poly(amino acid) chain (amino, hydroxyl and carboxylic groups) allows conjugation of different chemical entities to the polymeric backbone.

1.1.1.2. Polyion complex micelles – Polyion complex micelles can incorporate and deliver different therapeutic moieties that carry charge (e.g., small drugs [31, 32],

peptides [33], and DNA [34-36]). In this approach, drug incorporation is promoted through electrostatic interactions between oppositely charged polymer/drug combinations. Neutralization of the charge on the core-forming segment of the block copolymer will then trigger self assembly of the polyion complex and further stabilization of the complex within the hydrophobic environment of the micellar core.

1.1.1.3. Polymeric micellar nano-containers – In this system, formation of hydrophobic interactions or hydrogen bonds between the core forming block and drug provides basis for the physical encapsulation and stabilization of water insoluble drugs in the polymeric micelles. The compatibility of the micellar core and the incorporated drug, determines the final capacity of the polymeric micelle for the solubilization of a given therapeutic agent.

1.1.2. Methods of physical drug encapsulation in polymeric micelles

1.1.2.1. Direct addition- Polymeric micellar nano-containers may be prepared by direct addition and incubation of drug with block copolymers in an aqueous environment only if the block copolymer and the drug are water soluble [37-39]. The method, however, is not very efficient in terms of drug loading levels and not feasible for most block copolymer/drug structures.

1.1.2.2. Dialysis– Drug encapsulation by this methods is carried out through dissolution of block copolymer and drug in a water miscible organic solvent ,such as N,N-Dimethylformamide (DMF) followed by dialysis of this solution against water (Figure 1.3A) [37-45]. In this method, gradual replacement of the organic solvent with water, the non-solvent for the core forming block, triggers self-association of block copolymers and

entrapment of drug in the assembled structures. The semi-permeable membrane keeps the micelles inside the dialysis bag, but allows removal of unloaded drug. This method has been extensively used for the preparation of polymeric micellar formulations in a laboratory setting [46], but may not suit large scale production.

1.1.2.3. Oil/water emulsion– Preparation of micelles by emulsion method is accomplished by dissolving the drug in a water immiscible organic solvent (such as chloroform or methylene chloride), followed by the addition of organic phase to aqueous phase under vigorous stirring (Figure 1.3B). The polymer may be dissolved in either organic or aqueous phase. The organic solvent is then removed by evaporation [47-49].

1.1.2.4. Solvent evaporation method – Dissolving the drug and polymer in a volatile organic solvent and complete evaporation of organic solvent leading to the formation of polymer/drug films is the basis for solvent evaporation method (Figure 1.3C). This film is then reconstituted in an aqueous phase by vigorous shaking [50-52]. Although the solvent evaporation method of drug loading may have advantages in terms of scale up over the dialysis method, it can only be utilized for micelle-forming block copolymers with high hydrophilic lipophilic balance (HLB) values for which the polymer film can easily be reconstituted in an aqueous media.

1.1.2.5. Co-solvent evaporation method– In this method the drug and polymer are dissolved in a volatile water miscible organic solvent (co-solvent) (Figure 1.3D). Self assembly and drug entrapment is then triggered by the addition of aqueous phase (non-solvent for the core-forming block) to the organic phase (or vise versa) followed by the evaporation of the organic co-solvent [53-56].

1.1.2.6. Freeze-drying method– A freeze-dryable organic solvent like *tert*-butanol is used to dissolve the polymer and drug (Figure 1.3E). This solution is then mixed with water, freeze-dried and reconstituted with isotonic aqueous media. This procedure may be pharmaceutically feasible for large scale production but its application is limited to block copolymers and drug structures that can be solubilized in *tert*-butanol. Due to the insolubility of poly(ethylene oxide) (MPEO) in *tert*-butanol, the method can not be used for MPEO containing block copolymers [57, 58].

A) Dialysis method

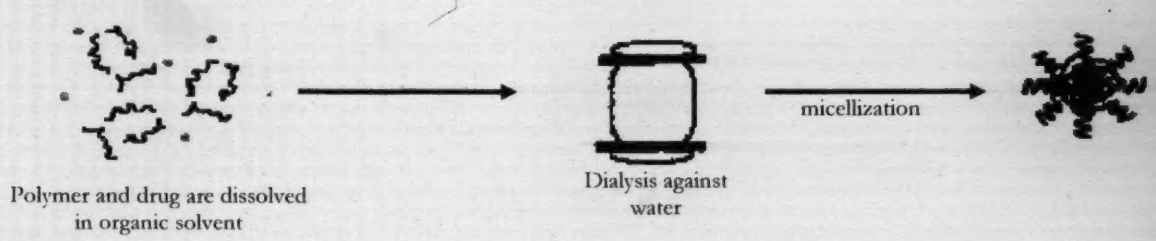

B) O/W emulsion method

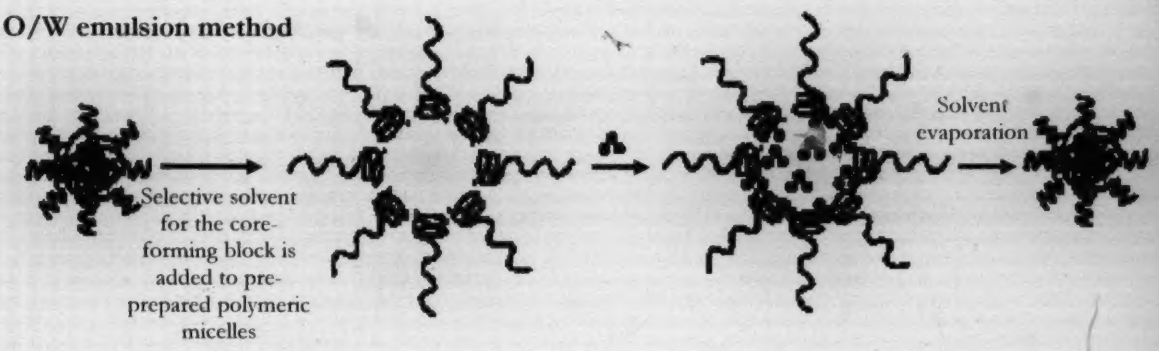

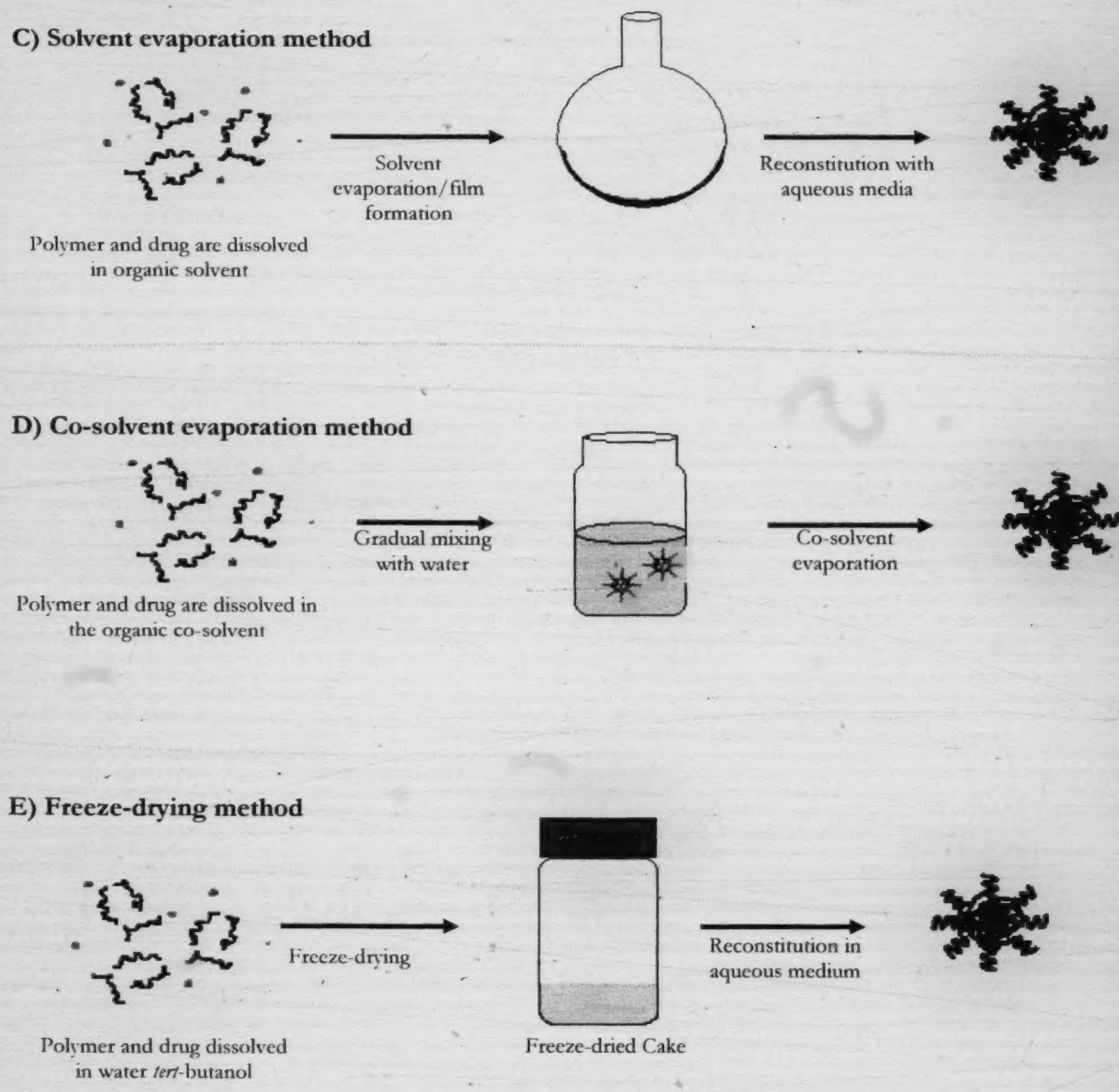
C) Solvent evaporation method
Solvent evaporation/film formation
Reconstitution with aqueous media
Polymer and drug are dissolved in organic solvent
D) Co-solvent evaporation method
Gradual mixing with water
Co-solvent evaporation
Polymer and drug are dissolved in the organic co-solvent
E) Freeze-drying method
Freeze-drying
Reconstitution in aqueous medium
Polymer and drug dissolved in water tert-butanol
Freeze-dried Cake

Figure 1.3 – Physical methods of drug encapsulation in polymeric micelles: **A)** dialysis; **B)** O/W emulsion; **C)** solvent evaporation; **D)** co-solvent evaporation; and **E)** Freeze-drying methods.

1.1.3. Applications of polymeric micellar systems in drug delivery

The interest in polymeric micelles has specifically been keen on the potential application of these delivery systems in three major areas in drug delivery so far: drug solubilization, controlled drug release and drug targeting.

1.1.3.1. Polymeric micelles as solubilizing agents – Effective application of many existing potent therapeutic agents or future entities emerging from drug discovery efforts is restricted by their poor water solubility. Conventional solubilizing agents currently in use for the formulation of such compounds are either ineffective or toxic. In this regard development of efficient solubilizing agents that can safely be administered to human is of great importance.

Polymeric micelles have been the focus of much interest as alternative vehicles for the solubilization of molecules with poor water solubility [46], rendering clear advantages over current solubilizing agents in drug delivery [11]. An increasing body of evidence points to a better safety profile for polymeric micelles as alternative solubilizing agents for the administration of hydrophobic drugs [42, 56]. Most solubilizing agents currently in use are shown to be biologically active and not entirely inert. For instance, Cremophor EL, a major component for the solubilization of potent water insoluble drugs such as paclitaxel (PXT) and cyclosporine A (CyA), causes a range of side effects, including hypersensitivity reactions, hyperlipidemia, neurotoxicity, and reversal of p-glycoprotein [59-62]. Tween 80 and sodium deoxycholate used for the solubilization of amiodarone and amphotericin B, respectively, are known to be hemolytic [42, 63, 64]. Moreover,

polymeric micelles have shown enhanced loading capacity, higher thermodynamic stability (based on the hydrophobicity of the core-forming block and critical micellar concentration [CMC] of the micelles) and kinetic stability (based on interaction of polymer chains below CMC), and more control over the rate of drug release. As a result, they may act as depot drug delivery systems after intravenous administration and have the potential to modify the biological disposition of the incorporated drug in a favourable manner. This is in contrast to the low molecular weight surfactant micelles that release their drug content immediately after administration and dilution in blood.

Perhaps one of the most successful examples for the application of polymeric micellar formulations as alternative solubilizing agents is the formulation of PXT in MPEO-*b*-POLY(D,L-lactide) (PDLLA) micelles developed by Burt *et al,* which have resulted in a 50,000 fold increase in the solubilized PXT levels in an aqueous media [51, 52, 65, 66]. Application of MPEO-*b*-PDLLA micelles is also reported to increase the water solubility of DOX up to 12,000 fold [67].

Compatibility between the micellar core and encapsulated drug molecule seems to be the most crucial factor which determines the final capacity of a polymeric micellar system for the solubilization of a given therapeutic agent. With this in mind, chemical conjugation of DOX to the poly(aspartic acid) (P(Asp)) block of MPEO-*b*-P(Asp) has been pursued to increase the entrapment of DOX inside the hydrophobic core of MPEO-*b*-P(Asp)-DOX micelles [27]. Further evidence for the importance of compatibility between the core-forming block and the encapsulated drug is provided in studies by

Kwon *et al* on the encapsulation of amphotericin B in polymeric micelles consist of MPEO-*b*-P(Asp) derivatives where replacement of the aromatic core with aliphatic ones has resulted in an increase in the level of encapsulated drug [50]. Partial replacement of benzyloxy group in MPEO-*b*-poly(β-benzyl-L-aspartate) (PBLA) with cetyl ester has also been used by Yokoyama *et al* to achieve polymeric micellar nanocontainers for KRN5500, an aliphatic antineoplastic agent [68-70]. Encapsulation procedure may play a significant role in determining the final solubilized levels of the encapsulated drug, as well [40, 48, 71].

1.1.3.2. Polymeric micelles as controlled release delivery systems – The mode of drug release from polymeric micelles mainly depends on the utilized design for their preparation; the chemical structure of micelle-forming block co-polymer and incorporated drug; their physicochemical properties; and the localization of the incorporated drug in the core/shell structure. Drug release from micelle-forming block copolymer-drug conjugates may proceed via two major pathways: either micellar dissociation followed by drug cleavage from the polymeric unimers or drug cleavage within the micellar structure and its further diffusion out of the micellar carrier (Figure 1.4A). Release of physically encapsulated drug from sufficiently stable micellar nanocontainers usually proceeds by diffusion (Figure 1.4B), whereas drug exchange with free ions and proteins in the physiological media triggers drug release from polyion complex micelles (Figure 1.4C). Potentially, it will be possible to tailor the chemical structure of the micelle-forming block copolymer and modify the physicochemical properties of the core/shell forming blocks to adopt instant, sustained, pulsed or delayed

mode of drug release for specific delivery requirements. For instance, hydrophobicity and rigidity of the micellar core may be enhanced to restrict the penetration of water and free ions to the micellar core in micelle-forming drug conjugates and polyion complex micelles, respectively. This may lead to a sustained or even delayed mode of drug release from the carrier [32, 72, 73]. Application of polymeric micelles that have glassy cores under physiological condition (37 °C); cross-linking of the micellar core structure and induction of strong hydrophobic interaction or hydrogen bonds between the core-forming block and solubilized may be utilized to lower the rate of micellar dissociation, drug diffusion, and the overall rate of drug release from the micellar carrier [33, 53, 74-76]. Introduction of hydrophilic or stimulus responsive groups to the core structure, on the other hand, may be utilized to provide an instant or pulsed mode of drug delivery. Finally, the method of drug incorporation in polymeric micelles may also be modified to improve the extent of drug loading, localization or physical state of the loaded drug providing other means for controlling the rate of drug release from polymeric micelles [71].

The *in vitro* rate of drug release from polymeric micelles has been assessed through different methods. The most popular method is dialysis of the polymeric micellar formulation against a physiological recipient phase. The molecular weight cut-off of the dialysis membrane in this experiment is chosen in a way to assure restriction of micellar structures inside the bag, but free diffusion of the released portion of drug to the recipient phase [30, 40, 48, 55, 56, 77]. An alternative method relies on the separation of the released from the encapsulated drug by gel permeation chromatography (GPC) after

direct incubation of the polymeric micellar formulation with the recipient phase [72]. In case of DOX, quenching of the fluorescence for the entrapped drug has been followed to investigate the *in vitro* rate of drug release from its polymeric micellar formulation [40].

Although these methods provide an approach to assess the relative effect of formulation parameters on drug release, they may not offer a realistic picture of drug release in a biological system. Firstly, because the required driving force for the release of poorly soluble compounds may not be reached under such conditions. Secondly, polymeric micelles are subject to sink condition in the biological system and extreme dilution after administration, which may bring the final concentration of the polymeric micellar system below its CMC. In this case, the kinetic stability of polymeric micellar system plays an important role in determining the final rate of drug release from these systems. Application of biomimetic recipients (e.g., lipid vesicles or serum albumin) has been tried in previous studies and shown a better insight into the rate and duration of drug release for these nanoscopic drug delivery systems [40, 50]. Nevertheless, the possibility of micellar dissociation upon dilution which may lead to a faster drug release after *in vivo* administration has to be accounted for.

Evidence gathered from *in vitro* experiments point to a sustained mode of drug release for many polymeric micellar delivery systems developed to date. Drug release from polymeric micellar nanocontainers is expected to be faster than micelle-forming drug conjugates. Yoo *et al* studied the chemical conjugation of DOX to MPEO-*block*-poly(D,L-lactic-co-glycolic acid) (MPEO-*b*-PLGA) forming an amide bond with pre-activated polymer. In phosphate buffered saline (PBS), MPEO-*b*-PLGA micelles released

A) Drug release from micelle forming block copolymer-drug conjugates

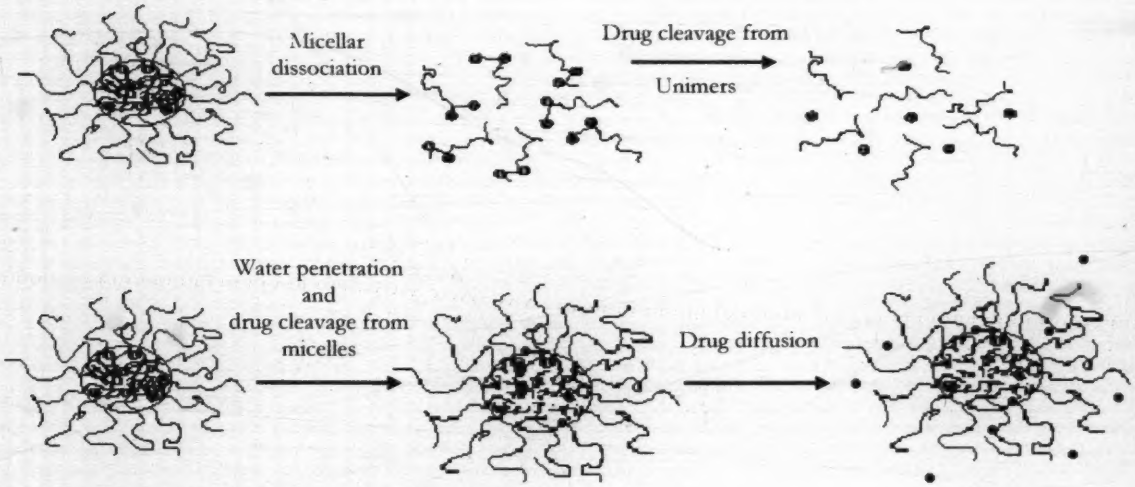

B) Drug release from micellar nanocontainers

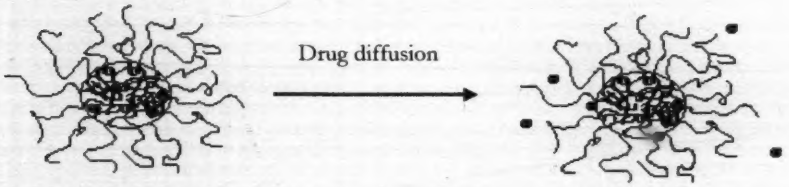

C) Drug release from polyion complex micelles

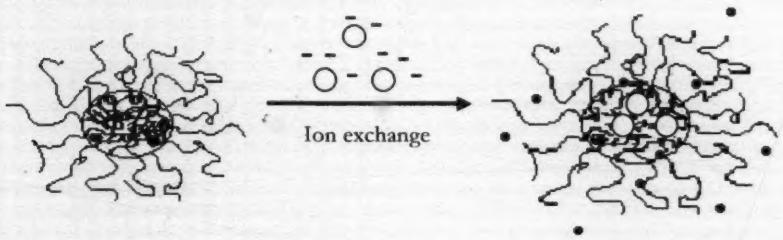

Figure 1.4 – Modes of drug release from: A) block copolymer-drug conjugate micelles; B) micellar nanocontainers; C) polyion complex micelles

50% of their drug content in a sustained manner over 2 weeks while release from physically encapsulated DOX in MPEO-*b*-PLGA only lasted for 3 days [30].

Application of drug compatible moieties in the micellar core is shown to lower the rate of drug release from the carrier. A slow mode of release for DOX from MPEO-*b*-PBLA nanocontainers to phosphate buffer (pH=7.4) and bovine serum albumin (BSA) containing recipient phases has been shown by Kwon *et al*, where 80 % of the drug content remained in the micellar carrier after 4 days of incubation [49]. The release profile was found to be rapid at initial stages and sustained in later stages. A decrease in the pH of the recipient phase from 7.4 to 5.0 accelerated the release of DOX from micellar carrier, pointing to a possibility for accelerated drug release from the carrier in the acidic environment of tumors [48]. It has been suggested that a more acidic pH would protonate the 3'-NH_2 group and catalyze the cleavage of DOX-DOX bound in DOX dimer, the presence of which in the micellar core is shown to reduce the release rate for DOX, probably due to an increase in the core/drug compatibility. The presence of DOX dimers is also shown to reduce the rate of DOX release from MPEO-*b*-P(Asp)-DOX nano-containers [78]. This concept has been used in studies for the development of modified release polymeric micelles for aliphatic drugs [13, 43, 50, 71, 79]. Through development of MPEO-*b*-P(Asp) derivatives having saturated fatty acid substitutes on their core-forming block, Kwon *et al* have made the core of polymeric micelles more compatible with amphotericin B. A reduced hemolytic activity as a result of reduced amphotericin B release from polymeric micelles bearing more drug compatible moieties in their core (> 50 % of stearic acid substitution) has been achieved.

Formation of hydrogen bonds between drug and core-forming block has been suggested as an alternative strategy to lower the rate of drug release in polymeric micelles. Lee *et al* reported on the preparation of functionalized MPEO-*b*-PDLLA bearing free carboxylic groups on the PDLLA block [75] and studied loading and release of papaverine. With an increase in the level of free carboxylic groups on the polymeric backbone, a significant increase in drug loading and reduction in drug release was observed, which was attributed to increased interactions between the loaded drug and the core forming block. Several groups have reported on an effect for the level of drug loading on the *in vitro* drug release rate from polymeric micelles [80, 81]. In micelles formed from assembly of MPEO-*b*-poly(β-benzyl-L-glutamate) (PBLG) star block copolymer, drug crystallization at higher DOX loading levels was correlated with slower drug release rates from this system. At 1 and 3 % DOX loading levels in poly(L-lactic acid) (PLLA)-*b*-MPEO-*b*-PLLA micelles, 50 and 17 % of encapsulated drug was released within 6 and 8 days, respectively [55]. Similarly, for DOX encapsulated at a 20 μM level in MPEO-*b*-P(Asp) -DOX micelles drug release continued for 72 h in saline, but at the encapsulation level of 2 μM almost all the loaded drug was released after 3 h [82].

1.1.3.3. Polymeric micelles as carriers for drug targeting– One of the major problems for a safe and effective pharmacotherapy is the fact that any given drug could potentially distribute throughout the body and create a toxic effect in non-target organs. On the other hand, in order to reach the site of action, a drug has to pass several obstacles such as epithelial cells of gastrointestinal tract, endothelial layer of blood vessels, subcutaneous or muscular tissue, depending on the route of administration. The drug may be

metabolized, inactivated, or even excretion from the body during this journey. This uncontrolled distribution will decrease the chance of a successful and effective treatment without causing undesired toxic effects.

1.1.3.3.1. Enhanced Permeation and Retention (EPR) Effect

Maeda *et al* were first to coin the expression of "EPR effect" as a mean to explain the reason behind accumulation of macromolecules in solid tumors [83, 84]. The EPR effect is caused by the increased permeability of the vasculature on one hand, and the lack of lymphatic drainage in solid tumors that normally remove macromolecules from normal tissue, on the other hand. Together, these two effects can increase the accumulation of i.v administered macromolecules in tumors (Figure 1.5). Plasma proteins were known to accumulate in inflammatory and tumor tissue due to EPR effect[85]. Entrapment of gallium-transferrin complex in solid tumors because of EPR effect has also been utilized in clinical radiology as gallium scintigraphy for diagnosis of various solid tumors and inflammation and their visualization by γ-scintillation camera [86].

The permeability of the vasculature in the tissue affected by inflammation and cancer growth is shown to be abnormally high. This will allow extravasation of particles in nanometer size range that normally cannot pass through the endothelial layer of the vessels [87]. The physiological changes in tight intercellular junction at the apical region of the lateral membrane in the endothelium are induced in response to stimulating factors such as cytokines and microbial toxins, which play an important role in the migration of immune cells (such as polymorphonuclear leukocytes (PMN)) across the paracellular

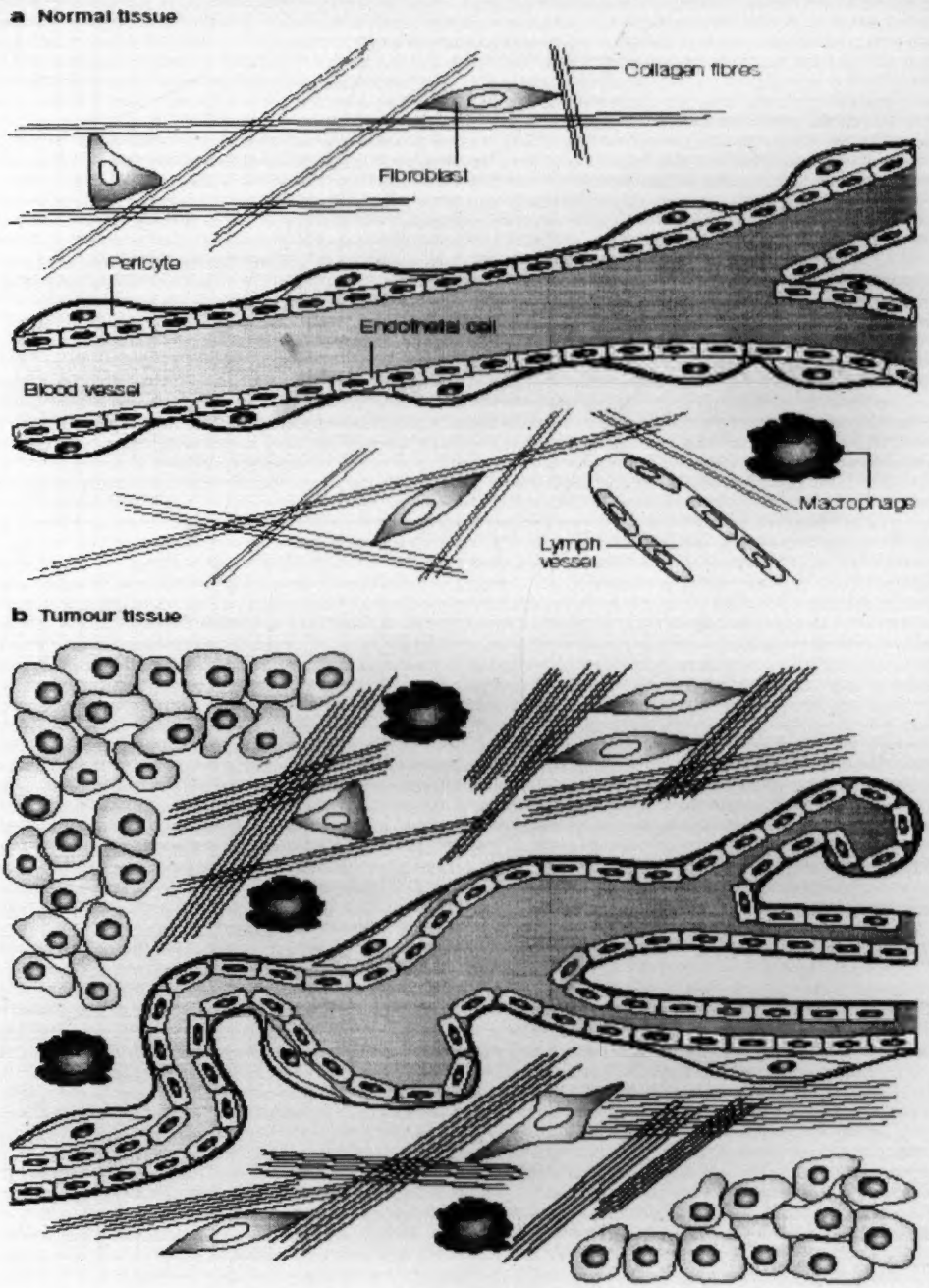

Figure 1.5 – Structural differences between normal and tumor tissue (from reference [88] with permission); a) Normal tissue containing linear blood vessels lined by a smooth layer of endothelial cells and lymph vessels; b) Tumor tissue with defective blood vessels that are leaky and irregularly shaped, usually without lymphatic drainage.

space during inflammation and immune response [89, 90]. The enhanced permeation of vasculature endothelium is known to occur in tumor tissue during angiogenesis, i.e. formation of new blood vessels in tumor.

Cancer is one of the medical conditions that cause hypoxia in the affected tissue because of the rapid growth rate and poor blood supply to malignant cells. Tumor cells that are more than 180 μm away from the blood vessels become necrotic; this is the calculated distance that oxygen diffuses from capillary to cells before it is completely metabolized [91]. In response to hypoxia, cells will produce different factors including hypoxia-inducible transcription factor 1 (HIF-1). In the absence of oxygen, HIF-1 binds to hypoxia-response elements (HREs) and activates the expression of many genes, including vascular endothelial growth factor (VEGF) [92] and one of its receptors, VEGF receptor 1 (VEGFR1) on endothelial cells and macrophage-lineage cells. Recent studies have placed a great importance on VEGF pathway [93] (also known as vascular permeability factor [94]) in cancer growth. VEGF is a ligand produced by tumor cells and associated stroma that functions predominantly on the VEGF receptor 2 (VEGFR2) to stimulate endothelial proliferation and migration to the tumor tissue, allowing for the rapid formation of functional neo-vessels [95]. Endothelial cells contributing to tumor angiogenesis originate from neighboring pre-existing vessels and bone-marrow-derived circulating endothelial progenitor cells (CEPs), which express VEGFR2 and are essential for angiogenesis in certain tumors [96] (Figure 1.6).

Most solid tumors also have elevated levels of vascular permeability factors such as bradykinin, which is produced via activated kallikrein-kinin cascade [97-100], nitric oxide (NO) generated by inducible form of nitric oxide synthase (NOS) [101, 102], peroxynitrite ($ONOO^-$), some prostaglandins [100, 103], and matrix metalloproteinases (MMPs/collagenases) [104]. NO that is predominantly synthesized by endothelial NOS (eNOS) in vascular endothelial cells, promotes angiogenesis directly and functions both

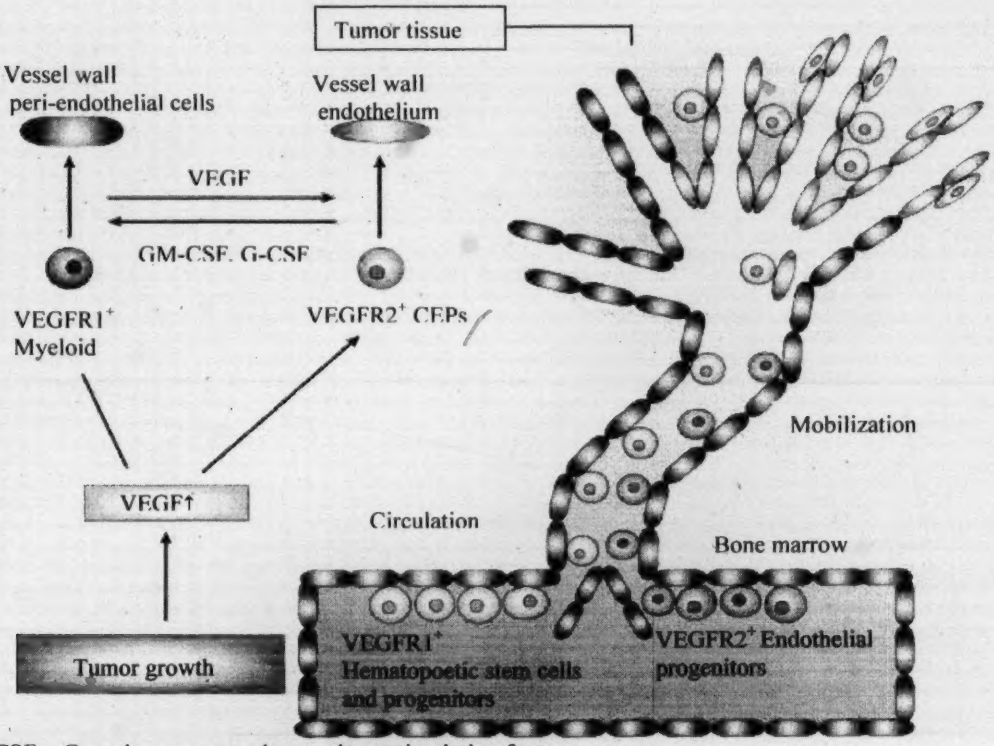

GM-CSF = Granulocyte macrophage colony-stimulating factor
G-SCF = Granulocyte colony stimulating factor

Figure 1.6 – The role of progenitor cells in angiogenesis (from reference [96]with modifications). Angiogenic factors that are released by tumor induce mobilization of VEGFR1-expressing hematopoietic stem cells ($VEGFR1^+$ myeloid cells) and VEGFR2-expressing circulating endothelial precursors ($VEGFR2^+$ CEPs) from the bone marrow.

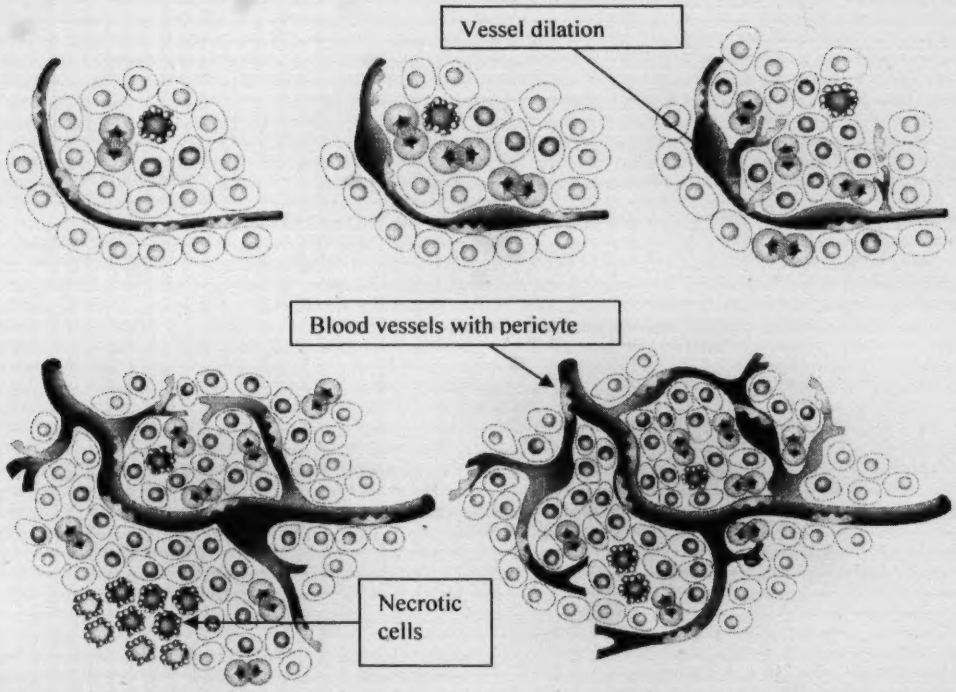

Figure 1.7 – The classical angiogenic switch (from reference [105] with permission). The 'angiogenic switch', has to occur to ensure exponential tumor growth. The switch begins with perivascular detachment and vessel dilation, followed by angiogenic sprouting, new vessel formation and maturation, and the recruitment of perivascular cells. Blood-vessel formation will continue as long as the tumor grows, and the blood vessels specifically feed hypoxic and necrotic areas of the tumor to provide it with essential nutrients and oxygen.

upstream and downstream of angiogenic stimuli. Moreover, NO mediates recruitment of perivascular cells and, therefore, remodeling and maturation of blood vessels. Nitric oxide promotes tumor progression through the maintenance of blood flow, induction of vascular hyperpermeability and reduction of leukocyte–endothelial interactions. Induction of vascular permeability by VEGF is also mediated by eNOS and its downstream signaling, and NO-mediated vascular permeability seems to share the same signaling pathway [106]. MMPs promote tumor progression by their extracellular matrix degrading activity, as well as signaling functions. In addition to angiogenesis, they are

also involved in apoptosis inhibition, regulation of innate immunity, and enhanced metastasis and tumor growth [107].

Tumor angiogenesis differs significantly from physiological angiogenesis. Differences include aberrant vasculature structure, altered endothelial cell-pericyte interactions, abnormal blood flow, increased permeability, and delayed maturation [105] (Figure 1.7). Formation of fenestrated (with trans-endothelial circular openings of 40-80 nm in diameter) and discontinuous capillaries (with openings of 100-1000 nm in diameter) in tumor capillaries is the main reason for the enhanced permeation of tumor vasculature [108]. It has also been shown that some tumor vessels have a defective cellular lining composed of disorganized, loosely connected, branched, overlapping, or spouting endothelial cells, which contribute to tumor vessel leakiness [87]. The absence of lymphatic drainage in tumor tissue is a key element in the EPR effect, allowing the entrapment of extravasated particles in the tumor for longer periods and higher extents [108, 109] .

The EPR effect has been observed in many experimental and human solid tumors, including hepatoma, renal cancer, lung cancer, and brain tumors [110, 111]. The accumulation of plasma proteins, synthetic polymers, polymer conjugates and macromolecular delivery systems in solid tumors at high concentrations for prolonged periods (more than 100 hours) [84]. The EPR effect is believed to be responsible for increased accumulation of many macromolecular-drug delivery systems of appropriate size to pass through the leaky tumor vasculature in solid tumors including dextran-

peptide-methotrexate conjugates [112], liposomal DOX [113], MPEO-modified Poly(β-amino ester) nanoparticles [114], platinum conjugates [115], micellar formulations of pirarubicin [116], and DOX-loaded MPEO-poly (L-histidine) (MPEO-PLH) polymeric micelles [117].

Enhanced permeation and retention effect (EPR), is the basic mechanism of passive targeting and considered a "gold standard" in the design of effective targeted delivery systems in cancer therapy [83, 118, 119]. Polymeric micelles are considered to be one of the most promising carriers for passive targeting by EPR in cancer, especially for hydrophobic drugs. In reality; however, to this point, only a few polymeric micellar formulations have demonstrated success in passive targeting of the incorporated drug to solid tumors [46]. Despite high accumulation of nanosized micelles in tumor tissue as a result of EPR effect, accumulation of the encapsulated drug at the cellular and molecular drug targets can not be guaranteed. Efficient drug targeting by polymeric micelles in most cases is hampered by either premature drug release from the micellar nano-containers before the carrier reaches the tumor targets, or insufficient intracellular delivery of the encapsulated anticancer drug to the tumor cells [46]. Finding the right polymeric micellar system that can provide a proper balance between the two properties, i.e., avoiding premature drug release outside tumor site, but promoting cellular internalization and/or obtaining triggered drug release at the tumor site poses a challenge for efficient targeted drug delivery by polymeric micelles.

1.1.3.3.2. Characteristics of ideal carriers for passive drug targeting by EPR effect

Longer blood circulation time of the delivery system in blood, increases the chance of extravasation and accumulation of delivery system in solid tumors by EPR effect. Therefore, delivery systems with stealth properties that can avoid uptake by the RES and excretion by kidneys and as a result reduce the volume of distribution (Vd), clearance (CL), and increase the area under blood (or plasma) concentration versus time curve (AUC) of the incorporated drug have a better chance for passive accumulation and targeted drug delivery in solid tumors. In general, an ideal delivery system for passive drug targeting should have the following characteristics:

a) Stealth properties of the nanocarrier (to enable the delivery system to avoid RES uptake and early elimination from blood circulation);

b) Optimum size (large enough to minimize extravasation from continuous capillary and renal clearance, but small enough to avoid RES uptake and extravasate at tumor site);

c) Stability in biological environment (the longer the drug is associated with the nanocarrier, more similar its pharmacokinetic pattern would be to the carrier);

d) Long circulation half-life (to increase the chance of tumor accumulation).

Many studies have shown the pharmacokinetic advantages of long circulating stealth nanocarriers that increase the blood circulation time, half life ($t_{1/2}$), and the AUC of the encapsulated drug, while decreasing the CL and Vd in passive tumor targeting [120-126]. Long circulating liposomes show dose-independent, non-saturable, log-linear (monophasic) pharmacokinetic. This log-linear kinetics results from a significant decrease in the first phase of clearance into the high affinity, low capacity, and saturable

reticuloendothelial system. Therefore, by switching to a slower, low affinity, high capacity elimination mechanism, a stealth nanocarrier is able to display dose-independent pharmacokinetics and change the kinetic pattern of the encapsulated drug dramatically [122].

1.1.3.3.3. Polymeric micelles for active or stimuli responsive drug targeting

The *in vivo* performance of polymeric micelles for tumor targeting can be further improved by taking advantage of differences between the cancerous and normal tissue at a cellular level.

The second generation of polymeric micelles (micelles for active targeting) can be categorized to immunomicelles that are prepared through chemical conjugation of monoclonal antibodies to micellar surface [18, 127], and ligand modified micelles [35, 128, 129]) in which micellar surface is modified through attachment of receptor specific probes such as small peptides, transferrin, or folate. An alternative targeting strategy by polymeric micelles relies on the responsiveness of the micellar structure to internal or external stimuli, i.e. ultrasound [130, 131], pH [132-134], and temperature [135, 136]. In recent years a third generation of these nanocarriers, known as multifunctional polymeric micelles, has also emerged. These micelles are designed to bear a combination of structural components required for various targeting strategies on an individual carrier [137-139].

1.1.4. Polymeric micellar delivery systems in clinical trials

To date, six polymeric micellar formulations, all developed for the delivery of anticancer drugs, have passed the phase of laboratory development and entered clinical trials. Among these systems, only a few have shown a favorable pharmacokinetic pattern for the encapsulated drug to achieve passive drug targeting. The results of preclinical animal investigations on the development of polymeric micellar delivery systems for the purpose of drug targeting are summarized in Table 1.1.

The list of polymeric micellar formulations that have found their way to clinical trials is given in Table 1.2. Physically encapsulated DOX in MPEO-*b*-P(Asp)-DOX micelles, namely NK911, is one of the few polymeric micellar formulations that have shown a favorable change in the normal pharmacokinetic parameters and bio-distribution pattern of the incorporated drug in animal models [140]. Compared to free drug, NK911 showed higher AUC in plasma (within 24 h), higher tumor drug levels, less toxicity and superior *in vivo* activity in solid and hematological cancers in mice (Table 1.1). After 24 h, the pharmacokinetics of encapsulated and free DOX became similar pointing to drug release from the micellar carrier. The results of phase I clinical trials and human pharmacokinetic studies on NK911 showed a similar spectrum in the side effects and recommended dose for NK911 and free DOX [141]. In pharmacokinetic evaluations in human, NK911 exhibited an increase in the half life and plasma AUC, and decrease in CL and Vd. A comparison of pharmacokinetic parameters of NK-911 and liposomal formulation of DOX showed a lower stability for NK-911 in the blood stream.

Table 1.1- The result of preclinical studies for tumor targeted micellar delivery systems

Incorporated drug	Polymer	Animal model	Change in MTD**	Change in plasma AUC**	Change in tumor AUC/antitumor activity**	Ref
Doxorubicin	MPEO-*b*-P(Asp)-DOX (Chemical conjugate)	P388 bearing CDF1 mice	↑	-	-	[25]
		Healthy ddy mice	-	↑	NA*	[22]
		Different tumors C57BL/6 mice	↑	-	-	[142]
		C26 bearing CDF1 mice	-	↑	tumor AUC ↑	[20]
	MPEO-*b*-P(Asp)-DOX (Physical encapsulation)	C26 bearing CDF1 mice	↑	↑	tumor AUC ↑ 7.4 fold)/antitumor activity ↑	[78]
		C26 bearing CDF1 mice	-	↑ (28.9 fold)	tumor AUC ↑(3.4 fold)/ antitumor activity ↑	[140]
	MPEO-*b*-PPO-*b*-MPEO	A2780 bearing nu/nu mice	-	-	tumor AUC ↑	[131]
		Different tumors and mice	No	↑ (2 fold)	tumor AUC ↑/ antitumor activity↑	[143]
	MPEO-*b*-PBLA	C26 bearing CDF1 mice	-	↑	antitumor activity↑	[48]
	MPEO-*b*-PLGA	KB bearing nu/nu mice	-	-	tumor AUC ↑/ antitumor activity↑	[129]
Paclitaxel	MPEO-*b*-PDLLA	P388 bearing B6DF1 mice	↑	-	-	[52]
		MV-522 bearing nu/nu mice	↑	↓	-	[65]
		LNCaP bearing BALB/c mice	↑	-	antitumor activity↑	[66]
		Different tumors and mice	↑	No change	tumor AUC ↑ /antitumor activity↑	[41]
	PVP-*b*-PDLLA	C26 bearing BALB/c mice	↑	↓	No Change	[57]
	MPEO-*b*-PPBA	C26 bearing CDF1 mice	-	↑ (86 fold)	tumor AUC ↑ 25 fold)	[144]
Cisplatin	MPEO-*b*-P(Asp)	LLC bearing C57BL/6N mice	-	↑ (5.2 fold)	tumor AUC ↑(4.6 fold)	[145]
		LLC bearing C57BL/6N mice	-	↑	tumor AUC ↑/no change in antitumor activity	[146]
	MPEO-*b*-P(Glu)	LLC and C26 bearing mice	-	↑	tumor AUC ↑ /Antitumor activity↑	[32]
		C26 bearing CDF1 mice‡	-	↑	tumor AUC ↑	[147]
	MPEO-*b*- poly (L-lysine)-Succinate	Adenocarcinoma bearing rats	-	-	tumor AUC ↑	[148]
HCPT†	MPEO-*b*-PCL	S180 bearing mice	-	↑	tumor AUC ↑	[149]

* Not applicable

** Compared to commercial formulation

‡ With dichloro(1,2-diaminocyclohexane)platinum(II) (DACHPt) † Hydroxycompthotecin

Table 1.2- Polymeric micellar delivery systems in clinical trials

Trade Name	Incorporated drug	Polymer	Company	Progress	Ref
NK911	DOX	MPEO-*b*-P(Asp)-DOX	Nippon Kayaku Co., Japan	Phase II	[141]
SP1049C	DOX	MPEO-*b*-PPO-*b*-MPEO	Supratek Pharma Inc., Canada	Phase II	[150]
PAXCEED®	Paclitaxel	MPEO-*b*-PDLLA	Angiotech	Phase I/II	http://www.angiotech.com
Genexol®-PM	Paclitaxel	MPEO-*b*-PDLLA	Samyang Corporation, South Korea	Phase II	[151]
NK105	Paclitaxel	MPEO-*b*-PPBA	Nippon Kayaku Co., Japan	Phase I	[144]
NC-6004	Cisplatin	MPEO-(Glu)	Japan	Phase I	

Pluronic® formulation of DOX, known as SP1049C, which is prepared from a combination of L61 with more hydrophilic Pluronics®, i.e., F127, at a ratio of 1:8 to avoid micellar aggregation, entered preclinical and clinical trials in Canada in 1999 [150]. In 2004, Danson *et al* reported on the results of the phase I clinical trials of SP1049C [150]. The pharmacokinetic profile of SP1049C was similar to conventional DOX but with a slower terminal clearance. An update on the results of phase II trials on this system reported partial responses in some patients after 4-6 cycles of treatment. However, data shows appearance of hematological and non-hematological signs of toxicity.

In 1996, Burt *et al* reported on the application of MPEO-*b*-PDLLA micelles for physical encapsulation of PXT by a solvent evaporation method [51]. Results of further studies on the biodistribution of MPEO-*b*-PDLLA in comparison to Cremophor EL formulation (Taxol®) showed a 5.5-fold decrease in the AUC of polymeric micellar PXT in blood after its i.v administration [65]. This is in contrast to the expected trend in pharmacokinetic parameters for carriers with stealth properties. The results of

biodistribution experiments in healthy rats using radiolabeled PXT demonstrated a rapid loss of drug from the micellar carrier. However, because of a higher maximum tolerable dose (MTD), this formulation (PAXCEED®) is now in clinical trials phase II for the treatment of rheumatoid arthritis, and is also evaluated for the therapy of psoriasis by Angiotech Pharmaceuticals in Canada (Table 1.2).

In 2001, Kim *et al* reported on the toxicity profile, pharmacokinetics and biodistribution of PXT loaded in a similar carrier, i.e., MPEO-*b*-PDLLA micelles prepared by an identical solvent evaporation technique, known as Genexol®-PM (Table 1.2) [41]. The MTD of Genexol®-PM and Taxol® in i.v administration in nude mice were determined to be 60 and 20 mg/ kg, respectively. Application of Genexol®-PM allowed administration of higher drug doses in clinical trials phase I studies in human but resulted in a lower AUC in plasma and a shorter half life for PXT [151].

Recently, Hamaguchi *et al* reported on the development of the first polymeric micellar formulation that has shown significant and favorable changes in the pharmacokinetic of incorporated drug, PXT: namely NK105. NK105 consists of micelle-forming block copolymers of MPEO-*b*-poly(4-phenyl-1-butanoate) L-aspartamide) (MPEO-*b*-PPBA) and has shown 86-fold increase in its AUC in plasma, 86-fold decrease in CL and 15–fold decrease in volume of distribution at steady state (Vdss) compared to Taxol®, commercial formulation of PXT, after i.v injection (Table 1.1) [144]. This has resulted in a 25-fold increase in drug AUC in tumor and stronger anti-tumor activity in C26 tumor bearing mice model, in turn. At a PXT-equivalent dose of 100 mg/kg, a single administration of NK105 resulted in the disappearance of tumors and all mice remained

tumor-free thereafter. This formulation is currently in clinical trials phase I in Japan (Table 1.2).

The most recent polymeric micellar formulation that has entered clinical trials and shown impressive results in passive drug targeting is the MPEO-*b*-poly(amino acid) based micellar formulation of cisplatin (CDDP). The MPEO-*b*-poly(glutamic acid) (MPEO-*b*-p(L-Glu)) formulation of CDDP, i.e., NC-6004, has shown to increase the AUC (65 fold) and decrease the clearance (19 fold) of the encapsulated drug in rats. It also demonstrated a comparable or higher antitumor activity compared to free CDDP. Toxicity experiments in rats also revealed a potential for this formulation to control the nephrotoxic and neurotoxic effects of CDDP; however, signs of a transient hepatotoxicity was observed in the animals that received NC-6004 (Table 1.2) [152].

1.1.5. Poly(ethylene oxide)-*block*-poly(ε-caprolactone) (MPEO-*b*-PCL) micelles for drug solubilization and delivery

MPEO-*b*-PCL is one of the block copolymers in the MPEO-*b*-poly(ester)s category. Compared to other core forming blocks in the poly(ester) group (such as poly(glycolic acid), PLLA or PDLLA), PCL is more hydrophobic, which makes it more compatible with hydrophobic drugs. The hydrophobicity of the PCL has pushed the CMC of MPEO-*b*-PCL block copolymers to extremely low concentrations in 100 nM range [153]. Besides, the semicrystalline structure of PCL may be considered an advantage over PDLLA leading to kinetic stabilization of and a potential for sustaining the rate of drug release for PCL based micellar structures.

Like other MPEO-poly(ester)s, MPEO-*b*-PCL copolymers are biocompatible and biodegradable [44, 45]. PCL has shown low toxicity and no immunogenicity in its record. Possible degradation products of PCL are caprolactone, succinic, butyric, valeric and hexanoic acid. With a rise in the popularity and potential applications of PCL, many researchers have paid attention to the biocompatibility and safety of this polymer [153]. Ory *et al.* found PCL capsules to be well tolerated and do not produce any side effects [154]. Rutledge *et al.* found no histological evidence of toxicity for PCL and determined bioabsorbable rods of PCL as safe and effective delivery systems for antibiotics [155]. Isotalo *et al* found PCL to be non-toxic and highly biocompatible [156].

MPEO-*b*-PCL block copolymers have been extensively used in solubilization of hydrophobic drugs (Table 1.3), and have shown potential for passive tumor targeting. The hydrophobic and semicrystalline nature of the PCL core was also shown to bring a high degree of kinetic stability to PEO-*b*-PCL micellar system below CMC [157]. In another study in Wistar rats by Shi et al, MPEO-*b*-PCL micelles were able to increase the AUC of hydroxycamptothecin (HCPT) up to 21-fold compared to the free drug after i.v injection. In S180 tumor bearing mice, the tumor accumulation of HCPT after administration of the polymeric micellar formulation was 8-fold higher than the free drug [149]. Higher blood levels and decrease in liver and spleen uptake compared to control has also been shown for MPEO-*b*-PCL micelles prepared for bone imaging [158].

Table 1.3 – Drug solubilization by MPEO-*b*-PCL polymeric micelles

Drug	Initial water solubility	Incorporation method	Final Concentration	Loading level (%w/w)	Ref.
Doxorubicin	≤ 50 μg/mL	Co-solvent evaporation	NR	4.3	[56]
Paclitaxel	1 μg/mL	Dialysis	NR	21	[41]
		Co-solvent evaporation	NR	5.1	[53]
Indomethacin	35 μg/mL	Dialysis	NR	42	[159]
Fenofibrate	0.1 μg/mL	Co-solvent evaporation	90 μg/mL	10	[54]
Nimodipine	45 μg/mL	Co-solvent evaporation	NR	4.9	[160]
Dihydroxytestosterone	28 μg/mL	Dialysis	1.3 mg/mL	39	[45]
Hydroxycamptothecin	2 ng/mL	Dialysis	NR	6.77	[149]

1.2. Multidrug resistance (MDR)

The development of MDR, i.e., resistance of cancer cells against a variety of chemotherapeutics with different chemical structures and mechanisms of action, is one of the major causes for cancer chemotherapy failure. Acquired MDR is the phenomenon in which exposure of tumor cells to a single cytotoxic agent results in cross-resistance to other structurally unrelated, classes of cytotoxins [161]. Various stimuli, such as DNA-damaging agents, heat shock, serum starvation, ultraviolet irradiation, glucose starvation and hypoxia are also known to activate different mechanisms of this resistance [162]. Innate MDR has been shown in some normal tissue cells including primitive hematopoietic stem cells, which express a constitutive up-regulation of MDR transporters, which is independent of drug exposure [163]. Neoplastic growth in such tissues can be an explanation for the innate MDR.

1.2.1. Responsible mechanisms for MDR

The responsible mechanisms behind emergence of MDR can be categorized into cellular and non-cellular mechanisms. The non-cellular mechanisms include the geometric resistance of vasculature, increased interstitial fluid (due to EPR phenomenon), reduced drug access to deeper parts of solid tumors, insufficient nutrients and oxygen (which causes stress and triggers different cellular mechanisms), existence of non-cycling cells (that are resistant to drugs dependent on cell proliferation), and acidic environment [164]. The cellular mechanisms play the major role in MDR and are categorized as: Reduced uptake or enhanced efflux of anticancer drugs, Overexpression of Detoxifying enzymes, Underexpression or mutation of anticancer drug targets, and Inhibition of apoptotic pathways.

1.2.1.1. Reduced uptake or enhanced efflux of anticancer drugs– The ATP-binding cassette (ABC) family of membrane transport ATPases are one of the largest membrane bound protein families that can reduce the cellular or nuclear accumulation of drugs (Table 1.4) due to attenuated uptake, altered intracellular distribution or enhanced efflux of the anticancer drug [165]. The ABC family of transporters has 48 members in human, which share sequence and structural homology. While this class of transporters has a large number of members, only 10 or so are reported to confer the drug-resistant phenotype [166]. Among the ABC transporters involved in MDR are P-glycoprotein (P-gp), lung resistance protein (LPR), breast cancer resistance protein (BCRP) and multidrug resistance associated protein (MRP), which can be overexpressed in malignant cells and serve to pump anticancer drugs out of the cell, resulting in intracellular drug

levels that is necessary for effective therapy [164]. MRP has been described as a glutathione S-transferase (GST) pump capable of transporting organic anion drug conjugates as well as intact anticancer drugs [167]. MRP, which was isolated as a transmembrane glycoprotein in non-P-gp expressing small lung cancer DOX resistant cell lines, is an asymmetrical molecule with eight subunits and four membrane-spanning domains [168].

Table 1.4 – ABC transporters involved in drug resistance [169]

Gene	Protein/ alias	Chemotherapeutic drugs effluxed by transporter	Other drugs and substrates
ABCA2	ABCA2	Estramustine	–
ABCB1	PGP/ MDR1	Colchicine, doxorubicin, etoposide, vinblastine, paclitaxel	Digoxin, saquinivir
ABCC1	MRP1	Doxorubicin, daunorubicin, vincristine, etoposide, colchicine, camptothecins, methotrexate	Rhodamine
ABCC2	MRP2	Vinblastine, cisplatin, doxorubicin, methotrexate	Sulfinpyrazone
ABCC3	MRP3	Methotrexate, etoposide	–
ABCC4	MRP4	6-mercaptopurine, 6-thioguanine and metabolites; methotrexate	PMEA, cAMP, cGMP
ABCC5	MRP5	6-mercaptopurine, 6-thioguanine and metabolites	PMEA, cAMP, cGMP
ABCC6	MRP6	Etoposide	–
ABCC11	MRP8	5-fluorouracil	PMEA, cAMP, cGMP
ABCG2	MXR/ BCRP	Mitoxantrone, topotecan, doxorubicin, daunorubicin, irinotecan, imatinib, methotrexate	Pheophorbide A, Hoechst 33342, rhodamine

1.2.1.2. Overexpression of Detoxifying enzymes– Altered activity of specific enzymes can decrease the cytotoxicity of drugs independent of intracellular drug concentrations. Glutathione S-transferase is an enzyme involved in xenobiotic detoxification. Specifically, biotransformation processes catalyzed by GST conjugate organic molecules with glutathione (GSH), resulting in excretable polar molecules [164]. The GSTs are extensively involved in the metabolic biotransformation of many anticancer drugs. Among these are nitrogen mustards, such as BCNU, and cyclophosphamides. In addition to GST, the cellular regulation of the thiol tripeptide, GSH, also appears to play a key role in detoxification and cellular repair following the damaging effects of DOX and

alkylating agents. Increases in GSH levels have been observed in many alkylating agent-resistant cell lines [170, 171].

1.2.1.3. Underexpression or mutation of anticancer drug targets– Topoisomerase is an important target for anticancer drugs. Two types of topoisomerase have been shown to be present in all eukaryotic cells. Type I topoisomerase, a monomeric 100-kDa protein, serves to alter DNA topology via single strand break, while topoisomerase type II alters DNA topology by causing transient double strand breaks. Both enzyme classes are intrinsically involved in the processes of DNA replication [164]. DOX and etoposide specifically target topoisomerase II [172], while camptothecin analogs target topoisomerase I. Cells become resistant to topoisomerase II inhibitors such as DOX and etoposide due either to the under-expression of topoisomerase II or topoisomerase II gene mutations. Reduced activity of topoisomerase II as well as reduction in topoisomerase II mRNA levels has been shown to cause cellular resistance to topoisomerase II inhibitors. Topoisomerase II gene mutations can also occur, where enzyme synthesis reduces following topoisomerase II gene transcription [173]. A compensatory overexpression of topoisomerase I has been observed in cells resistant to topoisomerase II inhibitors, where cells have reduced expression of topoisomerase II [174].

1.2.1.4. Inhibition of apoptotic pathways– Anticancer drugs typically induce programmed cell death or apoptosis. This form of cell death is characterized by nuclear condensation within cells, leading to DNA fragmentation caused by endonucleolytic cleavage of genomic DNA. The decision, whether a cell continues through cell cycle or

undergoes apoptosis, is dependent upon a complex interplay of a team of genes and proteins that exert a regulatory role in cellular events. It has been suggested that the tumor suppressor gene, p53, not only plays a key role in inducing cell cycle arrest in G_1 and apoptosis following DNA damage caused by anticancer drugs, but also in the regulation of expression of downstream proteins, B-cell lymphoma-2 (*bcl-2*) and bax [175]. The ability of cells to undergo apoptosis has been linked to the formation of hetero- and homo-dimers generated via bcl-2–bax interactions. For example, bax–bcl-2 heterodimers as well as bax homodimers promote apoptosis, whereas apoptosis is inhibited when *bcl-2* forms homodimers. Resistance may, therefore, develop with the loss of genes required for cell death such as p53 or overexpression of genes that block cell death. *Bcl-2* is a gene that plays a key role in the regulation of cell death pathways. *Bcl-2* serves to protect the cell from stimuli causing cell death, such as UV or gamma radiation, tumor necrosis factor, or drugs that induce free-radical production. *Bcl-2* can confer cellular resistance to the cytotoxic effects of a number of anticancer agents including DOX, paclitaxel, etoposide, camptothecin, mitoxantrone and cisplatin. When *bcl-2* is overexpressed and contributes as a resistance mechanism, it has been shown that the anticancer drugs promote cell cycle arrest; however, their effects are cytostatic rather than cytotoxic [176].

1.2.2. P-glycoprotein (P-gp)

P-glycoprotein is the most studied member of ABC transporters that can bind to a large variety of hydrophobic compounds with neutral or positive charge including several

anticancer agents. In fact, classic resistance to the cytotoxic drugs has most often been linked to the overexpression of P-gp [166].

1.2.2.1. Structure- P-glycoprotein is the 170-kD protein product of the human *MDR1* gene [177] (Mdr1a in mice). It is a dimer consisting of 1280 amino acids with 12 transmembrane segments and 2 adenosine 5'-triphosphate (ATP)-binding domains [178]. P-gp can be viewed as two half molecules or four distinct domains: two highly hydrophobic integral membrane domains and two hydrophilic nucleotide-binding domains (NBDs) located at the cytoplasmic face of the membrane (Figure 1.8). The amino acid sequences of the two half molecules are closely related to each other suggesting a pseudosymmetry to the protein structure. The two half molecules are separated by a highly charged 'linker' region which is phosphorylated at several sites by protein kinase C.

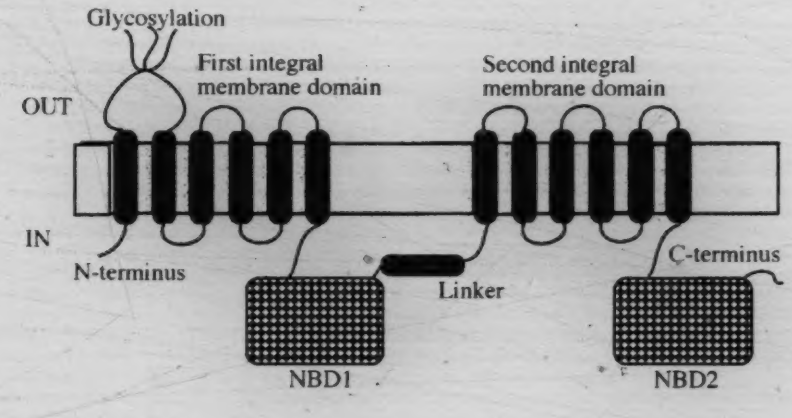

Figure 1.8 – Topological schematic map and domain organization of P-gp [179]

Binding of P-gp substrates to P-gp results in the hydrolysis of one ATP and a change in the shape of P-gp followed by the release of bound drug to the extracellular space. Hydrolysis of the second ATP restores the original conformation of P-gp[180]. In tumor cells expressing P-gp, this results in reduced intracellular drug concentrations which decreases the cytotoxicity of a broad spectrum of antitumor drugs including anthracyclines (e.g. DOX), vinca alkaloids (e.g. vincristine), podophyllotoxins (e.g. etoposide) and taxanes (e.g. Taxol).

The integral membrane domains of P-gp have two central roles in the transport process. First, they form the pathway through which solute is translocated across the membrane (parts of the nucleotide-binding domain can also, potentially, contribute to this pathway). Second, they provide the amino acid residues which interact directly with the substrate and form the substrate binding-site(s). Each integral membrane domain of P-gp consists of six membrane-spanning α-helices separated by hydrophilic loops, a total of 12 membrane-spanning α-helices per molecule (the 'six-plus-six' model) [179].

The two nucleotide-binding domains (NBDs) of P-gp share 30-40% amino acid sequence identity with each other and the equivalent domains of other ABC transporters. These domains bind and hydrolyze ATP and couple the hydrolysis of ATP to solute translocation across the membrane. Although the mechanism of energy transduction is unknown, it is likely to involve ATP hydrolysis-induced conformational changes: the binding of substrates to P-gp is known to stimulate ATP hydrolysis and conformational changes occur following drug binding and ATP hydrolysis [181]. The NBDs are located

at the cytoplasmic face of the membrane, consistent with a role in binding and hydrolyzing ATP. However, for several bacterial ABC transporters the NBDs are accessible to biochemical reagents from the extracellular surface of the membrane [182].

When viewed from the extracellular face of the membrane the protein is toroidal with a protein ring of diameter about 10 nm surrounding a large central pore (Figure 1.9.). The protein ring has two important features. First, it exhibits six-fold symmetry. Second, a 'gap' may be present in the protein ring, potentially providing access between the central pore and the lipid phase. The pore is large, about 5 nm in diameter, and is the entrance to a cup-shaped chamber within the membrane, presumably formed by the twelve membrane-spanning α-helices (Figure 1-8) [179]. An entry to this chamber from the lipid phase of the membrane is apparent, consistent with evidence that P-gp acts as a 'flippase' with drug substrates gaining access to their binding site(s) from the inner leaflet of the lipid bilayer [183]. This chamber narrows as it passes through the membrane and is closed at the cytoplasmic face of the membrane, presumably by sequences from the nucleotide-binding domains and the cytoplasmic loops separating the transmembrane α-helices. The two related halves of P-gp can be organized in true twofold symmetry (with helix 1 neighboring helix 12 and helix 7 neighboring helix 6), or in mirror symmetry (with helices 1 and 7 and helices 6 and 12 as neighbors). Cross-linking studies showing proximity between helix 6 and helix 12 suggest the latter organization [181]. The two intracellular lobes of P-gp which presumably correspond to the NBDs are asymmetrically organized in the structure and do not appear to interact with each other. Consistent with this, no interaction between the NBDs can be detected genetically using the yeast two-

hybrid system. However, the catalytic cycles of the two NBDs are coupled, and this has been taken to indicate that the two domains interact directly. It is possible that direct interactions between the NBDs only occur in the presence of ATP and/or substrate, and were therefore not apparent in the structure determined without these ligands [179].

A)

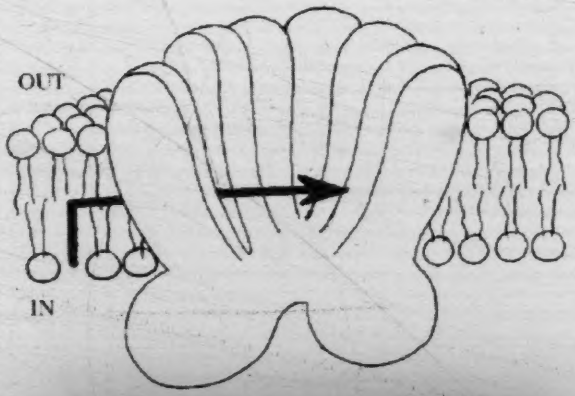

B)

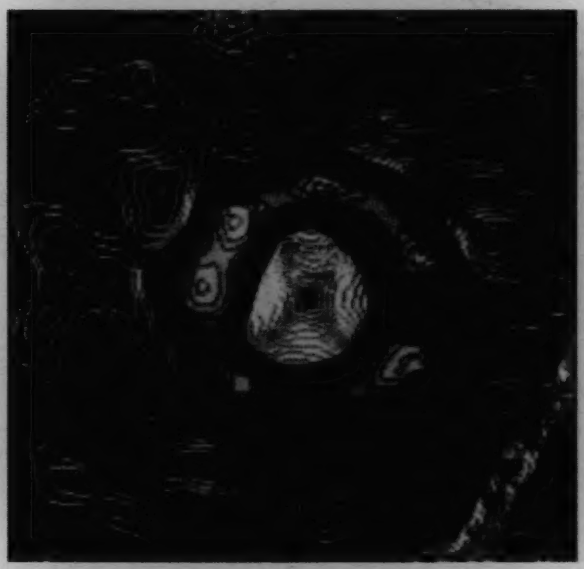

Figure 1.9 – P-gp structure; A) Cartoon based on electron microscopic images (courtesy of Kevin Hannavy); B) Projection map of P-gp from above the extracellular face of membrane (both from reference [179] with permission).

1.2.2.2. Distribution and role of P-gp in normal tissue- In addition to MDR cancer cells, P-gp is also expressed constitutively in many normal human tissues [184]. The expression of P-gp in some of the major organs associated with drug absorption, distribution, and elimination from the body has led to the hypothesis that P-gp might be part of a protective mechanism against a wide variety of potentially toxic substances, serving to limit distribution and facilitate elimination of P-gp substrates [185]. Determination of this distribution pattern and the exact location of P-gp leads to a better understanding of the role of this cell membrane pump.

1.2.2.2.1. Gastrointestinal (GI) tract

Absorption across the intestinal epithelium occurs either by facilitated or passive transport by a paracellular or transcellular mechanism [179]. The size, solubility, and lipophilicity of a drug molecule coupled with the effect of intestinal lumen pH, metabolism by intestinal flora, and hydrolytic and conjugative enzyme activity in the intestinal wall all affect intestinal absorption of a drug. P-gp and other transporters (e.g., MRP1) have been shown to be involved in modulating the absorption and/or intestinal elimination of drugs. P-gp is located on the apical membrane of intestinal epithelial cells, oriented such that substrates are secreted from the epithelial cell into the intestinal lumen [186]. An interesting aspect of P-gp is the interaction with drug metabolizing enzymes, specifically the 3A4 isozyme of cytochrome P450 (CYP3A4). P-gp and CYP3A4 share many substrates and inhibitors and have a common tissue distribution [187]. The isozyme CYP3A4 accounts for approximately 70% of the total CYP activity in the intestine, and P-gp may act with CYP3A4 to create a cycling effect to reduce systemic exposure to

certain xenobiotics by giving repeated chances to the enzyme to metabolize the substrate [178].

1.2.2.2.2. Liver

Bile formation is an osmotically driven process dependent on transport of bile salts and organic anions. Phospholipids, cholesterol, and other organic endogenous and exogenous compounds are also transported into the bile. Hepatocytes and cholangiocytes (bile duct epithelial cells) are the two cell types involved in bile formation and function. Hepatocytes contain over 10 known transport proteins and ion channels that are involved in bile formation and biliary secretion of endogenous and exogenous substrates. The sinusoidal (basolateral) membrane of the hepatocyte contains a number of transport proteins responsible for the uptake of cations, anions, and bile salts into the hepatocyte from the blood supply. The canalicular (apical) membrane contains a unique set of transport proteins responsible for transporting cations, anions, phospholipids, and bile salts from the interior of the hepatocyte into the canalicular lumen. P-gp is located on the canalicular membrane and functions to transport substrates into the canalicular space from the interior of the hepatocyte [188]. If the fate of a compound involves elimination by means of P-gp mediated biliary excretion, it must first traverse the sinusoidal membrane of the hepatocyte. Once in the hepatocyte, the compound may be sequestered and/or trafficked to the canalicular membrane, where P-gp will transport the compound into bile; ultimately, the compound may be reabsorbed from the intestine or eliminated in the feces. P-glycoprotein also may function to transport drug metabolites into bile [178].

1.2.2.2.3. Kidney

Renal clearance is a major route of elimination for many drugs. Three processes govern renal clearance: filtration, secretion, and re-absorption. Recent evidence suggests that P-gp plays a key role in the renal elimination of certain substrates by means of active secretion into the urine. P-gp is expressed on the apical (luminal) side of kidney proximal tubule cells and may be in other portions of the nephron, such as the loop of Henle [189]. Non-filtered substrates must cross the basolateral membrane (similar to the situation in the liver), either by diffusion or carrier-mediated processes, to interact with P-gp. In addition to increasing the direct flux of drugs from blood to urine [190], P-gp may limit re-absorption of substrates that are filtered at the glomerulus. The presence of P-gp on the luminal membrane of the kidney, where it transports substrates from the renal cell into urine, is consistent with a general protective role for the transporter [178].

1.2.2.2.4. Blood brain barrier (BBB)

Many drugs exert their pharmacologic effect and/or toxicity in the central nervous system (CNS). The BBB, which includes endothelial cells lining the brain capillaries, represents an important physical, biochemical, and transport barrier that serves to limit the access of many xenobiotics to the CNS [191]. Compared with vascular endothelial cells in other parts of the body, the endothelial cells of the BBB have narrow tight junctions with low paracellular transport, reduced pinocytotic activity, and specific transporters for the uptake of nutrients and extrusion of numerous compounds [192]. Although it is generally assumed that highly lipophilic drugs will achieve high concentrations within the CNS by passive diffusion across cell membranes, numerous

lipophilic agents penetrate the CNS poorly (e.g., loperamide, vinblastine, etoposide). Most of these compounds are substrates for P-gp [193]. The localization pattern of P-gp within the CNS is consistent with a putative protective role by either limiting brain uptake or increasing efflux of P-gp substrates from the brain. Studies have revealed the presence of P-gp on brain microvessel endothelial cells, specifically on the luminal membrane [194]. The results of several studies suggest that modulation of P-gp function at the BBB can result in substantially altered CNS pharmacokinetics, efficacy, and toxicity profiles for P-gp substrates [178].

1.2.2.2.5. Hematologic cells

Functional P-gp has been found in several types of human and murine leukocytes and in pluripotent stem cells [195]. Leukocyte P-gp expression is heterogeneous, with substantial variability between and within cell subtypes. However, among hematologic cells, P-gp expression is highest in natural killer cells, $CD4^+$ and $CD8^+$ lymphocytes, and bone marrow progenitor cells. Although the function of leukocyte P-gp is unknown, roles for this transporter in cell-mediated cytotoxicity, cytokine secretion, and protection from toxic substances have been proposed [196]. P-gp expression in B cells has been reported to be intermediate compared to natural killer cells [197].

1.2.3. Role of P-gp in MDR

P-gp is one of the major transport proteins implicated in MDR in neoplastic tissues. In cancer tissue, P-gp functions as a drug export pump that decreases intracellular concentrations of numerous chemotherapeutic agents. Several mechanisms have been put

forward to explain this transport function of P-gp. The model of Higgins and Gottesman (1992) postulates that P-gp encounters xenobiotics in the inner leaflet of the plasma membrane and flips the agents to the outer leaflet (Figure 1.10), where they diffuse into the extracellular region. In the hydrophobic vacuum cleaner model proposed by Gottesman and Pastan, 1993, P-gp interacts directly with substrates in the plasma membrane and pumps them out of the cell [164] (Figure 1.10).

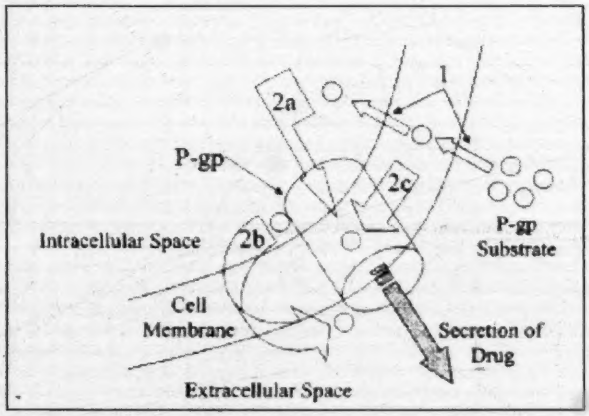

Figure 1.10– Proposed mechanisms of P-gp function in drug efflux: (1) passive drug uptake; (2a) hydrophobic channel between intracellular and extracellular space; (2b) "flip" mechanism; (2c) "vacuum cleaner model" [178].

A considerable number of cancers are either intrinsically resistant or exhibit treatment induced acquired resistance, which complicates efforts to successfully cause long-term regression. P-gp occurrence in clinical tumors has been extensively characterized and P-gp overexpression has been shown to occur both during diagnosis as well as during relapse [164]. P-gp expression has been shown to be the highest in tumors that arise from tissues known to physiologically express this protein, such as carcinoma of the colon,

kidney, adrenal gland, pancreas, and liver. Intermediate levels of expression have been reported in some neuroblastomas, soft tissue carcinomas, and hematological malignancies [198].

A fundamental role in regulating programmed cell death (apoptosis) has also been shown for P-gp. The exact mechanism by which P-gp inhibits apoptosis is not clear, however, different theories have been proposed, including interference with death-inducing-signaling-complex (DISC), inhibition of caspase 8 activation, an increase in pH, a decrease in the inner-leaflet-associated sphingomyelin (SM) pool, and inhibition of tumor necrosis factor (TNF)-induced ceramide production [177] (Figure 1.11).

1.2.4. P-gp inhibitors for chemosensitization of MDR tumors

The process of chemosensitization involves the co-administration of a P-gp inhibitor (MDR modulator) with an anticancer drug in order to cause enhanced intracellular anticancer drug accumulation via impairing the P-gp function. Numerous compounds have been shown to inhibit the drug efflux function of P-gp and therefore, reverse cellular resistance. The mechanism of this inhibition may be competitive (in which, the P-gp inhibitor itself is a substrate for P-gp), or non-competitive. P-gp inhibitors have been classified into three different generations.

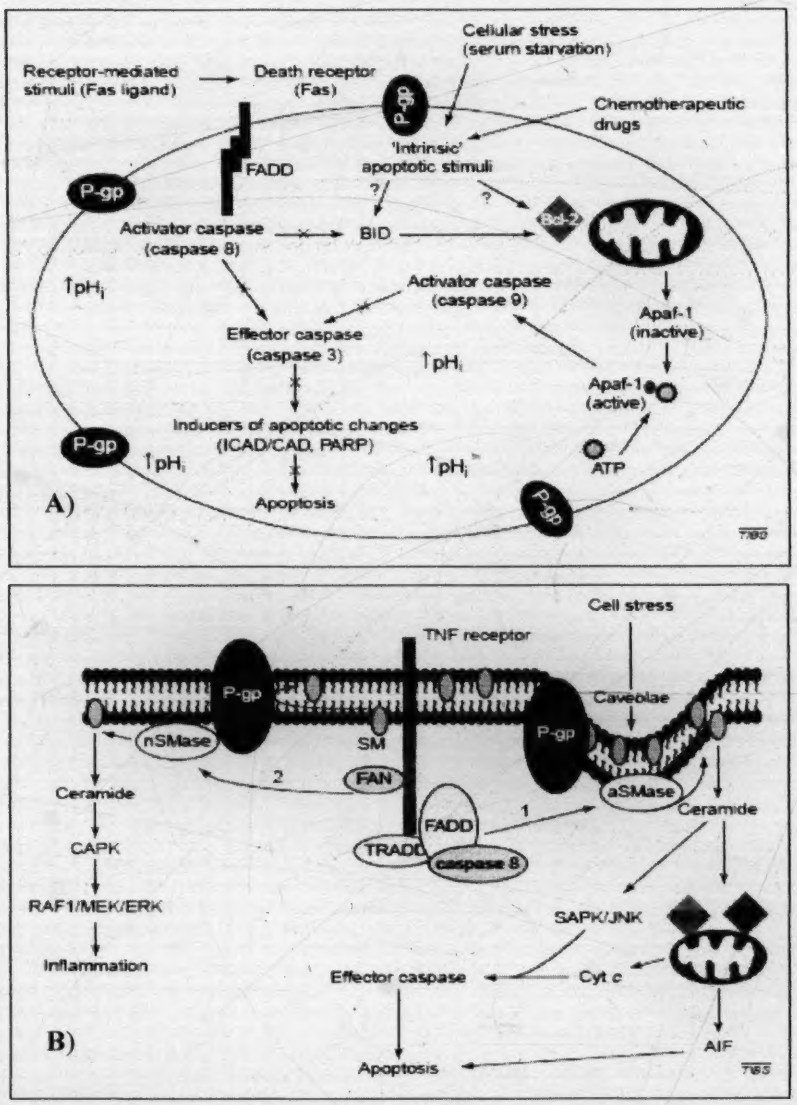

Figure 1.11– Regulation of apoptosis by P-gp: A) increase in pH and caspase 8 pathway (activated by Fas-associated death domain, FADD) inhibition; B) movement of SM and decrease in ceramide production; Binding of tumor necrosis factor (TNF) to its receptor results in formation of a DISC that links downstream to the acid sphingomyelinase and to the SAPK/JNK and caspase pathways (pathway 1). The effects of TNF on proliferation and inflammation are mediated by the activation of neutral sphingomyelinase (nSMase) through the TNF-receptor-binding protein FAN (pathway 2). P-gp has been reported to be present inside sphingomyelin (SM)- and cholesterol-rich caveolae. P-gp-mediated movement of SM out of the inner leaflet of the plasma membrane might decrease ceramide production [177].

1.2.4.1. First generation- Tsuruo et al [199] were the first to demonstrate the ability of the calcium channel blocker, verapamil, to reverse MDR in 1981. Verapamil has enhanced intracellular accumulation of many anticancer drugs, including DOX in numerous cell lines [200]. Later, the same effect was observed for many other calcium channel blockers, as well as many other therapeutic agents originally designed for different therapeutic purposes, including CyA [201] and digoxin [190]. A property shared by most first generation agents is that the concentrations at which they reverse MDR are much higher than those required for their original therapeutic activity. These agents modulated MDR at very high concentrations, ranging from 5 to 50 μM. A number of these first generation MDR modulators displaying excellent MDR reversal activities *in vitro* have been tested in murine tumor models. The exact mechanism of action for this class is still not clear, and probably not specific. It has been shown that CyA and verapamil activity is at least partially related to their effect on P-gp-associated ATPase [202].

1.2.4.2. Second generation- Second generation modulators are more potent and considerably less toxic. For instance, the tiapamil analog, Ro11-2933 is effective at 1–2 μM concentrations compared to 5–10 μM required for verapamil [203]. The non-immunosuppressive analog of CyA, PSC 833, has also demonstrated superior MDR reversal efficacy in many experimental cell lines *in vitro* at a concentration of 0.5–2 μM [202]. Studies on the mechanism of action of PSC833 indicate a very high affinity for P-gp and inhibition of P-gp ATPase activity [202].

1.2.4.3. Third generation- Several MDR modulators have recently been developed using structure–activity relationships and combinatorial chemistry approaches targeted against specific MDR mechanisms. These agents exhibit effective reversing concentrations in the nanomolar range (20–100 nM), thus requiring low doses to achieve effective reversing concentrations *in vivo*. Examples include specific P-gp blockers such as cyclopropyldibenzosuberane LY 335979 [204], acridonecarboxamide GF 120918 [205], diketopiperazine XR9051 [206], diarylimidazole OC144-093 [207], as well as bispecific (both P-GP and MRP) chemosensitizers such as VX-710 and VX-853 [208].

1.2.5. Clinical trials on the use of P-gp inhibitors in MDR

In spite of promising *in vitro* results, many clinical studies show that MDR modulators have had little success *in vivo* (Table 1.5) [209-211]. The failure has been attributed to one or a combination of following possible reasons: I) Extensive distribution of the P-gp inhibitor throughout the body causes insufficient concentrations of MDR modulator at the tumor site. Therefore, plasma concentrations of these modulators usually exceed the toxic level before approaching the therapeutic levels in tumor [212], and less accessibility of the solid tumors can worsen the problem [213]. II) Pharmacokinetic interaction of anticancer drugs with MDR modulators due to non-specificity of P-gp inhibitor that can interact with CYP450 and inhibit the metabolism of the chemotherapeutic agent, and/or non-specific distribution of P-gp inhibitor that can block the biliary and renal clearance of anticancer drugs as a result of P-gp inhibition in non-target sites [214, 215]. The pharmacokinetic interaction usually forces clinicians to decrease the dose of anticancer drug in therapy regiments that may lead to under dosing of patients [216-219]. III) P-gp

inhibition in non-target sites may increase the accumulation of anticancer drugs in healthy tissues that express P-gp leading to intolerable toxicity by the anticancer drug in co-administration with P-gp inhibitor. IV) It is now known that more than one mechanism of resistance is present in any given resistant tumor cell. Therefore, administration of drugs acting on single resistance mechanisms may not be the best choice for MDR modulation [165].

Among commercially available P-gp inhibitors, CyA has shown the most affinity for P-gp *in vitro* [220, 221] and promises to reverse drug resistance in oncologic patients(Table 1.5.) [220]. It has been tolerated better than verapamil by cancer patients. In 226 patients with acute myeloid leukemia (AML) randomly assigned to sequential therapy with cytarabine and infusional doxorubicin (DOX), patients who received CyA had a slightly higher complete response (CR) rate (40% vs. 33%) but a significantly better recurrence free rate (34% vs. 9%) and overall survival rate (22% vs. 12%), after 2 years [222]. The CyA effect was more significant in MDR-1 positive patients (median survival, 12 vs. 4 months). Even when doses of cytotoxic agents were reduced 3-fold, remission of drug resistance has been observed in the CyA treated group [223]. The rate of complete remission increased and the frequency of resistance decreased with increasing anticancer agent serum levels in CyA treated patients **only**, and not in the control group who received elevated doses of anticancer drug without CyA [223]. Unfortunately, CyA affects the pharmacokinetics of anticancer drugs through inhibition of non-tumorogenic P-gp and blockade of cytochrome P-450 3A (CYP3A) [214, 215, 224, 225]. Clinical studies involving etoposide, paclitaxel (PXT) and DOX show a 2-fold increase in the

AUC of anticancer agent when co-administered with CyA and its analogue, PSC833 [226, 227].

Table 1.5 – Clinical trials with P-gp inhibitors [169]

Inhibitor	Limitations	Toxicity	Cancer tested	Clinical benefit in clinical trials?
Verapamil	Low potency	Hypotension	Multiple myeloma Breast cancer NSCLC SCLC	No Yes Yes No
Quinidine	Low potency	Gastrointestinal disturbance	Breast cancer	No
Cyclosporine A	Pharmacokinetic interaction	Nephrotoxicity	AML Multiple myeloma	Yes No
Valspodar (PSC833)	Pharmacokinetic interaction	Ataxia	AML	No*
Biricodar (VX710)	Pharmacokinetic interaction	Not known	None	Not known
Elacridar (GF120918)	Not known	Not known	None	Not known
Laniquidar (R101933)	Not known	Not known	None	Not known
Tariquidar (XR9576)	Not known	Not known	None	Not known
Zosuquidar (LY-335979)	Not known	Not known	None	Not known
ONT-093 (OC-144-093)	Not known	Not known	None	Not known
CBT-1	Not known	Not known	Not known	Not known

1.3. Cyclosporine A (CyA)

CyA is a highly lipophilic cyclic endecapeptide (with water solubility of 23 μg/mL) (Figure 1.12). It is originally derived from the filamentous fungus *Tolypocladium inflatum* [228]. The introduction of CyA to the market was a major advance in immunosuppression and led to significant improvements in the outcomes of organ transplantation [229]. CyA was introduced to market more than 25 years ago, and is still one of the most potent immunosuppressive agents available. It is also one of the most

effective P-gp inhibitors, and therefore, subject to many studies focusing on MDR modulation.

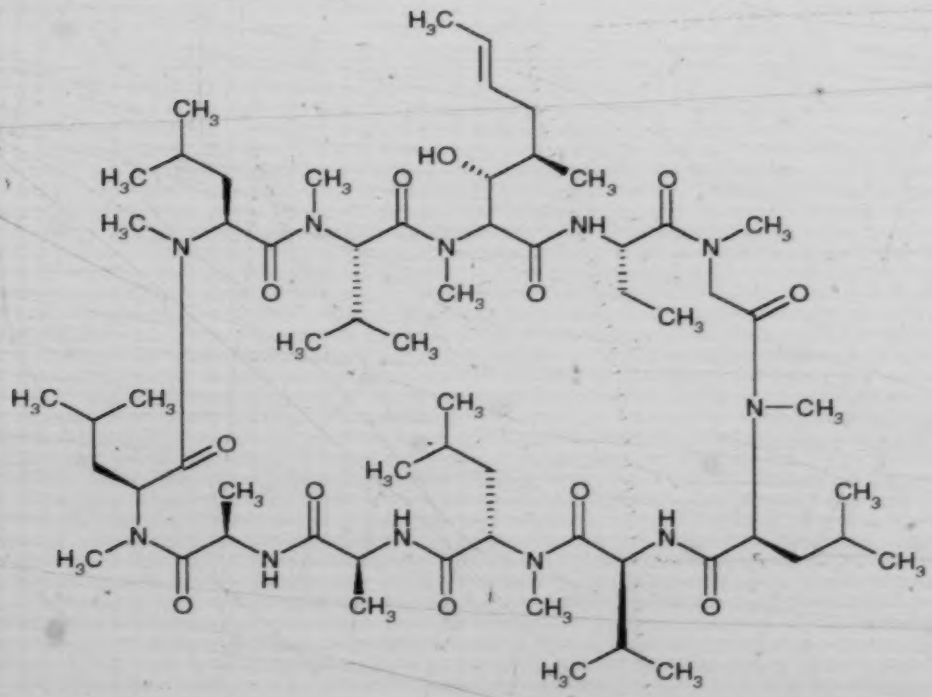

Figure 1.12 – Chemical structure of CyA (www.[illegible]abs.com/PRODFILE/A-C/C-6000.php4)

CyA is commercially available as oral formulations such as oil-based Sandimmune® that contains anhydrous alcohol and corn oil in the capsules; and alcohol, olive oil, and polyoxyethylated oleic glycerides in the oral solution. It is also available as microemulsion preparations, i.e., Neoral® that contains tocopherol and hydrogenated caster oil in both capsules and oral solution forms and Gengraf®, which has polyoxyl 40 hydrogenated castor oil in the oral solution and anhydrous alcohol and polyoxyl 30 castor oil in the capsules. Injectable formulation of CyA, i.e., Sandimmune®, contains Cremophor EL (surfactant) and ethanol (co-solvent) that solubilize 50 mg CyA/mL. For

i.v administration, Sandimmune® is diluted in sodium chloride for injection or 5% Dextrose to a final concentration of 0.5 – 2.5 mg/mL immediately before administration and infused at a dose of 5-6 mg/kg/day. While the therapeutic range for the immunosuppressive effect of CyA is 100-250 ng/mL [230], it has been shown that CyA is a potent P-gp inhibitor at concentrations ranging from 1000-2000 ng/mL [222].

1.3.1. Pharmacokinetics of CyA

The available data about pharmacokinetic parameters of CyA are not consistent. It has been shown that age, ethnicity, variability in gastrointestinal conditions (bile flow, concomitant ingestion of certain foods and medications), lipoprotein concentrations, and certain diseases like diabetes and cystic fibrosis can have a significant impact on CyA pharmacokinetic parameters [228]. A closer look at the different aspects of this data might help to understand the resulting complications better.

1.3.1.1. Absorption and distribution– The absorption of orally administered CyA is mainly in small intestine, slow, and variable, which makes it very difficult to predict the bioavailability of the drug. The absolute bioavailability of the oil-based formulation has been reported between 10 and 89%, with a mean value of 30% [231]. The development of Neoral® enhanced the bioavailability of CyA (measure by C_{max} and AUC) and minimized the effect of bile secretion on the absorption [232]. It also seems to increase the dose/AUC correlation and minimize the inter-patient variability in CyA pharmacokinetic [233]. The enterohepatic cycle seems to be insignificant, since only a small portion of the drug is excreted unchanged into the bile. It is extensively distributed

throughout the body. The apparent Vd in human varies between 4–8 L/kg [231]. The CyA levels are normally significantly higher in leukocyte-rich and fat-rich organs (especially liver) [234].

1.3.1.2. Metabolism– CyA is metabolized in the GI tract and liver, primarily by CYP3A4 member of the cytochrome P450 superfamily of mono-oxygenases [235]. CYP3A4 transforms CyA to more than 30 metabolites created by hydroxylation, demethylation, sulfation, and cyclization without ever disrupting the cyclic structure of CyA [236]. All of these metabolites display only minimal, if any, immunosuppressive activity [237]. Interindividual differences in the total CYP3A4 activity and the large number of drugs and endogenous substances capable of altering the function and expression of this family of enzymes can explain, in part, the significant differences in the CL of CyA [228].

1.3.1.3. Elimination– CyA is primarily excreted in bile (more than 90%) with less than 1% contribution of the parent drug [238]. Urine excretion accounts for about 6%, 0.15 of which is as the parent drug. Since metabolism plays the major role in the clearance of CyA, total clearance is almost equal to hepatic clearance. CyA does not have a high extraction ratio, so its clearance should be more sensitive to intrinsic enzyme activity and protein binding, and less sensitive to hepatic blood flow. Therefore, the negative correlation between age and CyA clearance has been explained by elevated levels of serum lipoproteins in the elderly [228].

1.3.1.4. Protein binding– CyA is highly bound to blood cells and plasma components. More than 50% of CyA in blood is bound to erythrocytes and about 33% to plasma lipoproteins [239]. Lipoproteins are macromolecular complexes of lipid and protein with the major function of transporting lipids (and highly lipophilic drugs) through the vascular and extravascular compartments. CyA is widely distributed among different classes of lipoproteins (mostly to low density lipoproteins [LDL] and high density lipoproteins [HDL]) [240]. The unbound fraction of CyA present in the plasma is typically less than 10% in humans, and up to 20% to 30% in rats [241].

1.3.2. The immunosuppressant activity of CyA

Cyclosporine A suppresses activated T- cells via calcineurin inhibition. Calcineurin is a phosphatase involved in the synthesis of proinflammatory cytokines and a sequence of events leading to allograft rejection [228]. Calcineurin inhibitors (e.g., CyA, tacrolimus, sirolimus) exert their cellular effect through binding to proteins called immunophilins [242] (Figure 1.13). Binding of CyA to immunophilins enhances the latter's affinity to calcineurin to from a complex that inhibits calcineurin's role in T-cell activation, which is the activation of nuclear factor of activated T-cell (NFAT) [243]. Members of NFAT family are also involved in transcriptional activation of interleukin-2 (IL2), IL4, and CD40L [244]. On the other hand, CyA treatment seems to be also associated with an up-regulation of transforming growth factor beta (TGF-β), which is a cytokine with significant immunosuppressive activities [245]. CyA has also been shown to interfere with p38 signaling pathway, necessary for the activation of AP-1, which is a transcription factor in T-cell activation process [246].

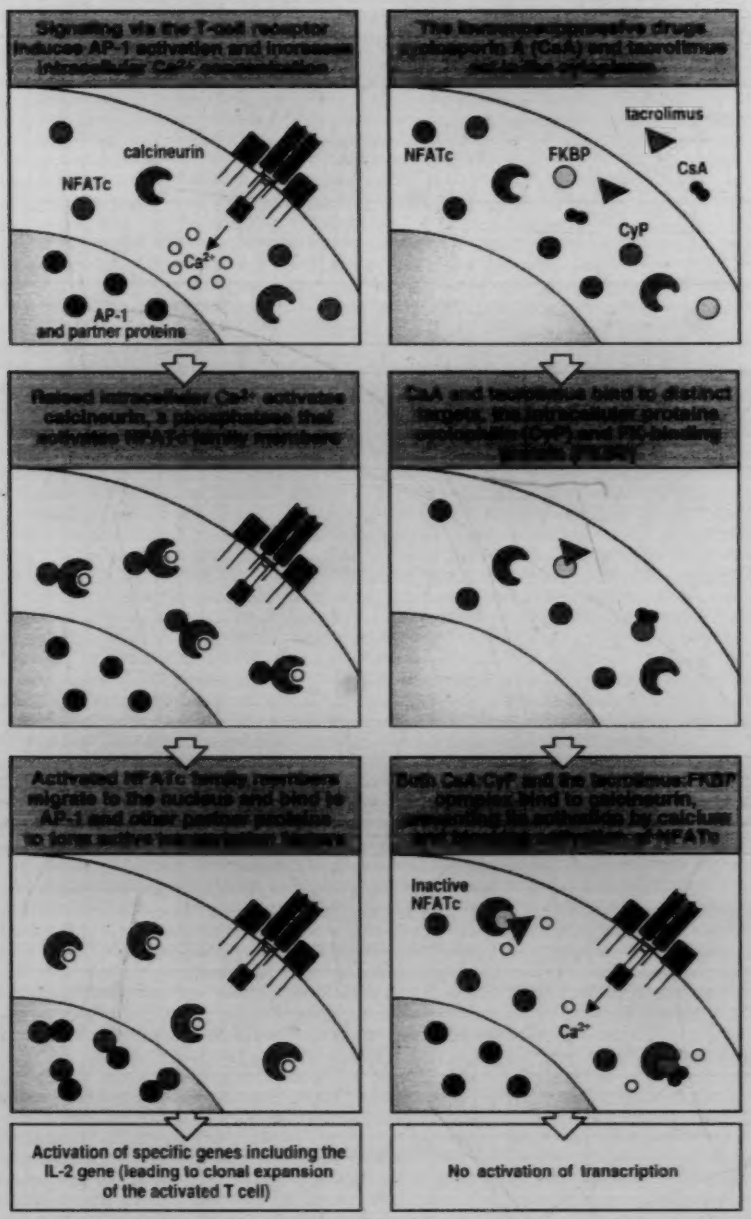

Figure 1.13– T-cell activation (left panels) and the mechanism of action of calcineurin inhibitors (right panels) [247]

1.3.3. Cyclosporine A as an MDR modulator

The chemosensitizing effect of CyA was first observed in the 1980s [248, 249]. Since then, many studies have shown the capability of CyA to reverse MDR in different resistant cell lines. In 1989, Foxwell et al showed the binding of CyA to P-gp by labeling P-gp and using ^{3}H-CyA [201]. Ten years later, using the same labeling technique in isolated perfused rat liver, Del Monache *et al* showed the role of P-gp in biliary excretion of CyA [250]. However, there are reports that deny the fact that cyclosporines are transport substrates for P-gp [251].

The effect of P-gp inhibitors on ATPase falls mainly in three different categories: a) compounds that stimulate ATPase activity at low concentrations but inhibit activity at high concentrations (such as vinblastine and verapamil); b) drugs that stimulate ATPase activity without inhibition (such as valinomycin); and c) drugs that inhibit both the basal and drug-stimulated ATPase activity (such as CyA) [185]. It has been shown that cyclosporines inhibit the P-gp associated ATPase activity. PSC-833 and other cyclosporine analogs are among the best reversers of P-gp. All these compounds are characterized by a high affinity (low *K*m, in the nanomolar range) for P-gp, and they are all strong ATPase inhibitors [252]. It has been shown that both CyA and PSC833 inhibit ATPase activity; however, the data on CyA being a substrate for P-gp are not clear. The latest reports consider PSC833 a substrate for P-gp, but a slow one, which means when it competes with a substrate, it will win because of a very high affinity. But since its transport rate is slower, it will slow down the turnover rate, which in turn will reflect in decreased ATPase activity [253].

CyA has entered many clinical trials with different cytotoxic agents for the reversal of MDR. In early 1990s, clinical trials on modulation of MDR by CyA combined with Vinblastine, daunorubicin, mitoxantrone, DOX, and etoposide showed increased risk of toxicity, increased bilirubin and leukopenia, which was accompanied by increased AUC for the cytotoxic agent, due to their decreased excretion and/or slowed metabolism [227]. Among several studies, one has showed a positive effect of CyA in acute myeloblastic leukemia by reducing resistance to daunorubicin and cytarabine, prolonging the duration of remission, and improving overall survival [222]. For more detailed discussion on the clinical trials of P-gp inhibitors in MDR please see pages 50 and 51.

1.3.4. Side effects associated with CyA administration

The clinical use of CyA has been restricted by severe toxic side effects of this drug on kidneys [254]. The toxic effect of CyA has been shown to be dose dependent [255]. With low-dose therapy, acute tubular nephrotoxicity is seldom encountered, and most nephrotoxic effects are reversible[256, 257].

Although CyA-induced nephrotoxicity has been extensively studied in different animal models, the exact mechanism of this toxicity is still in debate. CyA nephrotoxicity is characterized by renal vasoconstriction [258]. This might lead to ischemia and production of oxygen derived free radicals, which can exceed the capacity of the natural antioxidant system in tissue and cause damage [259, 260]. CyA is shown to induce renal failure and increase the synthesis of reactive oxygen species (ROS), thromboxane (TX) and lipid peroxidation products in kidneys. Satyanarayana *et al* have suggested that oxidative stress

[261, 262] and the renin-angiotensin system (RAS), and especially angiotensin II [263], the primary mediator of this system, may play a role in CyA induced nephrotoxicity. Functionally, the toxic effects of CyA on kidney in part take the form of a decrease in creatinine clearance (CLcr). Hepatotoxicity, hypertension, hyperplasia, and hirsutism are among other reported side effects of CyA.

1.4. Thesis proposal

1.4.1. Objective

To design and develop a long circulating delivery system based on polymeric micelles of MPEO-*b*-PCL that can solubilize, control the release rate, limit the toxicity, and enhance the effectiveness of CyA as a model P-gp inhibitor in the reversal of MDR.

1.4.2. Rationale and significance

MDR is the major cause for cancer chemotherapy failure. Over-expression of P-gp is one the most important mechanisms for MDR. Despite development of three generations P-gp inhibitors have shown little benefit in overcoming MDR in clinic. The negative therapeutic outcome is attributed to intolerable toxicities caused by the administration of P-gp inhibitors in cancer patients. P-gp inhibitors are hydrophobic and tend to distribute extensively in the body. As a result of nonspecific distribution, P-gp inhibitors may reach toxic levels in sensitive tissues by themselves, and/or enhance the accumulation and toxicity of P-gp substrates (e.g., anticancer drugs) in healthy organs that express P-gp (e.g., liver and kidney). Targeting of the site of action may increase the chance of accumulation of MDR modulator in tumor, protect the sensitive organs against the toxic

effects of the drug, reduce the risk of pharmacokinetic interaction with anticancer drug, and increase the chance of a more efficient reversal of resistance.

In this project the potential of MPEO-*b*-PCL micelles for the solubilization and site specific delivery of CyA, as a model P-gp inhibitor was evaluated. CyA has shown very promising results in clinical studies for MDR modulation. However, the pharmacokinetic interaction with the anticancer agents increases the risk of toxicity [214, 215, 224, 225, 264]. There are also evidence for the inhibitory effect of CyA and its analogue, PSC833, on membrane efflux pumps other than P-gp (such as MRP [265]). PSC833, the more potent analogue of CyA without the unwanted immunosuppressant effects, is probably the better choice; however, considering the similarity in the chemical structure of CyA and PSC833, and the fact that PSC833 is not commercially available, CyA seems to be the practical drug model for this project.

Ideally, the delivery system for CyA should be a safe replacement for Cremophor EL and be stable in blood circulation, to change the distribution of CyA and increase the accumulation of P-gp inhibitor in the tumor. Cremophor EL formulation causes hypersensitivity reactions and has been partially blamed for the nephrotoxic effects of the Sandimmune® [60], Liposomal formulations of CyA were shown to be unstable *in vivo* and released their CyA content upon i.v administration. As a results no change in the pharmacokinetic profile of liposomal CyA and its Cremophor EL formulation has been observed [266, 267]. MPEO-*b*-PCL micellar formulations of CyA may compensate for the short comings of both formulations. MPEO is known as a non-toxic polymer and

many studies have shown the biodegradable and biocompatible nature of PCL [44, 268-270]. Due to the very high hydrophobicity of PCL block, MPEO-b-PCL polymers have a very low CMC, and therefore a better chance of preserving their core/shell structure after i.v injection. On the other hand, high levels of CyA have been encapsulated in PCL nanoparticles (without MPEO modification), which reflect a compatibility and interaction between the PCL core and CyA [79, 271]. [159]. The interaction between encapsulated CyA and PCL core is expected to lead to a sustained mode of delivery for CyA from polymeric micelles.

1.4.3. Hypotheses

1. MPEO-*b*-PCL micelles are capable of encapsulating CyA at clinically relevant levels and control CyA release rate from micellar structures.
2. CyA-loaded MPEO-*b*-PCL micelles can serve as long circulating delivery systems for CyA changing its pharmacokinetic parameters and reducing the biodistribution the encapsulated drug in sites of drug toxicity (i.e., kidney).
3. Encapsulation of CyA in MPEO-*b*-PCL micelles can minimize the nephrotoxic effects of CyA.
4. Encapsulation of CyA in MPEO-*b*-PCL micelles can enhance the accumulation of this P-gp inhibitor in solid tumors, without jeopardizing the chemosensitizing effect of the encapsulated drug.

1.4.4. Specific aims

1. To develop polymeric micellar formulations of CyA (PM-CyA) and characterize these formulations for their size, drug loading, and release properties making comparisons with the commercially available i.v formulation of CyA, Sandimmune®.
2. To assess the pharmacokinetic and biodistribution profile of the micellar formulations compared to Sandimmune® in healthy animal models.
3. To evaluate the nephrotoxicity of PM-CyA in animal models.
4. To assess the distribution of PM-CyA in solid tumor bearing animal models and determine the efficacy PM-CyA in the reversal of MDR *in vitro*.

CHAPTER 2: EXPERIMENTAL PROCEDURES

2.1. Materials

Stannous octoate (96%) and biphenyl (99.5%) were obtained from Aldrich (Milwaukee, WI, USA). Methoxy polyethylene oxide (MPEO; average molecular weight of 5000 g/mol), ε-caprolactone, amiodarone HCl (98%), BSA, Cremophor EL, tetrazolium dye (MTT), poloxamer 407 (P407), and CyA (used as standard) were purchased from Sigma (St. Louis, MO, USA). Acetonitrile, methanol, and chloroform were supplied by Fisher Scientific (Nepean, Ontario, Canada). Sodium chloride injection 0.9% was obtained from Abbott Laboratories (Montreal, Quebec, Canada). Heparin sodium injection, 10,000 IU/mL was purchased from Leo Pharma Inc. (Thornhill, Ontario, Canada). Sandimmune® 50 mg/mL for intravenous administration (Novartis, Dorval, Quebec, Canada) was purchased from University of Alberta Hospital. Halothane BP was purchased from MTC Pharmaceuticals (Cambridge, Ontario, Canada). Methoxy polyethylene oxide (average molecular weight of 12,000 g/mol) was supplied by Polymer Source Inc. (Montreal, Quebec, Canada). CyA used to prepare micellar formulations was purchased from Wuhan Zhongxin Company, Hubei, China. Sucrose crystals were obtained from EM Science (Darmstadt, Germany). Triglyceride and total cholesterol kits were purchased from Diagnostic Chemicals Limited (Charlottetown, PE, USA). Cell culture media RPMI 1640, penicillin-streptomycin, fetal bovine serum, L-glutamine, and HEPES buffer solution (1 M) were purchased from CIBCO, Invitrogen Corporation (USA). All other chemicals were reagent grade.

2.2. Methods

2.2.1. Synthesis of MPEO-*b*-PCL block copolymers

Poly(ethylene oxide)-*block*-poly(ε-caprolactone) (MPEO-*b*-PCL) block copolymers were synthesized by ring opening polymerization of ε-caprolactone using MPEO (molecular weight of 5000 or 12,000 g/mol) as an initiator and stannous octoate as a catalyst [272]. MPEO (5 g), ε-caprolactone (different molar ratios to MPEO) and stannous octoate (molar ratio of 1:500 to ε-caprolactone) were added to a previously flamed 10 mL ampoule, nitrogen purged, then sealed under vacuum and put into the oven. The reaction product was dissolved in chloroform, precipitated and washed with an excess of cold methanol. The precipitate was collected by centrifuge and dried under vacuum oven. The molar feed ratio of monomer (ε-caprolactone) to initiator (M/I) was altered to achieve MPEO-*b*-PCL block copolymers with PCL average molecular weights of 5000, 13,000 and 24,000 g/mol. A nomenclature of 5000–5000, 5000–13,000, 5000–24,000, and 12,000–5000 (in which the left and right numbers define MPEO and PCL molecular weights, respectively) is used throughout the thesis to distinguish between different MPEO-*b*-PCL block copolymers used in the experiments.

2.2.2. Characterization of the block copolymers

^{1}H NMR spectrum of MPEO-*b*-PCL in CDCl3 at 300 MHz was used to assess the conversion of ε-caprolactone monomer to PCL and determine the number average molecular weight of the block copolymers [273]. ^{1}H NMR spectra were measured by a Bruker Unity-300 ^{1}H NMR spectrometer at room temperature, using deuterated N, N, dimethyl sulfoxide (DMSO-d_6) as solvent and tetramethylsilane as internal reference. The

percentage of ε-caprolactone conversion to PCL was determined comparing peak intensity of –O–CH2– (δ =4.223 ppm) for ε-caprolactone monomer to the intensity of the same peak for PCL (δ =4.075 ppm) in the ^{1}H NMR spectrum of MPEO-*b*-PCL. Gel permeation chromatography (GPC) was used to determine the average molecular weight and polydispersity of the synthesized micelles [274].

2.2.3. Preparation of MPEO-*b*-PCL micelles

A co-solvent evaporation method was used for the self-assembly of MPEO-*b*-PCL block copolymers [53-56]. The ratio of organic to the aqueous phase in the co-solvent evaporation method was changed to optimize the preparation method in terms of carrier size and encapsulation efficiency. Acetone the organic solvent of choice and the volume of organic solvent was either 0.5 or 1.5 mL, corresponding to a final 1:6 or 1:2 organic:aqueous phase ratio, respectively. MPEO-*b*-PCL (30 mg) was dissolved in acetone, and the solution was added in a drop-wise manner (1 drop/15 s) to 3 mL stirring aqueous phase (distilled water or normal saline). The mixture was then stirred at room temperature for 4 h. Vacuum was applied at the end to remove the remainder of the organic solvent.

2.2.4. Encapsulation of CyA in MPEO-*b*-PCL micelles

Drug encapsulation was accomplished by dissolving CyA in the organic solvent (2 or 3 mg/mL) and following identical procedures to the self-assembly condition. Again, different organic:aqueous phase ratios of 1:2 and 1:6 were tried for MPEO-*b*-PCL block copolymers with molecular weights of 5000–5000, 5000–13,000, 5000–24,000, and

12,000–5000. At the end of encapsulation process, the colloidal solution was centrifuged at 11,600×*g* for 5 min, to remove any CyA precipitate.

Two approaches were used to make the micellar solutions isotonic: a) addition of normal saline as the aqueous phase in the co-solvent evaporation method; b) addition of concentrated sucrose solution (0.255 mL of 1125 mg/mL sucrose aqueous solution) after completion of the micellization process.

2.2.5. Characterization of MPEO-*b*-PCL micelles

Mean diameter and polydispersity of self-assembled structures (with or without CyA) in aqueous media were defined using light scattering (3000 HS_A Zetasizer Malvern, Zeta-Plus ™ zeta potential analyzer, Malvern Instrument Ltd., UK). The concentration of block copolymer was 10 mg/mL of the final micellar solution. The value determined as the volume mean was reported as the size of the micelles in all experiments. Transmission electron microscopy (TEM) was also used to study the morphology of the prepared polymeric carriers [275].

Encapsulated levels of CyA were measured using reverse phase HPLC. An aliquot of the micellar solution in water was diluted 3-fold with acetonitrile to disrupt the micellar structure before injecting the samples to HPLC. The HPLC instrument consisted of a Chem Mate pump and a basic marathon auto-sampler (Spark Holland, Nederland). A C_{18} column (Hypersil BDS, 250×4.60 mm, 5 μ; Phenomenex, Torrance, CA, USA) was equilibrated with a mobile phase of acetonitrile:water (75:25, pH 3.1, adjusted using

phosphoric acid) at a flow rate of 1.2 mL/min. The column was heated at 72 °C using an Eppendorf CH-30 column heater. CyA concentrations were estimated by UV detection at 205 nm (Waters, model 481) after injection of 100 µL samples. CyA loading and encapsulation efficiency were calculated from the following equations:

$$\text{CyA loading (w/w)} = \frac{\text{amount of loaded CyA in mg}}{\text{amount of polymer in mg}}$$

$$\text{CyA loading (M/M)} = \frac{\text{moles of loaded CyA}}{\text{moles of polymer}}$$

$$\text{Encapsulation efficiency (\%)} = \frac{\text{amount of loaded CyA in mg}}{\text{amount of CyA added in mg}} \times 100$$

2.2.6. *In vitro* release study

A dialysis method was performed to evaluate the *in vitro* release rate for different CyA formulations involved in this study [30, 40, 48, 77]. CyA was dissolved in water at a concentration of 1 mg/mL with the aid of ethanol (40 % v/v). Aqueous solutions of Cremophor EL and polymeric micellar CyA (PM-CyA) formulations at a similar CyA concentration (corresponding to a concentration of 13 mg/mL for Cremophor EL and 8–11 mg/mL for block copolymers) were also prepared. One milliliter of each sample (ethanolic solution of CyA, Sandimmune®, or the PM-CyA formulation) was placed in a Spectra/Por dialysis bag (MW cut-off=12,000 – 14,000 g/mol). The dialysis bag was placed in BSA solution (4% w/v, 60 mL) while stirring at 37°C. Samples of 0.5 mL were taken from the BSA solution after definite time intervals, and replaced by identical volume of fresh media. This experiment was also performed at room temperature. Level of released CyA in each sample was measured by HPLC after drug extraction [276].

Amiodarone at a concentration of 10 μg/mL was used as internal standard. The internal standard solution (60 μL), deionized water (1.75 mL) and sodium hydroxide solution 1 M (200 μL) were added to release samples. Drug and internal standard were then extracted by ether–methanol 95:5 solution. After vortex mixing and centrifugation, the organic layer was removed and evaporated. The residue was solubilized in acetonitrile–phosphate buffer pH = 5.9 (65:35) and washed with hexane. Samples of 30 μL from the aqueous lower layer were injected into the HPLC system, (Chem Mate pump and auto-sampler) which was equipped with an LC1 column (Supleco) with a mobile phase of KH_2PO_4 (0.01 M), methanol and acetonitrile (25:50:25). The flow rate and column temperature were set at 1 mL/min and 65°C (Eppendorf CH-30 column heater), respectively. CyA concentrations were determined by ultraviolet (UV) detection at 205 nm (Waters 481). The calibration samples were prepared at a concentration range of 0.1–10 μg/mL. Each experiment was conducted in triplicate. The percentage of released drug for organic solution of CyA, Sandimmune®, and PM-CyA formulation was calculated and plotted versus time.

2.2.7. Optimization of CyA encapsulation

In order to achieve the optimum encapsulation efficiency for CyA in MPEO-*b*-PCL micelles, different starting CyA concentrations of 2 or 3 mg/mL (of organic phase), different organic:aqueous phase ratios, and different aqueous phases (distilled water and normal saline) were examined, and the final CyA level of loading and encapsulation efficiency was determined according the HPLC analysis method explained above.

Three different micellar formulations of CyA were prepared and examined for different studies throughout this manuscript: a) Dissolving CyA in acetone with an initial concentration of 2 mg/mL and adding acetone to normal saline with a ratio of 1:2, which will be referred as polymeric micellar CyA-low level of loading, **PM-CyA (L)**, throughout the manuscript; b) Dissolving CyA in acetone with an initial concentration of 3 mg/mL and adding acetone to normal saline with a ratio of 1:2, which will be referred as PM-CyA-intermediate level of loading, **PM-CyA (I)**, throughout the manuscript; c) Dissolving CyA in acetone with an initial concentration of 3 mg/mL and adding acetone to distilled water with a ratio of 1:6, which will be referred as PM-CyA-high level of loading, **PM-CyA (H)**, throughout the manuscript. In the formulations prepared with distilled water as the aqueous phase, sucrose was added to the polymeric micellar solution to achieve a final sucrose concentration of 95.76 mg/mL which is equal to isotonic sucrose concentration.

2.2.8. Determination of unbound fraction of CyA in rat blood

2.2.8.1. Sample preparation – For determination of CyA plasma protein binding *in vitro*, an erythrocyte vs. buffer or plasma partitioning method was used. Male Sprague-Dawley rats (Charles River Laboratories, Montreal, Quebec, Canada) were anesthetized using halothane/O_2 administered by anesthetic machine, and blood was collected by cardiac puncture into heparinized tubes. The collected blood (8 – 15 mL) was split equally into two tubes. Plasma was separated from blood cells by centrifugation of the whole blood at 2500 × g for 10 min. After removal of the plasma, the buffy-coat layers were discarded using a Pasteur pipette, and the blood cells were washed in an equal volume of isotonic

Sørenson's phosphate buffer (pH 7.4), followed by centrifugation at 2500 × g for 8 min. This washing procedure was repeated twice. After the third wash, the volume of total erythrocytes was estimated in each of the tubes using a calibrated tube, and either isotonic phosphate buffer (pH 7.4) or undiluted plasma was added to make a hematocrit (HCT) of 0.4 [277].

CyA was added to the erythrocytes suspended in buffer or plasma as Sandimmune® or different micellar formulations (details explained under the optimization of CyA encapsulation [2.2.7.]). The final concentration of CyA for all different formulations was 2.5 or 5 μg/mL. Erythrocyte suspensions were then incubated with CyA in quadruplicate at 37°C. For sampling plasma or buffer, blood was centrifuged at 2500 × g for 5 min. Samples of blood, plasma, and buffer were taken after one and two hours.

2.2.8.2. Determination of CyA levels – A similar HPLC method to what was used in the release studies was performed to determine the concentration of CyA in each fraction. Briefly, internal standard (amiodarone, 10 μg/mL), HPLC water, and sodium hydroxide (1 M) were added to samples, and CyA and internal standard were extracted from the mixture with ether:methanol (95:5). The organic layer was then removed and evaporated in vacuum (ISS110 Speedvac system, Thermo Savant, Milford, MA). The residue was then reconstituted in acetonitrile:Sørenson's phosphate buffer (pH 5.9) (65:35) and the solution vortexed with hexane. Samples of the aqueous lower layer were injected into the HPLC system (Waters 600 Multisolvent Delivery System and Waters 717 plus Autosampler, Milford, MA, USA) which was equipped with an LC1 column (Supleco,

Bellefonte, PA, USA) with a mobile phase of KH_2PO_4 (0.01M), methanol and acetonitrile (23:49:28). The flow rate and column temperature were set at 1 mL/min and 65°C (Waters temperature control module), respectively. CyA concentrations were determined by UV detection at 205 nm (Waters 486, Milford, MA, USA) based on calibration curve of different CyA concentrations ranging from 0.1 to 10 μg/mL. Corresponding blank drug-free blood, plasma, and buffer was used for the standard curve samples that were prepared at a concentration range of 0.1–10 mg/mL.

2.2.8.3. Measurement of the unbound fraction – Unbound fraction (*fu*) was determined using the equations explained by Schuhmacher et al [278]. The concentration of CyA in erythrocytes in erythrocyte-plasma samples (CE) and erythrocyte –buffer samples (CE*) was determined by the following equation:

$$CE = \frac{CB - Cp(1 - HCT)}{HCT} \qquad CE^* = \frac{CB^* - Cb(1 - HCT)}{HCT}$$

where CB and CB* are the concentration of CyA in the blood cell–plasma and blood cell-buffer suspensions, and Cp and Cb are the concentration of drug in the plasma and buffer. The partition coefficients for erythrocyte:plasma (Pp) and erythrocyte:buffer (Pb), and *fu* were determined by:

$$Pp = \frac{CE}{Cp},\ Pb = \frac{CE^*}{Cb},\ \text{and}\ \ fu(\%) = 100 \times \frac{Pp}{Pb}$$

2.2.9. Pharmacokinetic studies

2.2.9.1. Animals – All animal studies were performed according to the guidelines approved by Canadian Council of Animal Care (CCAC) and direct supervision of Health

Sciences Laboratory Animal Services (HSLAS), University of Alberta, using Sprague–Dawley rats (Charles River Laboratories, Montreal, Quebec, Canada), with body weights range of 250 to 350 g. All rats were housed in a temperature-controlled room with a 12 h light/dark cycle for at least one week prior to study. The animals were fed a standard rodent chow containing 4.5% fat (LabDiet1 5001, PMI nutrition LLC, Richmond, IN, USA). Free access to food and water was permitted prior to experimentation. The day before the pharmacokinetic experiment, the right jugular vein of all rats was catheterized with Silastic tubing (Midland, MI) under same anesthetic procedure explained for the unbound fraction experiments. Each cannula was filled with heparin (100 U/mL, diluted in normal saline). After surgery, animals were transferred to their regular cages and allowed free access to water, but not food overnight. The next morning, catheterized rats were transferred to metabolic cages and after assuring the effectiveness of cannula, dosing and blood sampling were performed [277, 279-281].

2.2.9.2. Procedure – Animals were randomly assigned to four different groups. In each group there were 4-6 rats receiving: a) CyA in Cremophor EL formulation, Sandimmune®, 5 mg/kg (diluted in 0.9% NaCl for injection); b) CyA in formulation PM-CyA (L), 2.5 mg/kg; c) CyA in formulation PM-CyA (I), 2.5 mg/kg; d) CyA in formulation PM-CyA (H), 5 mg/kg. Formulations were administered by a slow i.v injection over 60 seconds into the jugular vein cannula, immediately followed by 0.5 mL sterile 0.9 % normal saline to flush the cannula. At the first blood sample withdrawal, the first 0.2 mL volume of blood was discarded to avoid the drug residue in the cannula and to assure accurate estimation of CyA blood levels. Blood samples (0.15 – 0.2 mL) were

withdrawn from the cannula at approximate time points of 0.08, 0.33, 0.67, 1, 2, 4, 6, 8, 12, and 24 hours after the CyA administration . Each cannula was filled with heparin (100 U/mL) after each collection. Blood samples were stored at -20°C until HPLC analysis for CyA. Drug levels were assessed using the same HPLC method explained in section 2.2.8.2.

2.2.9.3. Pharmacokinetic data Analysis – To account for the difference in dose between different groups, blood, plasma and tissue concentrations for the test group (PM-CyA formulations) that were administered at a lower dose due to the limited loading efficiency, were normalized by multiplying each concentration to the ratio of injected CyA dose for Cremophor formulation over injected CyA dose for PM-CyA formulations. The pharmacokinetics of CyA have been shown to be linear at the administered CyA dose range of this study (≤5 mg/kg) in Sprague Dawley rats [282]. The elimination rate constant (λ_z) was estimated by linear regression of the blood concentrations in the log-linear terminal phase. In order to estimate the initial blood concentration (C_0) immediately after i.v injection, the linear regression of the log-linear initial state going through the first two time points was extrapolated to the time zero. The estimated C_0 was then used with the actual measured plasma concentrations to determine the area under the blood concentration–time curve (AUC). The AUC_{inf} was calculated using the combined log-linear trapezoidal rule for data from time of dosing to the last measured concentration, plus the quotient of the last measured concentration divided by λ_z. Noncompartmental pharmacokinetic methods were used to calculate mean residence time (MRT by dividing $AUMC_{inf}$ by AUC_{inf}) clearance (CL by dividing dose by AUC_{inf}), and volume of distribution (Vd by dividing CL by λ_z; and Vdss by multiplying CL by MRT) .

2.2.10. Biodistribution Studies

To assess the effect of formulation on the tissue distribution of CyA, rats were administered CyA in Cremophor EL formulation (Sandimmune® diluted 10-fold in 0.9% NaCl for injection) or PM-CyA (I) polymeric micelles at a similar dose to pharmacokinetic studies. Under light halothane anesthesia, each rat received the drug as i.v bolus doses by injection into the tail vein. At 5 min, or 1, 2, 6, 12, or 24 h after drug injection, each animal (n = 4 for each time point) was anaesthetized and exsanguinated by cardiac puncture. Heart, spleen, liver, kidney, fat, brain as well as samples of whole blood and plasma, were collected. In order to separate the plasma, blood samples where centrifuged at 2500 × g for 5 minutes and the supernatant plasma was saved for analysis. Tissue samples were blotted with paper towel, washed in ice-cold saline, bottled to remove excess fluid, weighed and stored in phosphate buffer (pH = 7.4) at -20 °C until assessed for drug concentration by HPLC. Tissue samples were homogenized in phosphate buffer before analysis. CyA levels were assessed using the same HPLC method explained in 2.2.8.2.

Tissue to plasma (Kp) concentration ratios were calculated by dividing CyA concentration in each tissue to CyA concentration in plasma and blood, respectively, for individual animals in the biodistribution studies.

2.2.11. Nephrotoxicity experiments

2.2.11.1. Animals – All animal studies were performed according to the guidelines approved by Canadian Council of Animal Care (CCAC) and direct supervision of Health

Sciences Laboratory Animal Services (HSLAS), University of Alberta, using Sprague–Dawley rats (Charles River Laboratories, Montreal, Quebec, Canada), with body weights range of 250 to 350 g. All rats were housed in a temperature-controlled room with a 12 h light/dark cycle for at least one week prior to study. The animals were fed a standard rodent chow containing 4.5% fat (LabDiet1 5001, PMI nutrition LLC, Richmond, IN, USA). Free access to food and water was permitted prior to experimentation. The day before experiments, the right jugular vein of all rats was catheterized with Silastic tubing (Midland, MI) under halothane anesthesia/O2, administered by anesthetic machine. The cannula was flushed and filled with 100U/mL heparin in 0.9% saline. After surgery, the rats were transferred to regular holding cages.

2.2.11.2. Treatments– Before each round of experiments a 24 h urine sample (collected in a metabolic cage) and a small blood sample was collected for each rat to assess the baseline renal function for each rat before entering the treatment phase. Animals were divided into five groups with 5 – 6 rats in each group. Group (1) received 20 mg/kg/day CyA as Sandimmune® (diluted with sterile normal saline) in three equal doses for 7 days via the cannula. Group (2) received the same dose and regiment of CyA as PM-CyA (H). Control animals received either Cremophor EL at a concentration of 260 mg/kg/day, equal to the dose of Cremophor EL administered as part of Sandimmune® in group (1); or unloaded MPEO-*b*-PCL micelles (at a concentration of approximately 87 mg/kg/day of polymer, equal to the dose of MPEO-*b*-PCL administered as part of PM-CyA (H) formulation in group (2); or normal saline. Injections were made into the cannula three times a day (6.67 mg/kg/dose).

All animals were weighed on daily basis at 0730 h. At the end of the 7-day administration period, another 24-h urine sample was collected. Animals were then anesthetized and exsanguinated by cardiac puncture.

2.2.11.3. Determination of CyA levels in blood and kidney after treatment period– Blood and kidney of rats that received CyA was collected for analysis, 3 hours after the last injection of CyA. The analysis method has been described in 2.2.8.2. Tissue samples were homogenized in phosphate buffer before analysis.

2.2.11.4. Assessment of renal function– Renal function was assessed by analyzing creatinine and urea levels in urine samples and creatinine, sodium, potassium and urea levels in blood samples using a Synchron LX® system at University of Alberta Hospital Laboratory Medicine and Pathology (accredited by the College of American Pathologists). Determination of creatinine levels was based on creatinine reaction with picric acid and formation of a red complex. A urea reagent and Synchron systems MULTI™ calibrator were used to measure the urea level concentrations by an enzymatic rate method. In this method urea is hydrolyzed to ammonia and glutamate dehydrogenase (GLDH) catalyzes the condensation of ammonia and α-ketoglutarate to glutamate with the concomitant oxidation of reduced β-nicotinamide adenine dinucleotide (NADH) to NAD. The Synchron LX system determines potassium and sodium ions concentration by indirect potentiometry utilizing ion selective electrodes. Creatinine and urea clearances

were calculated using the following equation, as an index of glomerular filtration rate (GFR):

$$Creatinine\ (or Urea)\ Clearance\ (mL/min/kg) = \frac{Urine\ Creatinine\ (or Urea)\ (mmol/L) \times Urine\ Volume\ (mL)}{Serum\ Creatinine\ (or Urea)\ (mmol/L) \times 24 \times 60 \times Body\ Weight\ (Kg)}$$

2.2.11.5. Histological studies – The kidneys were washed with ice-cold saline after extraction. For histological examination, the organ was fixed in 10% neutral buffered formalin solution and embedded in paraffin. Slices of 2-μm thickness were cut, deparaffinized, hydrated, and stained with hematoxylin-eosin. An additional section of each kidney was stained with periodic acid–Schiff (PAS). Sections were examined visually (magnification power 100-400×) for apical blebbing, interstitial vacuolization, hyaline casts, glomerular changes, arteriolopathy, and tubulointerstitial fibrosis in CyA-treated groups.

Each slide was assigned a code number before being sent off for microscopic assessment. The microscopic assessments were performed by a qualified veterinary pathologist, Dr Nick Nation, DVM, from HSLAS, University of Alberta. The assessor, who was blinded to the treatment groups and to the nature of the study design, was asked to look for qualitative evidence of microscopic changes consistent with renal toxicity. The sections (1 per kidney per animal) were each ~0.5 to 1 cm in diameter. Numerous fields were examined for evidence of consistent changes within the affixed kidney section.

2.2.12. Biodistribution of CyA loaded micelles in tumor bearing animals

2.2.12.1. Animal model – The C57BL/6 mice were chosen for the induction of tumor. Animals were maintained according to institutional guidelines approved by Health Sciences Animal Policy and Welfare Committee (HSAPWC). 3.5 $\times 10^6$ Lewis Lung Carcinoma (LLC) cells were injected subcutaneously to 12 mice with the body weight of 20-25 g. Tumor volume was calculated by measuring the length, width and depth of the tumor with calipers after one week.

2.2.12.2. Treatment– Animals were divided in two groups: 6 mice received Sandimmune® diluted to equivalent of 10 mg/kg CyA, and 6 mice received equal dose of CyA as PM-CyA (H) both via tail vein injection. After 6 hours animals were deeply anesthetized in CO_2 chamber and then exsanguinated by cardiac puncture. Samples of blood, tumor, kidney, liver, spleen, and heart were collected. Tissue samples were homogenized in phosphate buffer before analysis [41]. CyA levels in the samples were determined by the previously described HPLC method (see section 2.2.8.2).

2.2.13. Assessment of *in vitro* cytotoxicity of DOX in co-administration with CyA

3-(4,5-Dimethylthiazol-2-yl)-2,5-diphenyltetrazolium bromide (MTT, tetrazolium dye) method was used to evaluate the cytotoxicity of DOX against human breast cancer cell line MDA-MB435/LCC^{WT} (wild type) the mdr1-transfected MDR variant, MDA-MB435/LCC^{MDR} cells alone and in presence of CyA as Sandimmune® or PM-CyA (H), Cremophor EL and unloaded MPEO-*b*-PCL micelles. The latter two groups were used as controls. Toward this, 100 µL of growth medium suspending 4000 cells per well was plated out in 96-well plates and incubated overnight to allow cell attachment. The cells

were exposed to serial concentrations of DOX (dissolved in distilled water) with and without co-administration of CyA or controls for 48 h, followed by addition of 20 µL of MTT solution and incubation for another 3 h. Living cells metabolize MTT to a dark formazan dye. The cell culture media was removed by aspiration and replaced with 200 µL DMSO. The absorbance was measured by a UV/Vis spectrophotometer using a PowerwaveX340 microplate reader (BIO-TEK Instruments, Inc., Nepean, Ontario, Canada) at dual wavelengths of 570 nm and 650 nm. The mean and standard deviation of cell viability for each treatment was determined, converted to the percentage of viable cells relative to the control. The concentration of drugs required for 50% growth inhibition (IC_{50} values) was estimated from a plot of the percentage of viable cells versus log DOX concentration for each treatment as that giving a 50% decrease in absorbance as compared to controls [283-285] by fitting the straight line passing the 50% mark. The IC_{50} was calculated for the following treatment groups:

I. DOX only (0.04 – 5 µg/mL);
II. CyA (as Sandimmune®) only (0.16 – 20 µg/mL of CyA);
III. CyA (as PM-CyA [H]) only (0.16 – 20 µg/mL of CyA);
IV. Cremophor EL (2–260 µg/mL, the concentration range includes Cremophor EL concentration present in group treated with Sandimmune®);
V. Unloaded micelles (about 1-100 µg/mL), the concentration range present in group treated with PM-CyA (H);
VI. DOX (0.04 – 5 µg/mL) plus CyA as Sandimmune® (5 µg/mL of CyA);
VII. DOX (0.04 – 5 µg/mL) plus CyA as Sandimmune® (10 µg/mL of CyA);
VIII. DOX (0.04 – 5 µg/mL) plus CyA as PM-CyA (H) (5 µg/mL of CyA);

IX. DOX (0.04 – 5 μg/mL) plus CyA as PM-CyA (H) (10 μg/mL of CyA);

X. DOX (0.04 – 5 μg/mL) plus free CyA (5 μg/mL of CyA);

XI. DOX (0.04 – 5 μg/mL) plus free CyA (10 μg/mL of CyA);

XII. DOX (0.04 – 5 μg/mL) plus Cremophor EL (130 μg/mL, equivalent to Cremophor EL concentration present in 10 μg/mL Sandimmune® treated group);

XIII. DOX (0.04 – 5 μg/mL) plus unloaded polymeric micelles (about 50 μg/mL, equivalent to polymer concentration present in 10 μg/mL PM-CyA [H] group).

2.2.14. Statistical analysis

Compiled data are presented throughout the manuscript as mean±SD. The data were analyzed for statistical significance by unpaired Student's t-test except for cases specified in the following section.

In the tissue distribution studies, the AUC could not be determined in individual rats due to the destructive study design. Therefore, to permit an estimate of the variance associated with the composite mean AUC, the approach outlined by Bailer was utilized, which incorporates partial AUC and variability associated with each of the mean concentrations at each sampling point [286-288]. Pair wise comparisons of the AUC were then undertaken at α=0.05. The critical value of Z ($Z_{critical}$) for the two-sided test after Bonferroni adjustment was 2.24 [289], and the observed value of Z ($Z_{observed}$) was calculated as previously described .

In the nephrotoxicity experiments, the significance of changes for each individual rat in intragroup comparisons of means for renal function parameters before and after treatment period was analyzed by paired Student's t-test, whereas the significance of changes in these parameters for different rats in the intergroup comparisons of means were done by unpaired Student's t-test . The level of significance was always set at $\alpha = 0.05$. Differences in mean values of change in body wt, plasma potassium, CLcr, and CLur before and after experiments for different groups involved in the nephrotoxicity study were assessed and ranked using ANOVA followed by a post-hoc Duncan's Multiple Range test, using SSPS for Windows v.13 (Cary, NC, USA). Multiple comparisons for *fu* and pharmacokinetic parameters of different formulations were also assessed for significance using ANOVA. However, in this case, *Post hoc* analysis was performed using Dennett's T3 test using SSPS for Windows v.13 (Cary, NC, USA).

In the *in vitro* cytotoxicity experiments, intragroup comparisons of means for the IC_{50} of DOX was analyzed by unpaired Student's t-test, with the level of significance at $\alpha = 0.05$.

CHAPTER 3: RESULTS

3.1. Polymer synthesis and characterization

Synthesis of MPEO-*b*-PCL block copolymers through ring opening polymerization of ε-caprolactone by methoxy PEO (MPEO) in the presence of stannous octoate has been reported before [272]. In the present study optimal conditions for the preparation of MPEO-*b*-PCL block copolymers process were determined to be a temperature of 140 °C for 4 h and a catalyst to monomer ratio of 0.002. The molar ratio of ε-caprolactone (monomer, M) to methoxy PEO (initiator, I) was changed to prepare MPEO-*b*-PCL block copolymers having different degrees of ε-caprolactone polymerization. Prepared block copolymers were characterized for their average molecular weights by ^{1}H NMR (the results of GPC experiments are reported in [274]). Considering a MPEO molecular weight of 5000 g/mol, at M/I molar ratios of 44, 114 and 210, MPEO-*b*-PCL block copolymers with approximate PCL molecular weights of 5000, 13000 and 24000 g/ mol were synthesized. A nomenclature of 5000–5000, 5000–13000 and 5000–24000 is used throughout the manuscript to distinguish between the MPEO-*b*-PCL block copolymers. Another MPEO with molecular weight of 12,000 g/mol was also used to prepare MPEO-*b*-PCL block copolymers with the molecular weight of 12000–5000. Table 3.1 summarizes the characteristics of these synthesized polymers. As shown in this table, a good agreement between calculated and actual molecular weights was observed in most of the cases. Prepared block copolymers showed relatively narrow polydispersity indicating the absence of homopolymers.

3.2. Preparation and characterization of MPEO-*b*-PCL micelles

Micellization of MPEO-*b*-PCL block copolymers was achieved through a co-solvent evaporation method. A solution of MPEO-*b*-PCL block copolymers in acetone was added

to either water or normal saline (in order to prepare isotonic samples for the *in vivo* experiments) in a drop-wise manner followed by the evaporation of the organic solvent. The ratio of the organic solvent to the aqueous phase in the first series of experiments was 1:2. The micellar size and polydispersity index of the unloaded micelles prepared with different molecular weights of MPEO-*b*-PCL are summarized in Table 3.2. The differences in size between micelles prepared by polymers with different molecular weights was not statistically significant (unpaired student's t-test, $\alpha = 0.05$).

Table 3.1 – Characteristics of the prepared MPEO-*b*-PCL block copolymers

MPEO MW (g/mol)	PCL MW (g/mol)[a]	[M]/[I][b]	MPEO-*b*-PCL M_n[c]
5000	5000	44	9,984
5000	13000	114	23,008
5000	24000	210	30,035

a: Theoretical molecular weight
b: Monomer to initiator ratio
c: Number average molecular weight determined by ^{1}H NMR

Table 3.2 – Average size and polydispersity of unloaded MPEO-*b*-PCL micelles with different molecular weights (n=3-6).

Molecular Weight (g/mol)	Micellar Size ± SD (nm)	Polydispersity index*
5000-5000	87.5 ± 9.6	0.198
5000-13000	78.7 ± 11.8	0.111
5000-24000	99.8 ± 3.8	0.119

*: Determined by light scattering

3.3. Encapsulation of CyA in MPEO-*b*-PCL micelles

CyA reached a level of 1.277 mg/mL (CyA:polymer weight ratio of 0.128) in distilled water by MPEO-*b*-PCL micelles, and precipitated in water in the absence of the polymer (Table 3.3). Among MPEO-*b*-PCL block copolymers of different PCL block lengths, maximum CyA:polymer weight ratio was achieved by MPEO-*b*-PCL block copolymers with the molecular weight of 5000-13000. However, the molar CyA loading levels increased from 0.9 to 2.4 (mol CyA/mol polymer) with an increase in the molecular

weight of the PCL block from 5000 to 24000 g/mol. CyA encapsulation resulted in an increase in the average diameter of MPEO-*b*-PCL micelles with the molecular weight of 5000-13000. An increase in the initial level of applied drug from 2 to 3 mg did not increase the solubilized CyA levels (Table 3.4).

Table 3.3 – The effect of PCL molecular weight on CyA encapsulation in MPEO-*b*-PCL micelles (using water as the aqueous phase and 2 mg CyA initial level) (n=3-6).

MPEO-PCL	Loading level ± SD (mg/mg)	CyA loading ± SD (M/M)	Encapsulation efficiency ± SD (%)	Micellar size ± SD (nm)	Poly-dispersity index
5000-5000	0.104±0.015	0.9±0.1	52.2±7.4	100.3±9.0	0.157
5000-13000	0.128±0.013	1.9±0.2	63.8±6.6	98.6±13.2	0.127
5000-24000	0.099±0.001	2.4±0.3	49.5±6.6	102.3±17.2	0.152

The presence of salt in the aqueous phase in the co-solvent evaporation method did not have a significant impact on the final size of the prepared micelles (Table 3.4); however, this was proved to be a decisive factor for the encapsulation efficiency of CyA in the polymeric micelles. When water was replaced with normal saline to prepare isotonic polymeric micellar solutions of CyA for *in vivo* experiments, the efficiency of CyA encapsulation in MPEO-*b*-PCL micelles was reduced (Table 3.4). While in water, CyA reached an average aqueous concentration of 1.28 and 1.07 mg/mL applying initial CyA levels of 2 and 3 mg in the loading process, respectively, this level was reduced to an average concentration of 0.74 and 0.83 mg/mL when normal saline was used as the micellization medium. Premature precipitation of CyA during the micellization process in an acetone:normal saline solvent mixture in comparison to acetone:water environment might be the reason for lower levels of CyA encapsulation .

Table 3.4 – The effect of initial CyA level and ionic strength of the aqueous phase on the CyA encapsulation in MPEO-*b*-PCL micelles (n=3-20).

MPEO-PCL	Aqueous phase	Initial CyA level (mg/mL)	Loading level (mg/mg) ± SD	CyA Loading ± SD (M/M)	Encapsulation efficiency ± SD (%)	Micellar size ± SD (nm)	Poly-dispersity index
5000-13000	Water	2	0.128± 0.013	1.9±0.2	63.8± 6.6	98.6±13.2	0.127
5000-13000	Saline	2	0.074± 0.002	1.1±0.1	37.0±1.1	105.2±4.4	0.163
5000-13000	Water	3	0.107± 0.007	1.6±0.1	35.7± 2.4	118.0±16.7	0.144
5000-13000	Saline	3	0.083± 0.014	1.2±0.1	27.5± 4.8	118.0±16.2	0.161

Increasing the initial level of CyA from 2 to 3 mg increased the micellar size, regardless of the aqueous phase used (Table 3.4). However, the CyA loading level and the loading efficiency of the polymeric micelles for CyA changed in two different directions depending on the aqueous phase: Increasing the CyA initial level from 2 to 3 mg caused a decrease in loading level from 0.128 to 0.107 mg/mg when the aqueous phase was water; in saline, the same change in the initial CyA level increased the loading level from 0.074 to 0.083 mg/mg (α = 0.05, unpaired student's *t*-test). However, because of the higher starting CyA concentration, the 0.083 mg/mg loading level translated to a lower loading efficiency (α = 0.05, unpaired student's *t*-test, Table 3.4). The results of TEM experiments are reported in [275].

3.4. *In vitro* release

Lipid vesicles formed by lipid film method in PBS using disteryl phosphatydilcholine (DSPC) and cholesterol at a molar ratio of 3:1 had previously been used in our laboratories for *in vitro* release studies on polymeric micellar formulations [50, 290]. However, they were found to be poor recipients for CyA, possibly due to the weak

association of CyA with the lipid carrier (data not shown). Instead, BSA was used as a bio-mimetic recipient phase to maintain sink condition for the release of CyA from its vehicle. Encapsulated drug was separated from the recipient phase by a dialysis membrane having a molecular weight cut-off of 12,000–14,000 g/mol. Transfer of CyA through dialysis membrane to BSA was assumed to take place rapidly, and the release of CyA from its vehicle was assumed to be the rate limiting step in this process.

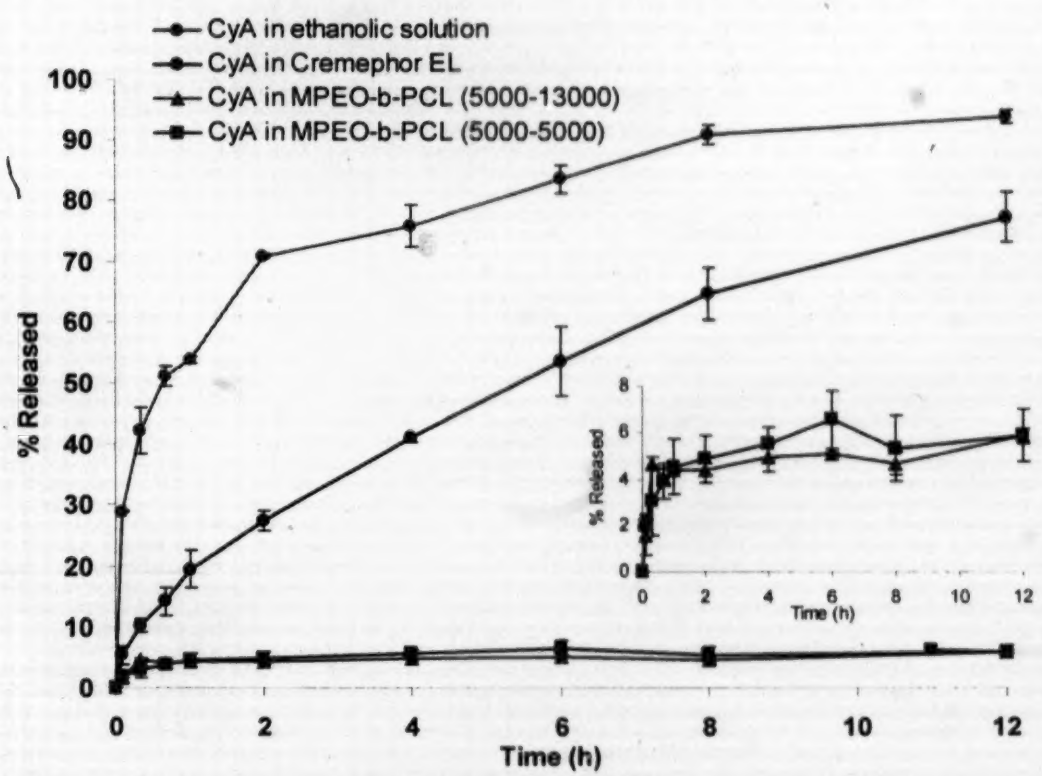

Figure 3.1 – The effect of solubilizing vehicle on the *in vitro* rate of CyA release; Data are presented as mean ± SD (n =3). Inset depicts the release profile of the polymeric micellar formulations using a larger y-axis.

In fact, 71% of unencapsulated CyA from its ethanolic solution was transferred to BSA within 2 h at 37 °C (Figure 3.1). The release of CyA from Cremophor EL micelles

(Sandimmune®) was found to be slower (27% of CyA was released in 2 h). In this stage of project, CyA-loaded micelles (with molecular weights of 5000-5000 and 5000-13000) using saline as aqueous phase and 3 mg CyA initial level (Table 3.4) were prepared and examined for their ability in sustaining the rate of CyA release. After 12 h, Cremophor EL formulation released 77% of its drug content, while polymeric micellar vehicles released only 5.8% of encapsulated CyA . There was no significant difference between the release profiles of the two CyA-loaded micellar formulations which were prepared using 5000-5000 and 5000-13000 MPEO-*b*-PCL in this experiment (Figure 3.1, inset).

3.5. Pharmacokinetics of CyA as Sandimmune and polymeric micellar formulation

Linearity in the standard curves was demonstrated for each of the tissues over the concentration range studied, and chromatograms were free of interference from endogenous components. At this stage, the polymeric micellar formulation of CyA used for pharmacokinetic studies was prepared using 3 mg CyA initial level and normal saline as the aqueous phase (row 4 in Table 3.4). The blood CyA concentration vs. time profiles observed for Sandimmune® and polymeric micellar CyA were similar in shape (Figure 3.2). A rapid decline in concentrations, representing a distribution phase, was observed for the first 2 h after dosing. This was followed by an elimination phase with $t_{1/2}$ of 9–12 h. However, CyA-loaded polymeric micelles yielded higher blood concentrations than the Cremophor EL formulation. Non-compartmental analysis of the blood concentrations showed a significant change in pharmacokinetic parameters of CyA in polymeric micelles in comparison to Sandimmune® (Table 3.5). CyA-loaded polymeric micelles provided significantly higher (6.1 fold) blood AUC compared to Sandimmune®. CyA-

loaded polymeric micelles also significantly decreased the volume of distribution (Vdss) and clearance (CL) of CyA by 10.0 and 7.6 fold, respectively. The terminal phase half life of CyA did not differ significantly between the two formulations.

Table 3.5– Non-compartmental pharmacokinetic parameters (±SD) of CyA after i.v administration of polymeric micellar CyA in comparison to Sandimmune®

	Sandimmune®	polymeric micellar CyA
AUC_{0-24} (μg.h/mL)	25.3 ± 7.64	167 ± 18.8[a]
AUC_{inf} (μg.h/mL)	32.7 ± 13.8	199 ± 20.9[a]
$t_{1/2}$ (h)	11.5 ± 4.58	9.40 ± 1.20
MRT (h)	14.4 ± 6.62	9.24 ± 2.06
CL (L/kg/h)	0.195 ± 0.131	0.0255 ± 0.00319[a]
Vd_{ss} (L/kg)	2.33 ± 0.785	0.232 ± 0.0425[a]

[a] Denotes significant difference between groups
Data for polymeric micelles is normalized to the injected dose of CyA in Sandimmune® and presented as mean ±SD (n = 4).

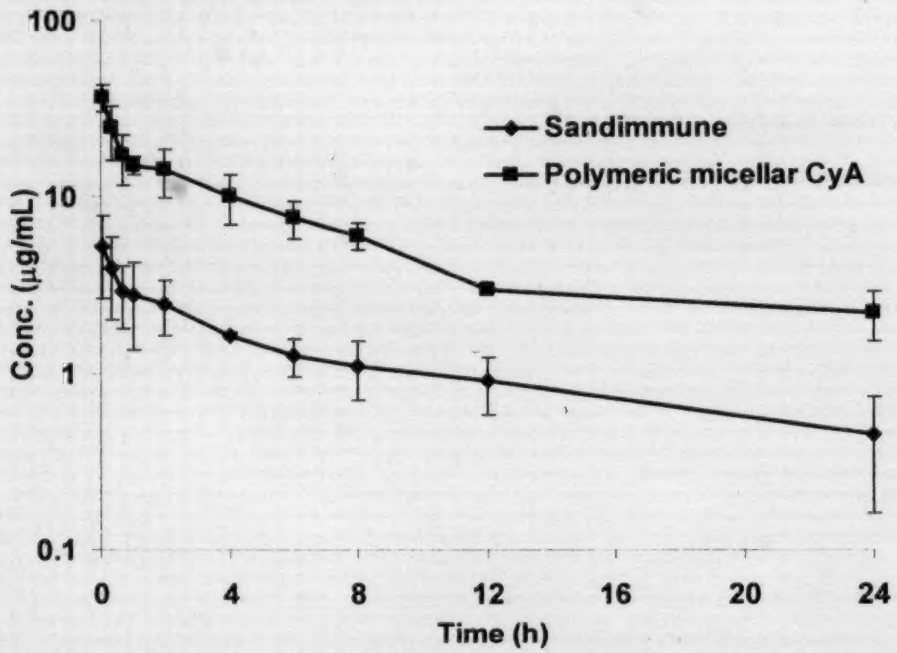

Figure 3.2 – CyA concentration–time profile in whole blood after i.v injection of Sandimmune® and polymeric micellar CyA. Data for PM-CyA is normalized to injected dose of CyA in Sandimmune® and presented as mean ± SD (n = 4).

3.6. Biodistribution

The biodistribution experiments were performed on Sandimmune® and polymeric micellar formulation of CyA (characteristics described in row 4 of Table 3.4). After single-dose i.v administration of CyA as Sandimmune®, the plasma and blood concentrations declined rapidly for 2 hours, after which the post-distributive phase appeared to be reached (Figure 3.3). In the tissues analyzed for drug content, CyA was detected in all tissue specimens at quantifiable concentrations except in the brain and fat. In those specimens in which CyA was detected, the order in mean AUC from highest to lowest in the Sandimmune® group was spleen > liver > kidney > heart > blood > plasma .

In contrast to the pattern observed for Sandimmune®, the corresponding order for AUC of CyA as part of polymeric micellar formulation in different examined tissue was blood>heart>plasma>liver>kidney>spleen. CyA-loaded polymeric micelles showed 1.5, 1.4 and 2.1-fold lower AUCs of CyA in liver, kidney and spleen, respectively, when compared to Sandimmune®. On the other hand, the AUC of CyA as part of polymeric micellar formulation was 5.7 and 4.9 times higher in blood and plasma, respectively.

Consistent with the pharmacokinetic experiments in rats in which serial blood collection was obtained (Figure 3.2, Table 3.5), in the biodistribution study the blood and plasma concentrations and resultant AUC of CyA were significantly higher for the micellar formulation (Figure 3.3, Table 3.6) than the available commercial formulation.

There were some significant formulation-related differences detected at some discreet CyA concentrations in kidney, spleen, liver and heart (Figure 3.3). Furthermore, in the tissues, a significantly lower AUC of CyA after administration of the polymeric micellar formulation was detected in spleen and kidney (Table 3.6). Heart, however, displayed a higher AUC after administration of the polymeric micellar CyA.

Variations in the Kp of CyA were followed over time for both formulations (Figure 3.4). The resultant profiles between the polymeric micellar formulation and Cremophor EL formulation were quite different. Compared to the commercial formulation, polymeric micelles showed much lower Kp values in kidney, liver, spleen and heart at all time points. Tissue to plasma ratios of polymeric micellar CyA remained below one for all organs up to 6 hours and gradually increased afterwards (Figure 3.4A-C), except for the heart in which a sharp raise after 12 hours has been observed (Figure 3.4D). In kidney, liver and spleen of Sandimmune® group, CyA showed a biphasic pattern with maximum values at one and 12 hours after injection for Kp. One hour after i.v injection of Sandimmune®, the Kp ratio was 7.4, 10.6, 13.3 and 2.1 for kidney, liver, spleen and heart, respectively, compared to Kp values of 0.4, 0.9, 0.6 and 0.5 for CyA-loaded polymeric micelles.

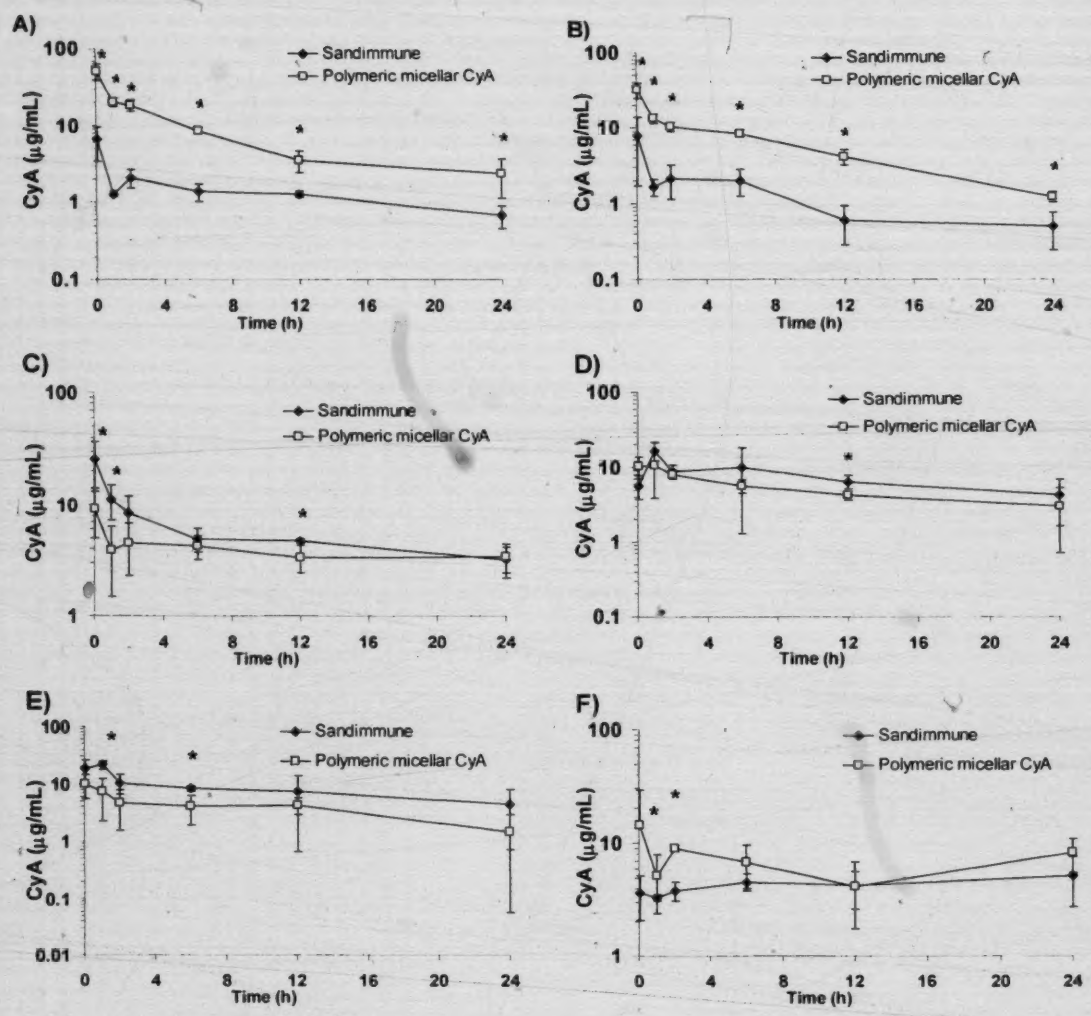

Figure 3.3– CyA concentration vs. time profiles in (A) blood, (B) plasma, (C) kidney, (D) liver, (E) spleen and (F) heart following i.v administration of polymeric micellar CyA in comparison to CyA in Cremophor EL (Sandimmune®) formulation in rats. Micellar data is normalized to injected dose of Cremophor EL and presented as mean ± SD (n = 4). * Denotes a significant difference between concentrations at that time point ($p<0:05$, unpaired t-test).

Table 3.6 – Area under the blood, plasma, and tissue concentrations versus time curve (±SD) for CyA after i.v administration of Sandimmune® and polymeric micellar CyA to rats (n=4). Data for polymeric micelles is normalized to injected dose of CyA in Sandimmune® and presented as mean ±SD (n = 4).

Tissue	Sandimmune® (μg·h/g)	Polymeric micellar CyA (μg·h/g)
Blood	31.8 ± 1.59	181 ± 8.7[a]
Plasma	29.5 ± 3.23	143 ± 5.61[a]
Kidney	128 ± 7.12	91.4 ± 6.12[a]
Liver	176 ± 27.5	119 ± 8.52
Spleen	188 ± 32.1	90.0 ± 10.1[a]
Heart	107 ± 13.8	155 ± 13.4[a]

[a] Denotes significant difference between groups

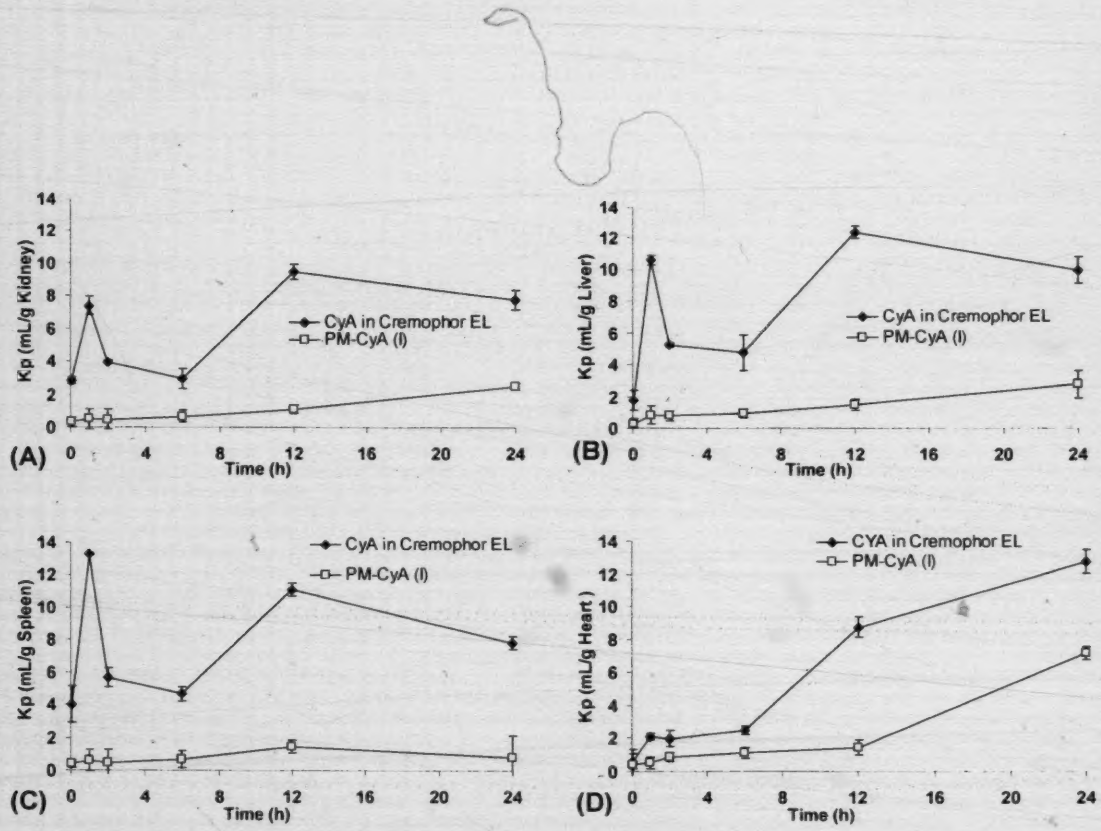

Figure 3.4 – kp vs. time profiles for CyA after i.v administration of polymeric micellar CyA and Sandimmune®. The data presents A) kidney, B) liver, C) spleen, and D) heart to plasma ratios. The data for polymeric micelles is normalized to injected dose of CyA in Sandimmune® and presented as mean ± SD (n = 4).

3.7. Modification of the characteristics of CyA loaded MPEO-*b*-PCL micelles

It has been shown that preparation method can have a significant impact on the *in vitro* and *in vivo* behavior of polymeric nanocarriers. Therefore, after the *in vivo* evaluation of CyA-loaded polymeric micelles, the need for the improvement of the micellar formulation justified a closer look at the details involved in the micellar preparation method, with the objective of increasing the loading efficiency of CyA in MPEO-*b*-PCL micelles, and improving the biological stability and performance of the prepared formulations in restricting CyA in blood circulation. Such formulation was expected to attenuate the CL, Vd of encapsulated CyA and restrict its access to kidneys while enhancing CyA concentration and residence time in blood circulation.

The volume fraction of the organic to aqueous phase was shown to affect the average diameter of self-associated nanocarriers. Application of lower acetone:water ratios led to the formation of smaller particles for 5000-5000, 5000-13000 and 12000-5000 MPEO-*b*-PCL block copolymer molecular weights under the study ($\alpha = 0.05$, unpaired student's *t*-test) (Table 3.7). Compared to other block copolymers, 12000–5000 MPEO-*b*-PCL micelles had a higher polydispersity and secondary peaks were present in the micellar population. However, the diameter of nanostructures formed from assembly of 5000–24000 MPEO-*b*-PCL was not significantly different between the 1:2 and 1:6 organic:aqueous phase ratios ($\alpha = 0.05$, unpaired student's *t*-test) .

Table 3.7- The effect of solvent/co-solvent composition on the average diameter and polydispersity index of unloaded MPEO-*b*-PCL micelles of different PCL molecular weights (n=3-6).

MPEO-*b*-PCL	Ratio (Organic: Aqueous)	Average diameter of particles ± SD (nm)	PI
5000-5000	1:2	68.5 ± 2.0	0.136
	1:6	50.2 ± 3.8‡	0.169
5000-13000	1:2	87.8 ± 9.4	0.111
	1:6	63.0 ± 4.0‡	0.142
5000-24000	1:2	93.6 ± 1.7	0.112
	1:6	92.0 ± 3.13	0.223
12000-5000	1:2	401 ± 47.7†	0.559
	1:6	92.3 ± 24.3‡*	0.382

‡: Significantly different from 1:2 ($p < 0.05$)
†: Secondary peak observed at approximately 60 nm (peak population < 25 % total population)
*: Secondary peak observed at about 300 nm (peak population < 25 % total population).

The effect of organic to aqueous phase volume ratio on the level of CyA loading in MPEO-*b*-PCL micelles and the diameter of loaded particles was also evaluated (Table 3.8). For 5000–13000 MPEO-*b*-PCL (similar to unloaded particles) the average diameter of CyA loaded micelles was significantly smaller when organic:aqueous phase ratio was 1:6 (unpaired student's *t*-test, $\alpha = 0.05$). Application of 1:6 organic to aqueous phase ratio also led to a higher polydispersity for the assembled structures (except for 12000–5000). Similar to unloaded carrier, CyA loaded 12000–5000 MPEO-*b*-PCL micelles have shown higher polydispersity in the micellar population. The average diameter of loaded 5000–24000 MPEO-*b*-PCL micelles was not significantly different for 1:2 and 1:6 acetone to water ratios.

Table 3.8- The effect of solvent/co-solvent composition on the encapsulation efficiency of CyA in MPEO-*b*-PCL micelles of different MPEO and PCL molecular weights.

MPEO-PCL	Ratio (Organic: Aqueous)	CyA loading ± SD (w/w)	Encapsulation Efficiency ± SD (%)	Average diameter of particles ± SD (nm)	PI
5000-5000	1:2	0.0969 ± 0.0270	32.3 ± 12.5	74.1 ± 4.80	0.206
	1:6	0.1678 ± 0.0036‡	55.9 ± 8.5‡	59.9 ± 6.27‡	0.231
5000-13000	1:2	0.1071 ± 0.0072	35.7 ± 2.4	118 ± 16.73	0.121
	1:6	0.2286 ± 0.215‡	75.9 ± 7.51‡	89.3 ± 15.30‡	0.207
5000-24000	1:2	0.1176 ± 0.0163	39.2 ± 8.5	105 ± 3.66	0.072
	1:6	0.1827 ± 0.0097‡	60.9 ± 3.2‡	101 ± 4.84	0.245
12000-5000	1:2	0.0351 ± 0.0247	11.7 ± 8.2	550 ± 175†	0.724
	1:6	0.1512 ± 0.0247‡	50.4 ± 8.2‡	384 ± 11.4‡	0.174

‡: Significantly different from 1:2 ($p < 0.05$)

†: Secondary peak observed at approximately 60 nm (peak population < 25 % total population).

The results also showed that organic to aqueous phase ratio to affect the final CyA loading in MPEO-*b*-PCL micelles (Table 3.8). CyA reached a final aqueous concentration of 2.3 mg/mL in the presence of 5000–13000 MPEO-*b*-PCL micelles when acetone was added to water at an initial organic to aqueous phase ratio of 1:6. However, a ratio of 1:2 led to a final aqueous CyA concentration of 1.07 mg/mL on average. A similar trend in CyA loading was observed for 5000–5000, 5000–24000 and 12000–5000 MPEO-*b*-PCL micelles (Table 3.8). Addition of acetone to water at 1:6 phase ratio led to 1.7, 2.1, 1.5 and 4.3-fold increase in CyA encapsulated levels in 5000–5000, 5000–13000, 5000–24000 and 12000–5000 MPEO-*b*-PCL micelles, respectively (Table 3.8, Figure 3.5) . An increase in the PCL molecular weight from 5000 to 13000 and 24000 led to an increase in the molar loading of CyA in polymeric micelles for the acetone:water ratio of 1:6 ($\alpha = 0.05$, student's *t*-test) (Figure 3.5). Identical results were observed with a ratio of 1:2 ($\alpha = 0.05$, student's *t*-test). A comparison between 5000–5000 and 12000–

5000 MPEO-*b*-PCL micelles showed no significant difference in molar CyA loading between these two structures (irrespective of the organic:aqueous phase ratio) .

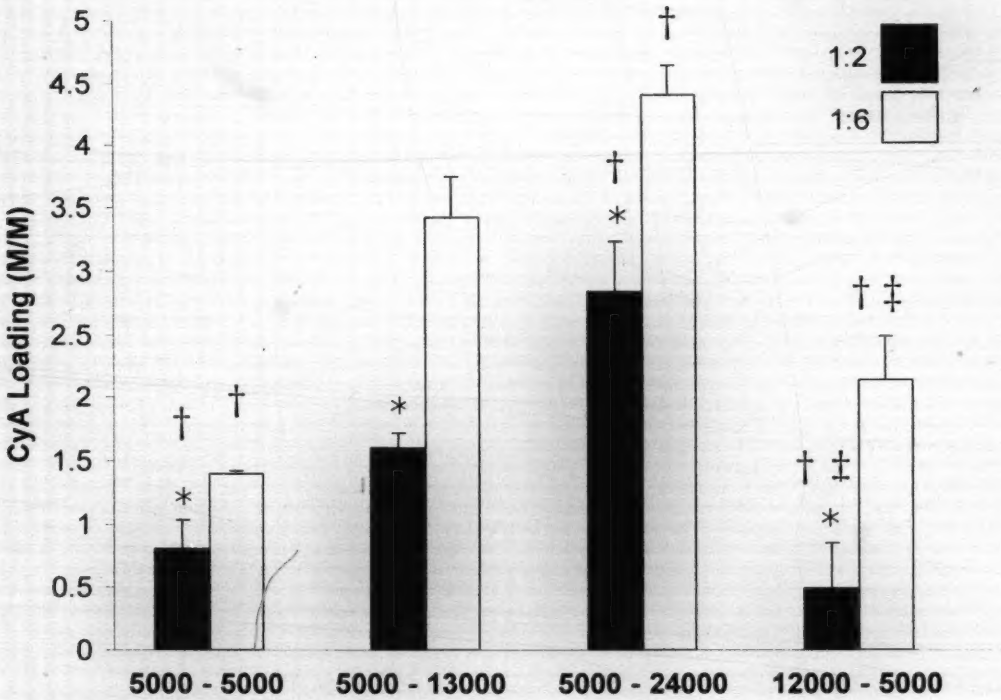

*: Significantly different from 1:6 ($p < 0.05$).
†: Significantly different from 5000-13000.
‡: Not significantly different from 5000-5000.

Figure 3.5 - The effect of solvent/co-solvent composition on molar CyA loading in MPEO-*b*-PCL micelles of different MPEO/PCL molecular weights. Data presented as mean +SD (n = 3-5).

3.8. Novel use of an *in vitro* method to assess the *in vivo* stability of CyA polymeric micellar formulations

3.8.1. The effect of CyA loaded levels on the *in vitro* release for different polymeric micellar formulations of CyA

Three polymeric micellar formulations containing different CyA to polymer loading levels were prepared in different stages of this project. The characteristics of these polymeric micellar formulations are described in Table 3.9. In order to assess the release profile of the different micellar formulations of CyA *in vitro*, and to compare their ability to control the release rate of the encapsulated drug, the *in vitro* release test was performed for PM-CyA (L), (I), and (H) denoted to low, intermediate and high level of CyA loading, respectively. CyA was rapidly released from Sandimmune®, with almost complete release being achieved by 24 h (Figure 3.6). In comparison, the different micellar formulations prepared for this study showed a significant ability to retain the drug (maximum 5.3% CyA released after 24 hours). However, no differences were discerned in the release pattern between these different polymeric micellar formulations (Figure 3.6, inset).

Table 3.9 – Characteristics of different PEO-*b*-PCL based nanocarriers prepared for this project. Values are recorded as mean ± standard deviation (n = 3 – 20).

Micellar nanocarrier	Aqueous phase	Organic: aqueous ratio	CyA initial level (mg/mL)	Average diameter (nm)	CyA loaded level (mg/mg)	Encapsulation efficiency (%)
PM-CyA (L)	Normal saline	1:2	2	105 ± 4.42	0.740 ± 0.022	37.0 ± 1.11
PM-CyA (I)	Normal saline	1:2	3	118 ± 16.2	0.825 ± 0.143	27.5 ± 4.79
PM-CyA (H)	Distilled water	1:6	3	89.3 ± 15.3‡	2.286 ± 0.215*	75.9 ± 7.51

* Significantly different with PM-CyA (L) and (I)
‡ Significantly different with PM-CyA (I)

This experiment showed the limitations of this *in vitro* test to reveal the subtle differences in the release profile of nanocarriers prepared with different loading levels. This was

consistent with our previous observation on a similar level of CyA release from MPEO-*b*-PCL micelles bearing 5000 and 13000 g/mol of PCL (Figure 3.1). Therefore, determination of unbound fraction was chosen as an *in vitro* substitute for dialysis method to compare the stability of these nanocarriers in terms of CyA release in the presence of blood components. This test has been originally designed to determine the protein binding of mostly hydrophobic drugs *in vitro*. We hypothesized that a more stable nanocarrier could change the protein binding pattern of the encapsulated drug significantly.

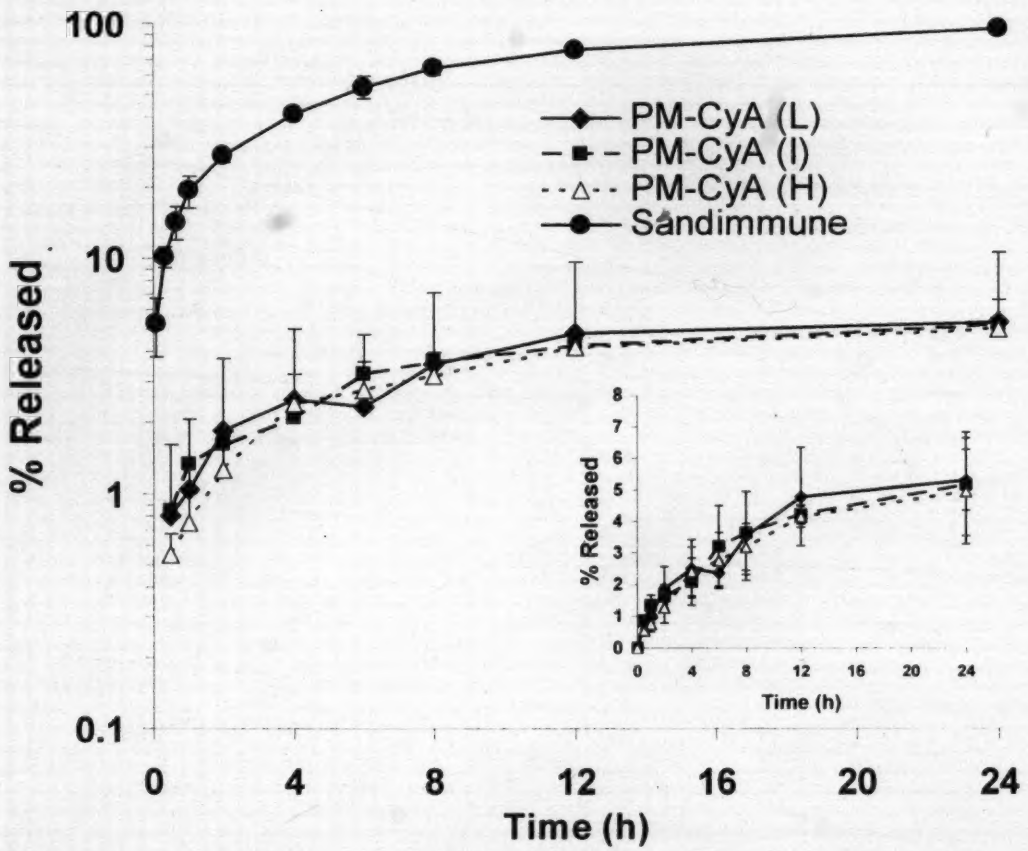

Figure 3.6– The *In vitro* rate of CyA release from Cremophor EL and polymeric micellar formulations at 37°C; the inset depicts an enlargement of the release rate data for the

micellar formulations only on linear y-axis scale. Each point represents average release ± SD (n=3).

3.8.2. Determination of unbound fraction (*fu*)

In the protein binding experiments, equilibrium was achieved within 1 h for all formulations. Each of the micellar formulations showed a significantly lower *fu* for CyA compared to the Sandimmune® (Table 3.10). In contrast to the release experiment (Figure 3.6), differences in *fu* were observed for each of the polymeric micellar formulations (Table 3.10). Specifically, with an increase in CyA loading levels in polymeric micelles, there was a progressive increase in the *fu*. The rank ordering in *fu* was PM-CyA (H)<PM-CyA (I)<PM-CyA (L)<Sandimmune® .

3.8.3. Pharmacokinetics of different micellar formulations

In the pharmacokinetic studies, as shown previously, amongst the tested formulations, Sandimmune® displayed the lowest observed mean concentrations *in vivo* at all time points, including 5 min after injection (Figure 3.7). The PM-CyA (L) formulation, possessing the lowest loading of CyA amongst the polymeric micellar formulations, also had the lowest mean *in vivo* concentrations (Figure 3.7). In contrast, the mean concentration versus time curve appeared to overlap at the early time points for PM-CyA (I) and PM-CyA (H); however, by 6 h after i.v administration CyA levels maintained a higher level for PM-CyA (H) (Figure 3.7).

Calculation of AUC_{0-24} and $AUC_{0-\infty}$ (Table 3.10) confirmed the observations noted from the blood concentrations versus time curves (Figure 3.7). The AUC values were lowest

for Sandimmune®, and increased with an increase in CyA loading content in the MPEO-*b*-PCL micelles (Table 3.10, Figure 3.8). The CyA mean CL was highest in the animals given Sandimmune®, and was inversely related to the amount of CyA loading content in the polymeric micellar formulations (Table 3.10, Figure 3.8). Vc, Vλ and Vdss were calculated for each of the tested formulations, and the rank order was the same as for CL (Table 3.10, Figure 3.8). There were no significant differences in mean $t_{½}$ (Figure 3.8). The ranking for mean AUC_{0-24} was in the exact opposite direction to what observed for *fu*, where Sandimmune®< PM-CyA (L)<PM-CyA (I)<PM-CyA (H). A similar trend was noted for $AUC_{0-\infty}$ (Table 3.10, Figure 3.8). On the other hand, CL, Vd, and Vc of the different formulations yielded essentially the same relative rank ordering as *fu*.

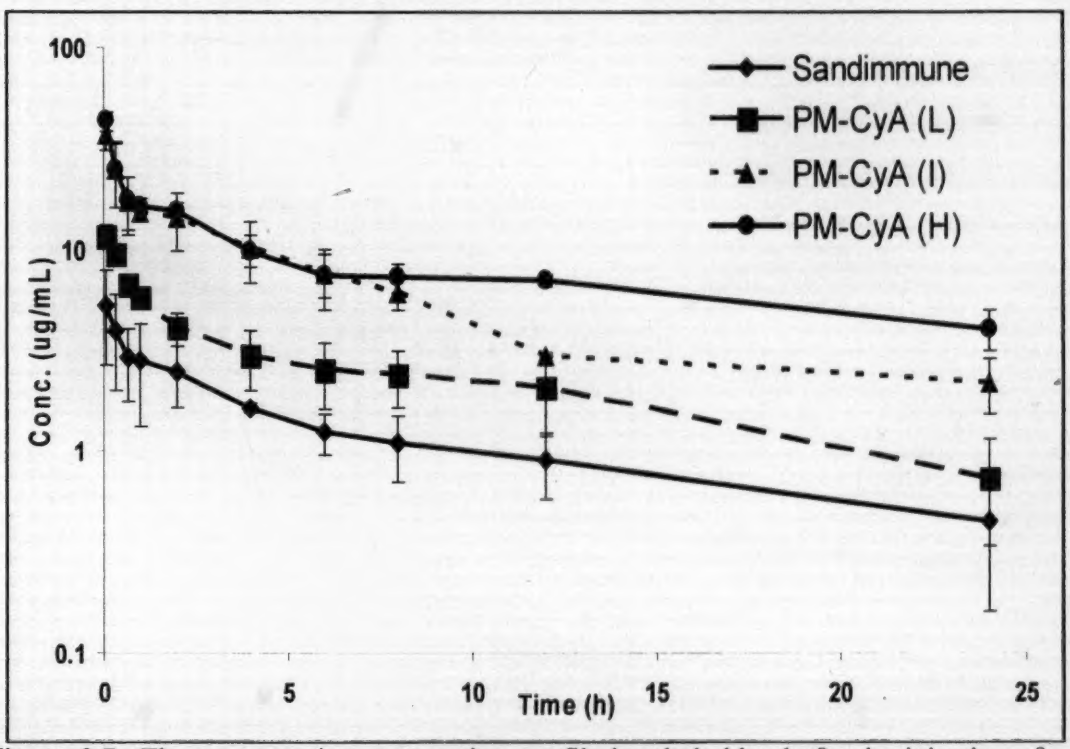

Figure 3.7– The concentrations versus time profile in whole blood after i.v injection of different CyA formulations. Data for PM-CyA (L) and PM-CyA (I) is normalized to injected dose of Sandimmune® and PM-CyA (5 mg/kg). All data are presented as mean ± SD (n=4 to 6 rats/group).

Table 3.10 – Pharmacokinetic parameters (mean±SD) for the different formulations of CyA under study in rat (n=4 to 6 rats/group).

	Sandimmune®	**PM-CyA (L)**	**PM-CyA (I)**	**PM-CyA (H)**
$AUC_{0\text{-}24}$ (μg.h/mL)	25.3 ± 7.64	53.7 ± 11.3	167 ± 18.8	214 ± 18.1
$AUC_{infinity}$ (μg.h/mL)	32.7 ± 13.9	63.0 ± 16.5	199 ± 20.9	240 ± 26.9
$t_{1/2}$ (h)	11.5 ± 4.59	8.53 ± 1.00	9.39 ± 1.20	14.5 ± 3.24
MRT (h)	14.4 ± 6.62	11.6 ± 1.93	9.24 ± 2.06	11.1 ± 0.687
CL (L/kg/h)	0.195 ± 0.131	0.0829 ± 0.0183	0.0255 ± 0.00319	0.0223 ± 0.00270
Vd (L/kg)	2.85 ± 1.40	1.02 ± 0.244	0.343 ± 0.0468	0.167 ± 0.0296
Vdss (L/kg)	2.33 ± 0.786	0.939 ± 0.147	0.232 ± 0.0426	0.242 ± 0.0303
Vc (L/kg)	0.936 ± 0.461	0.404 ± 0.0535	0.0933 ± 0.0205	0.0672 ± 0.0150
fu (%)	37.4 ± 2.34	34.0 ± 3.36	30.1 ± 1.91	15.1 ± 1.88

There were some interesting relationships noted between the *in vitro fu*, the formulation specifications and the *in vivo* pharmacokinetic behaviors of each formulation (Figure 3.9). There appeared to be a linear relationship between the *fu* of CyA and the level of loading in the polymeric micelles (r^2=0.9787) (Figure 3.9). However, there seemed to be no perceptible relationship between the size of the micelles and the *fu*. In contrasting the pharmacokinetic data of the Sandimmune®, PM-CyA (L) and (I) formulations, there appeared to be a nearly linear relationships between the *fu* and each of the AUC, CL, Vc, Vdss and Vd_{λ}. The PM-CyA (H) formulation, however, was not linearly related to the other formulations (Figure 3.9).

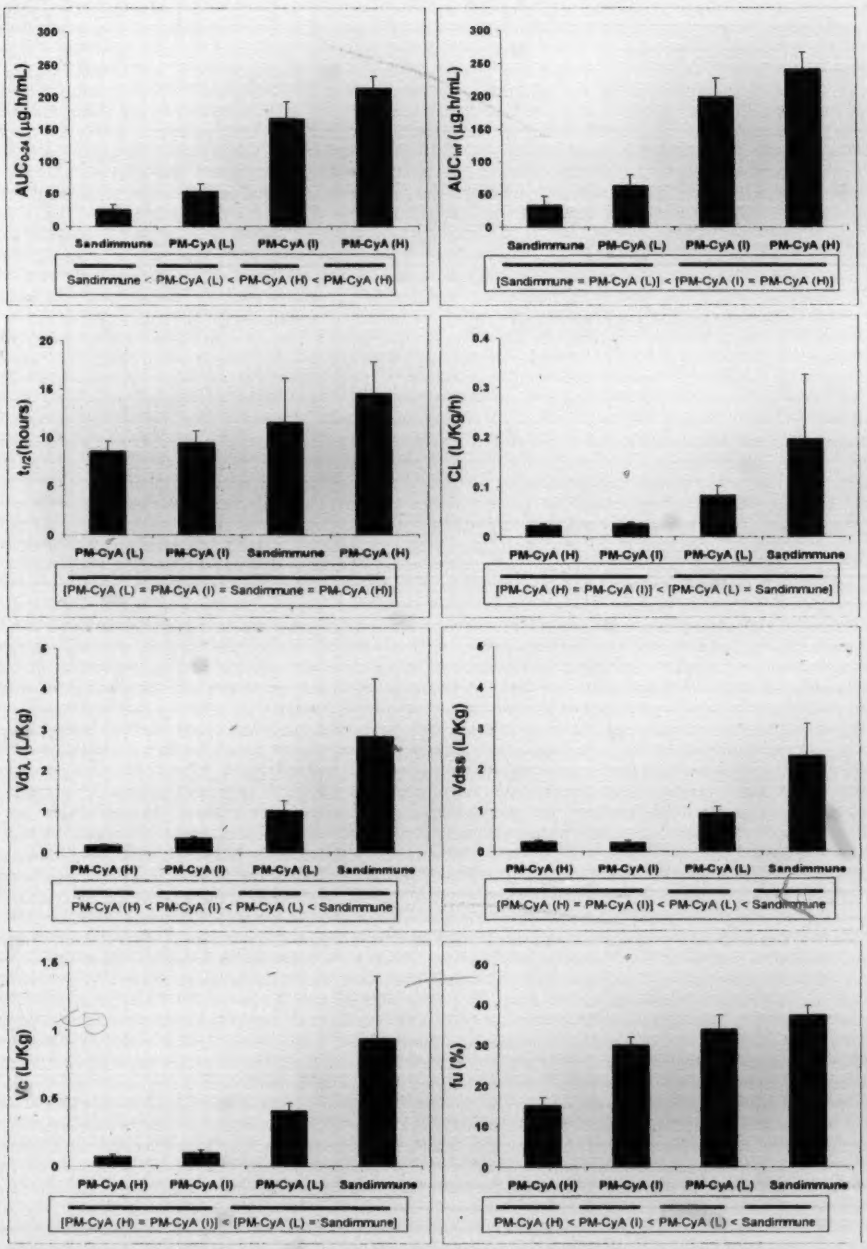
AUC0-24 (µg.h/mL)
Sandimmune PM-CyA (L) PM-CyA (I) PM-CyA (H)
Sandimmune < PM-CyA (L) < PM-CyA (H) < PM-CyA (H)
AUCinf (µg.h/mL)
Sandimmune PM-CyA (L) PM-CyA (I) PM-CyA (H)
[Sandimmune = PM-CyA (L)] < [PM-CyA (I) = PM-CyA (H)]
t1/2(hours)
PM-CyA (L) PM-CyA (I) Sandimmune PM-CyA (H)
[PM-CyA (L) = PM-CyA (I) = Sandimmune = PM-CyA (H)]
CL (L/Kg/h)
PM-CyA (H) PM-CyA (I) PM-CyA (L) Sandimmune
[PM-CyA (H) = PM-CyA (I)] < [PM-CyA (L) = Sandimmune]
Vd1 (L/Kg)
PM-CyA (H) PM-CyA (I) PM-CyA (L) Sandimmune
PM-CyA (H) < PM-CyA (I) < PM-CyA (L) < Sandimmune
Vdss (L/Kg)
PM-CyA (H) PM-CyA (I) PM-CyA (L) Sandimmune
[PM-CyA (H) = PM-CyA (I)] < PM-CyA (L) < Sandimmune
Vc (L/Kg)
PM-CyA (H) PM-CyA (I) PM-CyA (L) Sandimmune
[PM-CyA (H) = PM-CyA (I)] < [PM-CyA (L) = Sandimmune]
fu (%)
PM-CyA (H) PM-CyA (I) PM-CyA (L) Sandimmune
PM-CyA (H) < PM-CyA (I) < PM-CyA (L) < Sandimmune

Figure 3.8– Ranking of *fu* and pharmacokinetic parameters for CyA formulations. Continuous lines over the symbol of groups indicate lack of significance between groups encompassed by the lines; groups not encompassed within lines are significantly different (one way ANOVA and post-hoc Dunnett T3 test, $p<0.05$). Data presented as mean + SD ($n = 4 – 6$).

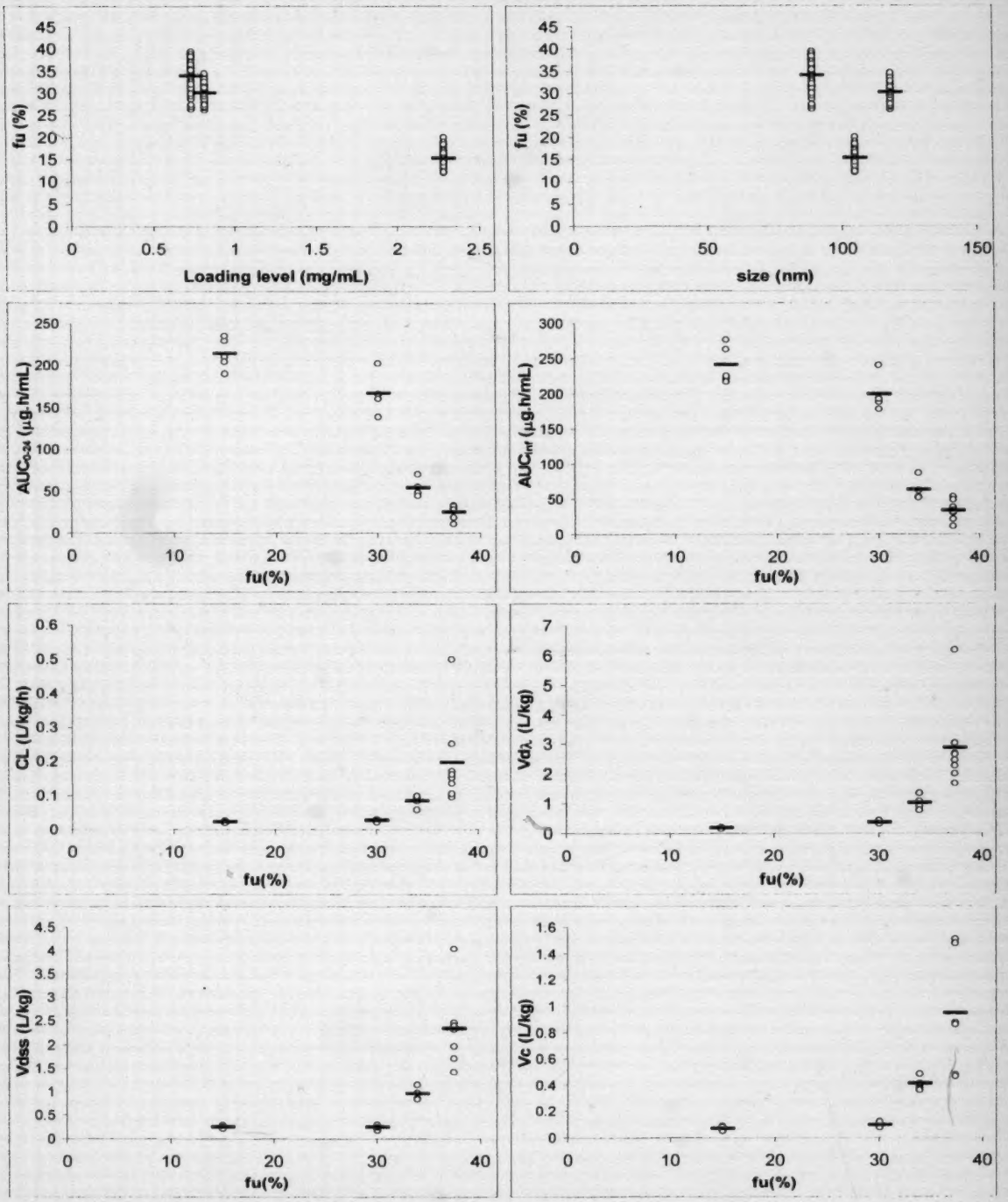

Figure 3.9 – Relationships between *fu* and drug loading content, micellar size, and pharmacokinetic parameters for different CyA formulations.

3.9. Nephrotoxicity of PM-CyA (H) in comparison to Sandimmune®

The isotonic solutions of PM-CyA (H) and saline-diluted Sandimmune® were administered to healthy Sprague-Dawley rats intravenously at a dose of 20 mg/kg/day for 7 days. Control animals received empty MPEO-*b*-PCL micelles, Cremophor EL and saline. There was no significant difference between the weights of animals in different treatment groups at the commencement of the study (Figure 3.10). Over the course of the study, rats given saline, unloaded micelles or Cremophor EL gained weight on a regular daily basis, with means of 3.11, 3.35, and 3.22% daily body weight gain being observed, respectively. In contrast, animals receiving Sandimmune® displayed no significant change in their total body weight over the course of treatment. Unlike the rats given Sandimmune®, animals receiving PM-CyA did gain body weight (1.82% per day), although it was not as high as the control animals. After 7 days the relative weight gain in animal receiving different treatments was ranked based on the following order determined by Duncan's multiple range test, and the analysis indicated that [saline = Cremophor EL=unloaded micelles]>PM-CyA>Sandimmune ® (Figure 3.11A) .

There was no significant difference between the baseline (Day 0) indices of renal function in rats allocated to each treatment group (Table 3.11). The overall mean CLcr in all rats before the treatment period was 8.41±2.12 mL/min/kg, which is comparable to the reported values for CyA CLcr in rat [258]. After 7 days of treatment, no significant changes in CLcr, CLur, plasma potassium or sodium were observed from baseline for control animals given saline, unloaded MPEO-*b*-PCL, or Cremophor EL. In contrast, repeated dose administration of Sandimmune® to rats resulted in significant decreases in

CLcr (47%) and CLur (61%). This treatment also caused significant increases in urea (73%) and potassium (21%) levels in rat plasma. Unlike Sandimmune®, administration of PM-CyA did not cause a significant change in CLcr in animals (7.74 vs. 7.39 mL/min/kg before and after treatment, respectively). However, over the study duration, a significant decrease in CLur (42%), increase in plasma urea (57 %), and increase in plasma potassium levels (19 %) were detected in animals given PM-CyA. Plasma sodium levels did not change significantly in any of treatment groups. The level of decrease in mean CLcr for different treatment groups was ranked as [saline=Cremophor EL=unloaded micelles=PM-CyA]< Sandimmune® (Figure 3.11D). The degree of increase in mean plasma potassium for different groups was ranked as [saline=Cremophor EL=unloaded micelles]<[PM-CyA=Sandimmune®] determined by Duncan's multiple range test (Figure 3.11B). The degree of decrease in CLur followed the same order (Figure 3.11C). No significant trend of changes in urinary output was observed in any of the studied groups .

Analysis of kidney and blood samples after treatment with CyA revealed a reduced delivery of CyA by PM-CyA to kidneys by 2.6-fold, and increased CyA levels in blood by 2.1-fold, in comparison to Sandimmune® (Figure 3.12A). The kidney to blood concentration ratios of CyA after 7 days administration of PM-CyA was significantly lower than that of Sandimmune® (0.6 vs. 2.9 mL/g) (Figure 3.12B) .

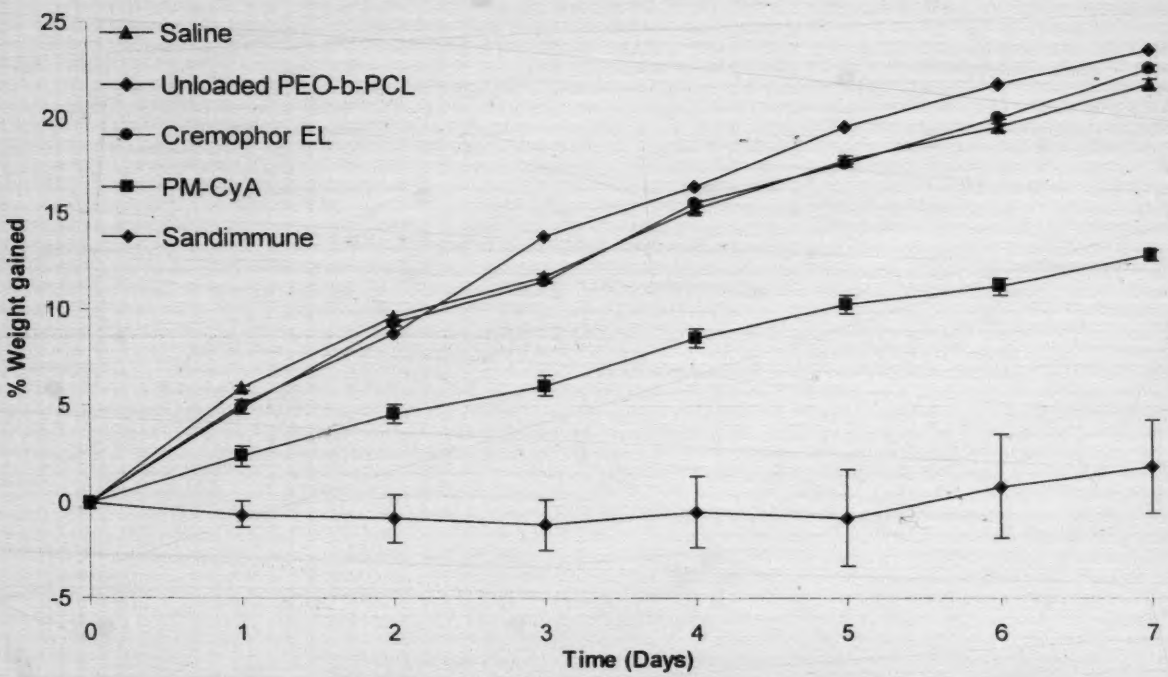

Figure 3.10 – Average weight gain ± SD (%) in rats treated with saline, 20 mg/kg/day of CyA as part of Sandimmune® and PM-CyA (H), corresponding concentrations of Cremophor EL and empty MPEO-*b*-PCL micelles as appeared in the Sandimmune® and PM-CyA (n=5-6).

Table 3.11 – Indices of renal function in rats before (day 0) and after (day 8) treatment

Treatment		PNa ± SD (mEq/L)	PK ± SD (mEq/L)	PU ± SD (mmol/L)	CLur ± SD (mL/min/kg)	CLcr ± SD (mL/min/kg)
Saline	Before:	141 ± 2.06	4.50 ± 0.59	7.08 ± 1.52	5.74 ± 1.41	7.95 ± 1.13
	After:	141 ± 1.71	4.60 ± 0.48	6.13 ± 0.17	5.21 ± 0.89	8.50 ± 1.17
Cremophor EL	Before:	142 ± 0.447	4.54 ± 0.55	5.92 ± 0.55	4.93 ± 0.48	6.98 ± 0.96
	After:	141 ± 2.07	4.36 ± 0.25	6.22 ± 0.62	4.64 ± 0.25	8.14 ± 0.44
Unloaded micelles	Before:	139 ± 1.34	4.64 ± 0.56	6.52 ± 0.51	5.24 ± 1.32	9.18 ± 1.35
	After:	140 ± 0.707	4.58 ± 0.66	6.2 ± 0.72	4.99 ± 0.50	8.90 ± 1.19
Sandimmune®	Before:	142 ± 1.58	3.92 ± 0.29	5.96 ± 1.03	5.78 ± 1.55	10.2 ± 2.48
	After:	146 ± 4.47	4.74 ± 0.35*	10.1 ± 1.11*	2.14± 0.14*	5.35 ± 1.51*
PM-CyA	Before:	139 ± 2.43	4.38 ± 0.45	5.07 ± 0.65	6.50 ± 1.27	7.74 ± 2.64
	After:	137 ± 2.95	5.15 ± 0.31*	7.83 ± 0.74*	3.76 ± 1.13*	7.39 ± 2.14

PNa: Plasma sodium; PK: Plasma potassium; PU: Plasma Urea; CLur: Urea Clearance; CLcr: Creatinine clearance

*: Significant difference compared to "before" ($\alpha = 0.05$, paired Student's t test) ($n \geq 3$).

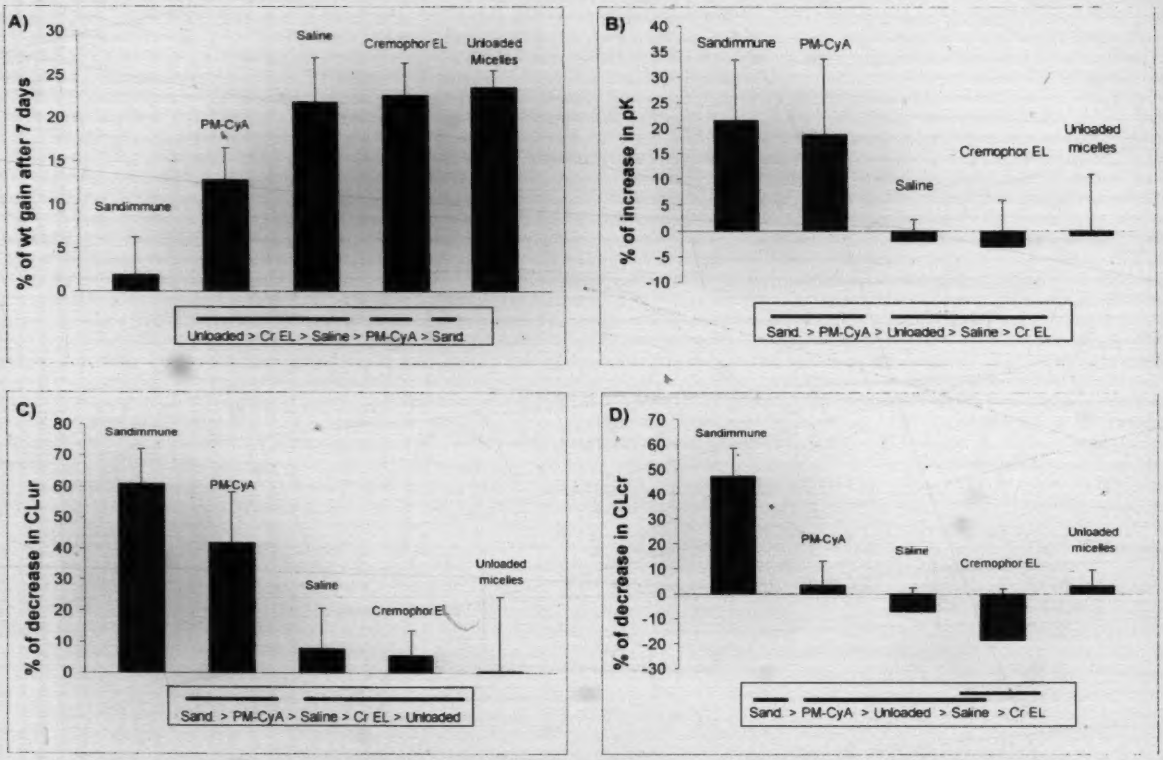

Figure 3.11- Changes in **A)** body weight, **B)** plasma potassium level, **C)** CLur, and **D)** CLcr for animals treated with saline, Cremophor EL, unloaded polymeric micelles, Sandimmune® and PM-CyA expressed as a percent of variable measured in the same treatment group on day zero. Continuous lines over the symbol of groups indicate lack of significance between means encompassed by the lines; means not encompassed within lines are significantly different from those encompassed by the lines (one way ANOVA followed by a post-hoc Duncan's Multiple Range test, $p<0.05$). Each bar represents the mean + SD for the group.

Histopathological examination of kidney tissues after H&E and PAS staining was performed for rats treated with normal saline, PM-CyA and Sandimmune® at the end of the study (Figure 3.13A-F). The histology of kidneys for rats treated with PM-CyA was very close to being microscopically normal. The changes that were present should not be considered toxic, but rather, within the normal range of changes/responses that occur when the kidney removes and metabolizes xenotic compounds (Figure 3.13A-D). Abnormalities presented as finely vacuolated cytoplasm in tubular epithelial cells were

only seen in kidney of rats treated with Sandimmune® (arrows in Figure 3.13E and F). Glomerular cellular defects, which presented as finely vacuolated cytoplasm, were noted in only one of the kidneys from the Sandimmune® treated animals.

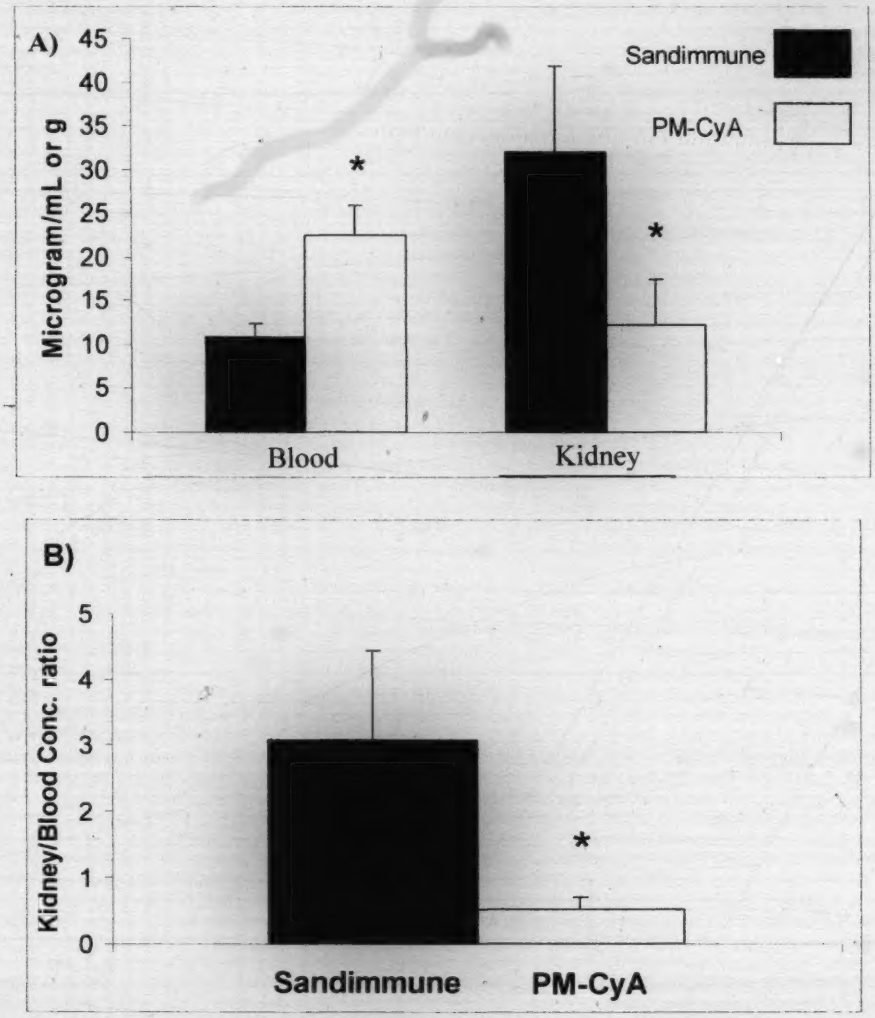

Figure 3.12 – A) Average CyA levels + SD (μg/g or mL) in rat blood and kidneys after 7 day treatment with Sandimmune® and PM-CyA at 20 mg/Kg/day of CyA; **B)** Kidney/Blood levels ratios for after 7 day treatment with Sandimmune® and PM-CyA at 20 mg/Kg/day of CyA (asterisks indicate a significant difference [$p < 0.05$]).

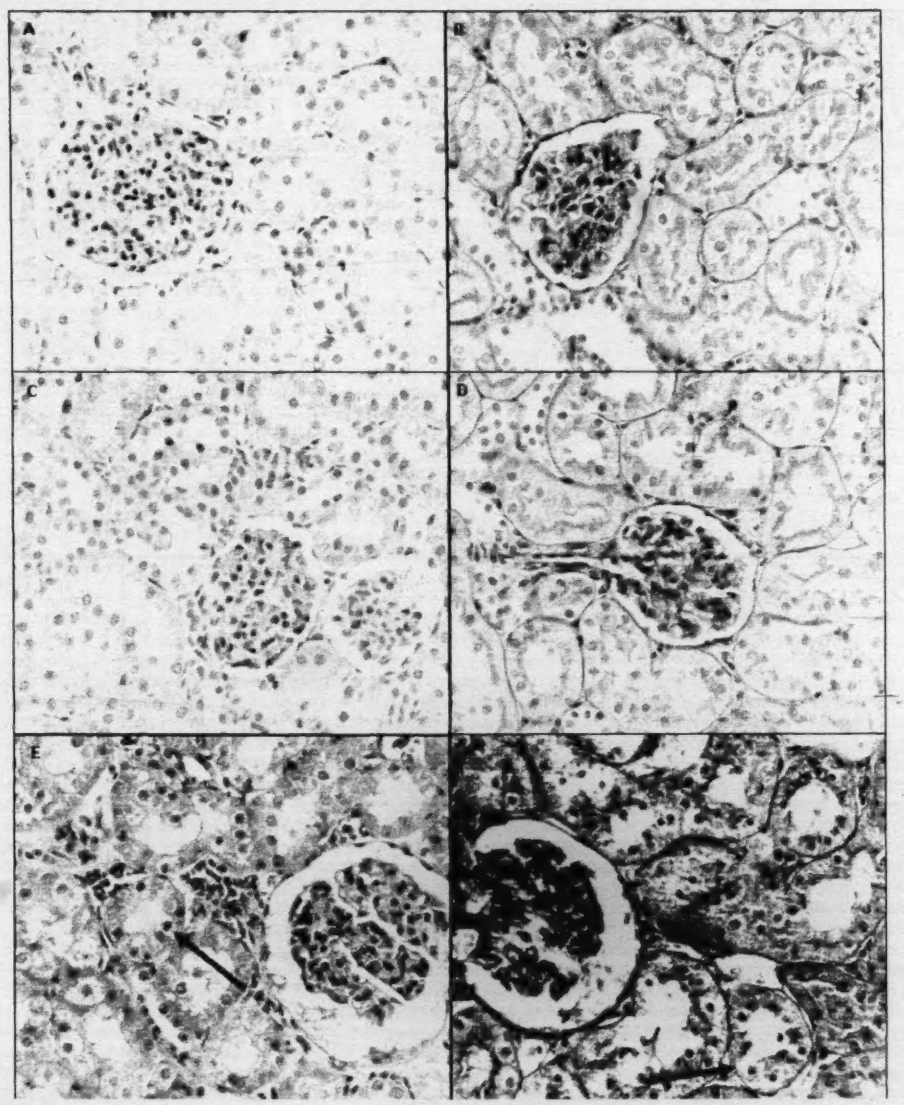

Figure 3.13 – Stained kidney sections of rats given saline, PM-CyA and Sandimmune® (n=3; optical magnification is × 400): **A)** a representative H&E stained kidney tissue from saline treated rats; **B)** a representative PAS stained kidney tissue from saline treated rat; **C)** a representative H&E stained kidney tissue from rats treated with PM-CyA. The cell structures are within the normal limits and cannot be distinguished from the saline treated control group; **D)** a representative PAS stained kidney tissue from rats treated with PM-CyA. There are no unusual PAS positive structures in the tubules, and again, not distinguished from the saline treated control group (Figure 3B); **E)** a representative H&E stained kidney tissue from rats treated with Sandimmune®. The fine perinuclear vacuolation of tubular epithelial cells, shown by arrows, was present throughout the cortex in the kidney sections obtained from this group; **F)** a representative PAS stained kidney tissue from rats treated with Sandimmune®. The tubular epithelium shows occasional PAS positive intracytoplasmic droplets, but most of the vacuoles were PAS negative.

3.10. Assessing the *in vitro* efficacy of PM-CyA (H) in the reversal of drug resistance to DOX

Determination of IC_{50} for DOX against MDA-MB435/LCC^{MDR} and MDA-MB435/LCC^{WT} cells was carried out as a test for *in vitro* efficacy of CyA in different formulations for the reversal of MDR. Unloaded MPEO-*b*-PCL micelles and Cremophor EL alone were not cytotoxic against the wild type cell line at the applied concentration range (corresponding concentrations of Cremophor EL and unloaded micelles in Sandimmune®, and PM-CyA (H), respectively) (Figure 3.14). CyA as Sandimmune®, and PM-CyA (H) seemed to start to show some cytotoxic effects at concentrations above 10 μg/mL (Figure 3.14).

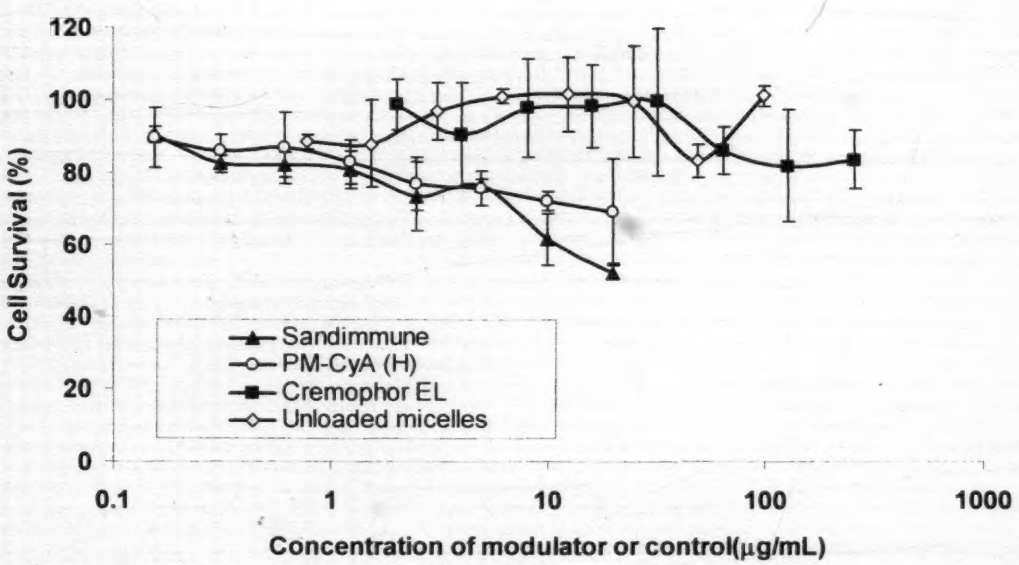

Figure 3.14 – Cell survival for the wild type cell line in the presence of different formulations of CyA and controls. Data presented as mean ± SD (n=3).

In the wild type cell line, an IC_{50} of 0.69 μg/mL was observed for DOX (Table 3.12). Adding unloaded MPEO-*b*-PCL micelles to DOX did not change the IC_{50} of DOX

significantly. However, adding Cremophor EL had a significant impact on the cytotoxic effect of DOX against the wild type cell line (Figure 3.15, and Table 3.12) decreasing the IC_{50} of free DOX by 3.1 fold.

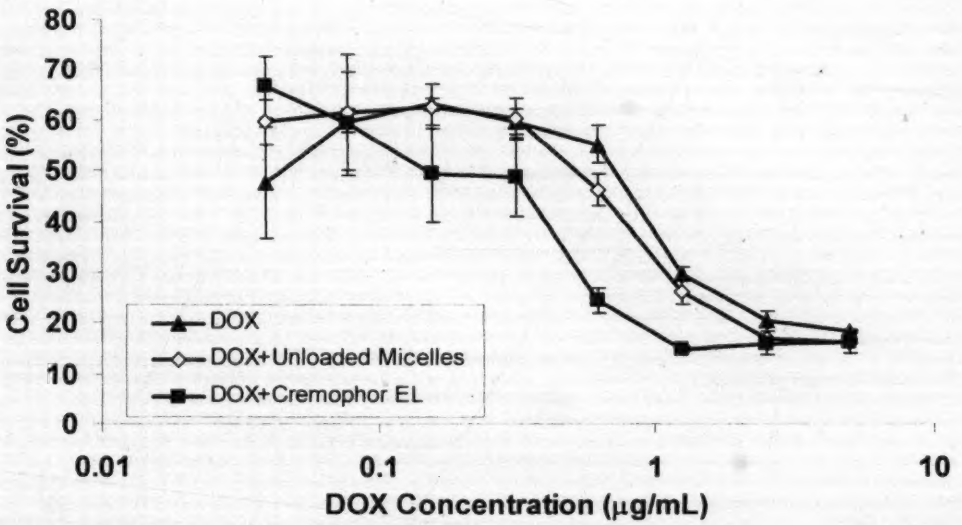

Figure 3.15– Cytotoxicity profile of DOX alone and DOX in the presence of unloaded micelles and Cremophor EL at identical concentrations to what are present in Sandimmune® and PM-CYA (H) formulations, respectively, against MDA-MB-435/LLC6^{WT} cells. Data presented as mean ± SD (n=4).

Addition of CyA at two concentrations of 5 and 10 μg/mL (either as Sandimmune® or PM-CyA (H)) to DOX treatment, even in the wild type cell line, significantly decreased the IC_{50} of DOX. The sensitizing effect of CyA at 5 μg/mL was statistically the same for Sandimmune® and PM-CyA (H). Sandimmune® with the concentration of 10 μg/mL showed a greater effect in reducing IC_{50} of DOX than the corresponding concentration of PM-CyA (H) (Figure 3.16 and Table 3.12). The degree of change in cytotoxicity was very similar to the effect of Cremophor EL alone.

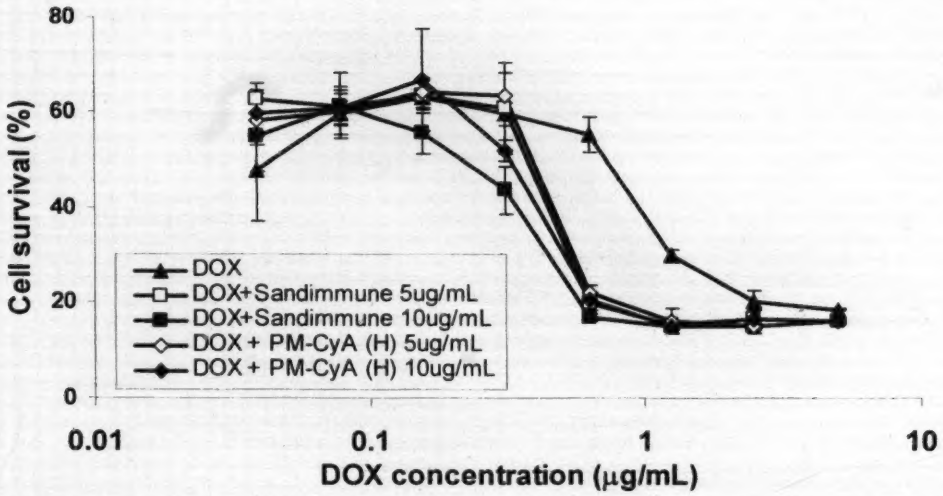

Figure 3.16– Cytotoxicity profile of DOX alone and DOX in the presence of 5 and 10 μg/mL CyA as Sandimmune® and PM-CyA (H) against MDA-MB-435/LLC6^{WT} cells. Data presented as mean ± SD (n=4).

Table 3.12– IC_{50} and sensitivity factor for DOX alone and in combination with CyA formulations and controls against MDA-MB-435/LLC6^{WT} cells

	IC_{50} (μg/mL)	**Increase in sensitivity factor[c]**
DOX	0.69 ± 0.11	-
DOX + Cremophor EL	0.22 ± 0.15[a]	3.14
DOX + Unloaded MPEO-*b*-PCL	0.52 ± 0.09	1.33
DOX + Sandimmune® 5 μg/mL	0.37 ± 0.04[a]	1.86
DOX + Sandimmune® 10 μg/mL	0.22 ± 0.06[a]	3.14
DOX + PM-CyA (H) 5 μg/mL	0.39 ± 0.02[a]	1.77
DOX + PM-CyA (H) 10 μg/mL	0.33 ± 0.01[a,b]	2.09

[a] Significantly different with DOX
[b] Significantly different compared to Sandimmune® 10 μg/mL
[c] Increase in sensitivity factor = IC_{50} (DOX alone)/IC_{50} (DOX + modulator)

Unloaded MPEO-*b*-PCL micelles, Cremophor EL, CyA as Sandimmune®, and PM-CyA (H) alone, were found to be non-toxic against the MDR cells (Figure 3.17).

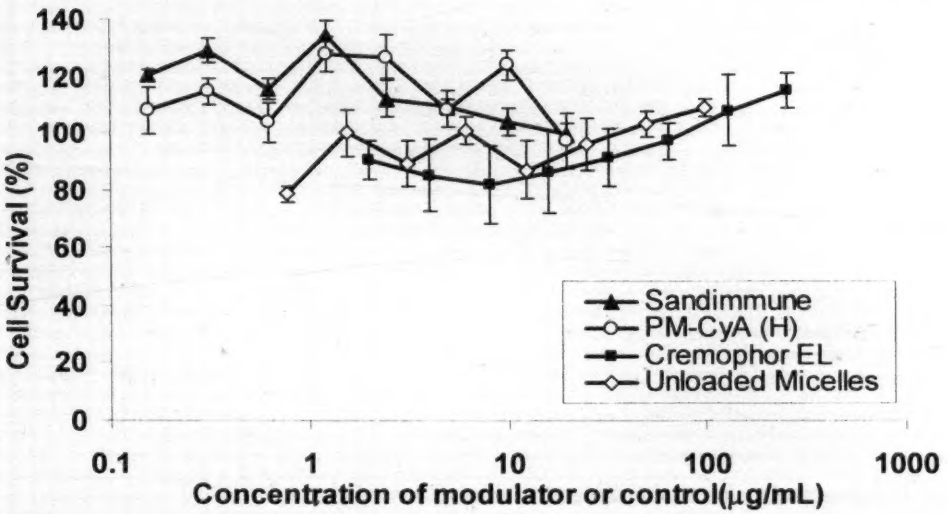

Figure 3.17 – Cytotoxicity of CyA formulations and the carriers present in each formulation against MDA-MB-435/LCC6^{MDR} cells. Each point represents mean cell viability ± SD (n=4).

The IC_{50} of DOX in the resistant type was 11.6 μg/mL, which is significantly higher than the IC_{50} of DOX in wild type cells (Figure 3.18 and Table 3.13). Unloaded MPEO-*b*-PCL micelles did not change the cytotoxicity of DOX in MDR cells significantly (unpaired student's t-test, $\alpha = 0.05$), while Cremophor EL increased DOX Cytotoxicity (Figure 3.18). The IC_{50} of DOX was reduced by 6.5 folds in the presence of Cremophor EL in MDR cells (Table 3.13). CyA at a concentration of 5 μg/mL as free CyA dissolved in water:ethanol (95:5), Sandimmune® and PM-CyA (H) dropped the IC_{50} of DOX from 11.6 μg/mL to 0.36, 0.36, and 0.48 μg/mL, respectively, corresponding to 32.3, 32.3 and 24.2 times increase in the sensitivity factor of MDR cells to DOX. The difference in IC_{50} of DOX in the presence of PM-CyA (H) and Sandimmune® was not significant ($\alpha = 0.05$, unpaired Student's t-test). Increasing the concentration of CyA to 10 μg/mL decreased the IC_{50} of DOX even further. The IC_{50} of DOX dropped to 0.39, 0.24, and 0.44 μg/mL in presence of 10 μg/mL CyA as free drug, Sandimmune®, and PM-CyA (H), respectively.

At this concentration, Sandimmune® was more efficient in lowering the IC_{50} of DOX compared to free drug and PM-CyA (H) (α = 0.05, unpaired student's t-test) (Figures 3.19 and 3.20, and Table 3.13).

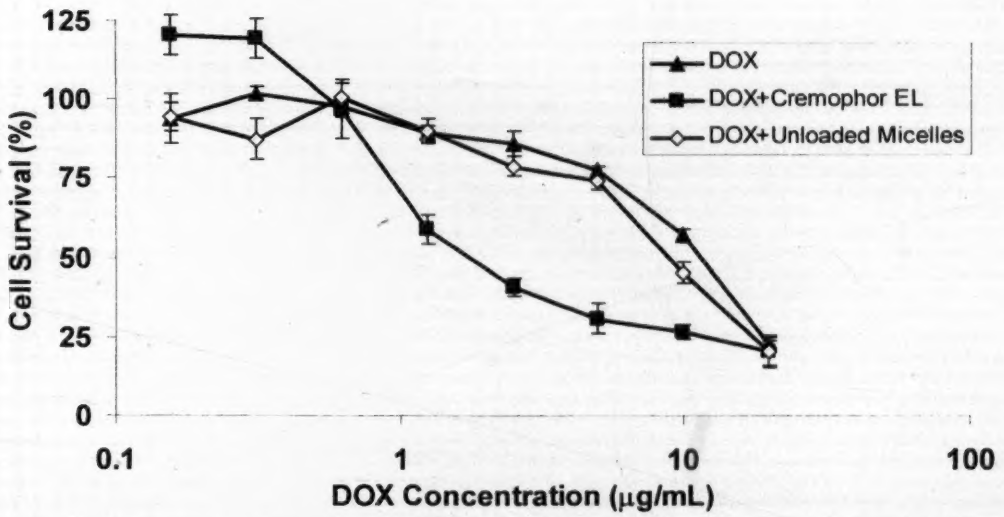

Figure 3.18 – Cytotoxicity profile of DOX alone and DOX in the presence of unloaded micelles and Cremophor EL at identical concentrations to what are present in Sandimmune® and PM-CyA (H) formulations, respectively against MDA-MB-435/LLC6^{MDR} cells. Data presented as mean ± SD (n=4).

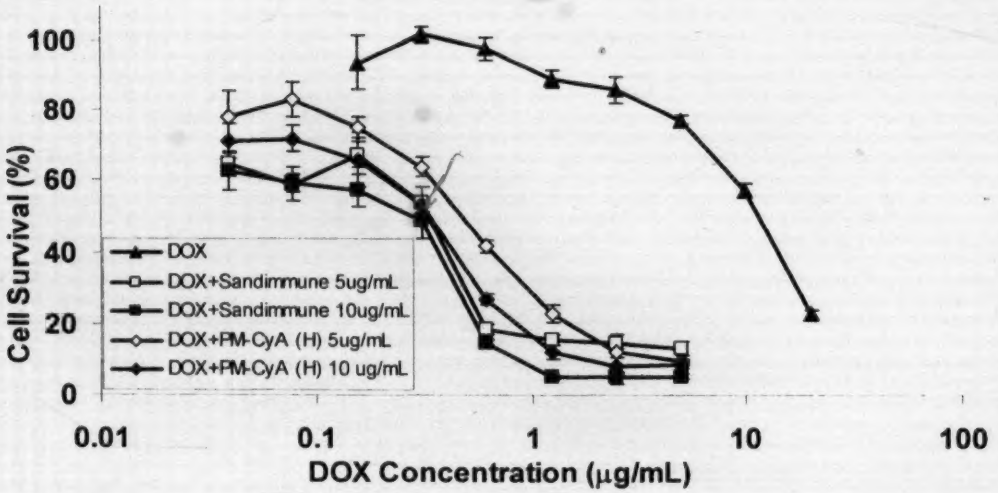

Figure 3.19 – Cytotoxicity profile of DOX alone and DOX in the presence of 5 and 10 μg/mL CyA as Sandimmune® and PM-CyA (H) against MDA-MB-435/LLC6^{MDR} cells Data presented as mean ± SD (n=4).

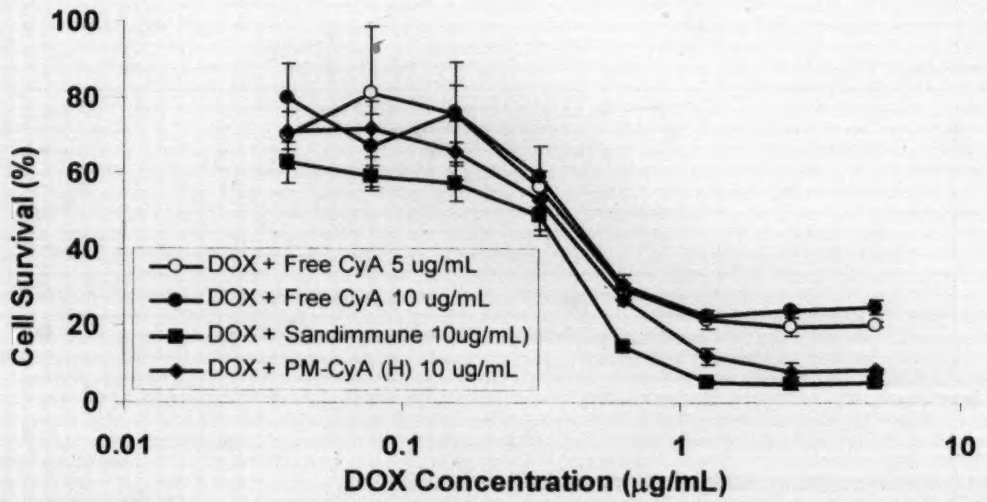

Figure 3.20 – Cytotoxicity profile of DOX in the presence of 5 and 10 μg/mL CyA as free drug, and 10 μg/mL as Sandimmune® and PM-CyA (H) against MDA-MB-435/LLC6^{MDR} cells. Data presented as mean ± SD (n=4).

Table 3.13 – IC_{50} and sensitivity factor for DOX alone and in combination with CyA formulations and controls in the resistant cell line (n=3).

	IC_{50} ± SD (μg/mL)	Increase in sensitivity factor	Residual resistance
DOX	11.63 ± 1.87	-	-
DOX + Cremophor EL	1.80 ± 1.83[a]	6.64	17.10
DOX + Unloaded MPEO-*b*-PCL	8.95 ± 0.58[a,b]	1.30	12.97
DOX + Sandimmune® 5 μg/mL	0.36 ± 0.03[a]	32.31	0.52
DOX + Sandimmune® 10 μg/mL	0.24 ± 0.13[a]	48.45	0.35
DOX + PM-CyA (H) 5 μg/mL	0.48 ±0.10[a]	24.23	0.70
DOX +PM-CyA (H) 10 μg/mL	0.44 ± 0.04[a,c]	26.43	0.64
DOX + Free CyA 5 μg/mL	0.36 ± 0.08[a]	32.31	0.52
DOX + Free CyA 10 μg/mL	0.39 ± 0.01[a,c]	29.82	0.57

[a] Significantly different from DOX
[b] Significantly different from all other DOX + modulator or control groups
[c] Significantly different from DOX + Sandimmune 10 μg/mL
[d] Increase in sensitivity factor = IC_{50} (DOX alone)/IC_{50} (DOX + modulator)
[e] Residual resistance = IC_{50} (DOX + modulator in MDR cells)/IC_{50} (DOX alone in wild type cells)

3.11. Tumor accumulation

Tissue analysis of CyA, 6 hours after single-dose i.v administration of Sandimmune® and PM-CyA (H) to tumor (Lewis lung carcinoma [LLC]) bearing mice showed a significant difference in the distribution pattern of the drug. While the order in mean CyA concentration from highest to lowest in the Sandimmune® group was kidney>heart>liver>tumor>spleen>blood, in the PM-CyA (H) group, the corresponding order was tumor>kidney>heart>liver>spleen>blood. CyA levels were significantly different in blood, kidney and tumor samples from mice treated with Sandimmune® and PM-CyA (H). Blood and tumor levels of CyA were 1.7 and 2.5 fold higher for the micellar formulation compared to the group that received Sandimmune®. On the other hand, kidney level was 1.5 fold lower (Figure 3.21). CyA levels in other organs for

polymeric micellar formulation and Sandimmune® were not significantly different (α = 0.05, unpaired student's t-test).

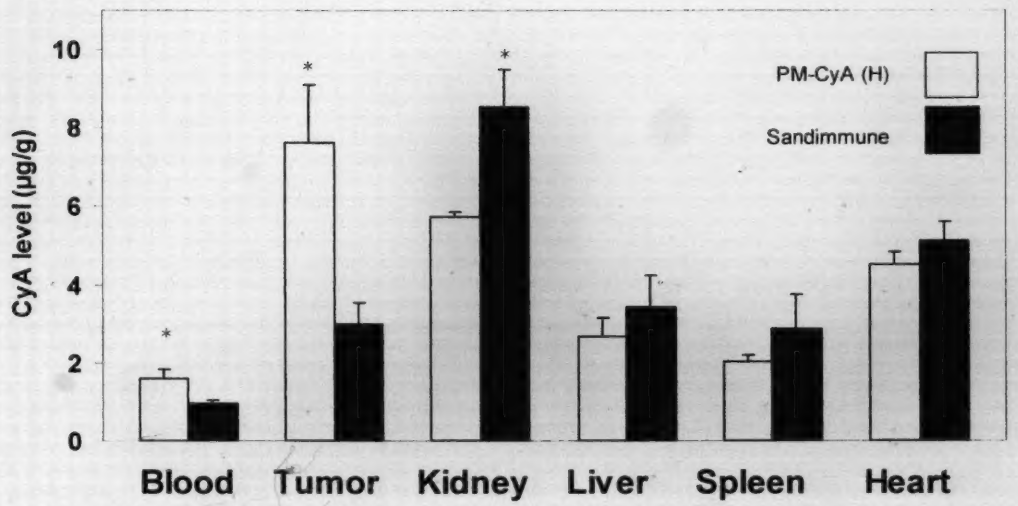

Figure 3.21 – Tissue distribution (6 h post-dose concentrations) of CyA after a single i.v dose of 10 mg/Kg as Sandimmune® and PM-CyA (H) to tumor (Lewis lung carcinoma) bearing mice. Data is presented as mean + SD (n=3). * denotes a significant difference between the CyA levels in that tissue.

CHAPTER 4: GENERAL DISCUSSION AND CONCLUSION

4.1 Discussion

Cyclosporine A (CyA) is a potent drug primarily used for its immunosuppressive function in organ and tissue transplant and autoimmune diseases [291]. The drug is also one of the most effective inhibitors of P-glycoprotein (P-gp), modulation of which has been a focus for improving antineoplastic therapy by overcoming drug resistance [222, 292]. It is a neutral, lipophilic cyclic endecapeptide with very low water solubility (23 μg/mL). The commercial formulation of CyA for injection (Sandimmune®) uses ethyl alcohol and Cremophor EL as major components for CyA solubilization, although Cremophor EL and ethyl alcohol present parenteral safety limitations. Acute and chronic nephrotoxicity caused by CyA and/or Cremophor EL has restricted the clinical use of this important molecule. The main objective of this research is to develop a site specific delivery system that can replace the toxic solubilizing agent in the formulation of CyA and minimize CyA distribution to sites of drug toxicity allowing a reduction in CyA side effects, while enhancing the accumulation of this MDR modulator in the tumor site. The potential of this strategy in enhancing the therapeutic benefit of CyA or other P-gp inhibitors in overcoming MDR will be assessed in future studies.

Several carriers, including liposomes and phospholipid micelles, have been investigated as potential vehicles that can overcome the poor water solubility and excessive toxicity associated with CyA administration. Lipid-based carriers have been able to replace Cremophor EL and reduce the toxicity of CyA formulation for intravenous administration [293, 294], but were shown to be inefficient in keeping the incorporated drug within the lipid membrane *in vitro*, and were thus ineffective at changing CyA disposition *in vivo*

[266, 267, 295, 296]. Considering the hydrophobic nature of CyA, polymeric micelles were hypothesized to be superior to liposomes in retaining CyA within their hydrophobic core and avoid its leakage from the carrier *in vivo* Among different micelle-forming block copolymers poly(ethylene oxide)-*block*-poly(ε-caprolactone) (MPEO-*b*-PCL) micelles were chosen for this purpose. The hydrophobicity and semicrystalline nature of PCL was not only expected to result in thermodynamic and kinetic stability of polymeric micelles but also enhance CyA's solubility and sustain its rate of release from the micellar carrier.

4.1.1. Polymer synthesis and characterization

Synthesis of MPEO-*b*-PCL was carried out through ring opening polymerization of ε-caprolactone in the presence of stannous octoate as catalyst. Yuan et al. have reported on the application of a similar process at a temperature of 140 °C for 24 h [272]. In the present study, reaction conditions for the preparation of MPEO-*b*-PCL block copolymers through ring opening polymerization were optimized with respect to time, temperature and catalyst concentration. Inadequate time or temperature of the reaction in the ring opening polymerization of lactones may lead to incomplete conversion of the monomer to polymer [297], whereas long reaction times and/or high temperatures may result in transestrification or back biting degradation of the polyester chain leading to an increase in the polydispersity of the prepared block copolymers [272]. At a reaction temperature of 140 °C and a reaction period of 4 h sufficient conversion of ε-caprolactone to PCL occur. Also, a catalyst to monomer ratio of 0.002 was chosen as the optimal condition for this synthesis. Prepared block copolymers were characterized for their average molecular

weights by ^{1}H NMR. Considering a MPEO molecular weight of 5000 g/mol, at M/ I molar ratios of 44, 114 and 210, MPEO-*b*-PCL block copolymers with PCL molecular weights of 4984, 12,318, and 22,800 g/mol were synthesized, which is close to the targeted molecular weights of 5000, 13,000 and 24,000 g/mol (Table 3.1).

4.1.2. Micelle preparation and characterization

Prepared block copolymers were assembled to micellar structures by a co-solvent evaporation method and characterized for their functional properties in drug delivery. Direct dissolution and solvent evaporation/film formation has been shown to be inappropriate methods for the self-assembly of MPEO-*b*-PCL block copolymers, especially for those with long PCL chain lengths having molecular weights of 13,000 g/mol and more, because of the high hydrophobicity of the PCL. The co-solvent evaporation method bears several advantages over dialysis method including more feasibility for scale up and less chance for drug loss during dialysis in the encapsulation process, as well.

Preparation of MPEO-*b*-PCL micelles having relatively short PCLs through the evaporation of a co-solvent azeotrope with acetonitrile/water has been reported by Jette et al. [54]. In the current study, an acetone/water co-solvent system has been used to match the higher hydrophobicity of the core-forming block utilized here. Recently, tetrahydrofuran (THF)/water co-solvent systems have been used by Gao *et al.* for the micellization of MPEO-*b*-PCL block copolymers having long PCL blocks (PCL molecular weights of 2500–24,700 g/mol) [56]. The acetone:water system may be

beneficial in terms of scale-up because of a lower boiling point, however. In this project we started with a ratio of 1:2 for acetone:water, by adding the organic phase to the aqueous phase. Using this ratio, MPEO-*b*-PCL block copolymers with molecular weights of 5000-5000, 5000-13,000, and 5000-24,000 produced polymeric micelles with an average diameter of 79–100 nm (Table 3.2). At a similar block copolymer molecular weight range, application of a THF:water (1:10) system has resulted in the formation of smaller micelles (an average diameter of 41–86 nm) [56]. The difference in size is specially marked for self-assembled structures formed from 5000–5000 MPEO-*b*-PCL block copolymers (an average diameter of 41.0 nm for THF:water versus a diameter of 87.5 nm for acetone:water system). Although the size distribution of the self-assembled structures prepared from 5000–5000 MPEO-*b*-PCL micelles in the acetone:water co-solvent mixture in this study were unimodal, a higher polydispersity index (Table 3.2) might be an indication of a trend towards aggregate formation with a larger average diameter of this particular structure. Application of dialysis methods for the self-assembly of MPEO-*b*-PCL block copolymers having similar PCL chain lengths has resulted in the formation of larger particles, even when THF has been used as the selective solvent for the core-forming block in the micellization of MPEO-*b*-PCL [298].

The co-solvent composition used in this study, i.e. acetone:water at a ratio of 1:2, was shown to be efficient in the production of polymeric micellar formulations having appropriate micellar diameters and sufficient CyA solubilization (Table 3.3). Aqueous solubility of CyA was increased up to 50-fold, reaching to a level of 1 mg/mL, in the presence of MPEO-*b*-PCL micelles with this system. This level is comparable to injected

CyA concentrations in Sandimmune®, which is between 0.5 and 2.5 mg/mL. To provide a CyA aqueous concentration of 0.5–2.5 mg/mL, 6.5–32.5 mg/mL of Cremophor EL is required in the Sandimmune® formulation. This level corresponds to a drug to vehicle loading weight ratio of 0.078 mg/mg. To achieve a similar CyA level, the polymeric micellar formulation requires 10 mg/mL (of the final solution) of MPEO-*b*-PCL, which corresponds to drug to vehicle loading weight ratios of 0.09–0.13 mg/mg for block copolymers of various PCL lengths.

4.1.3. Optimization of the micellar characteristics for CyA delivery

A comparison between various studies on the preparation of MPEO-*b*-PCL micelles demonstrates that several factors such as block copolymer molecular weight, micellization procedure and solvent composition to play a significant role in determining the average diameter, size distribution, drug loading levels and rate of release from the assembled nano-carriers [53, 54, 56, 71, 298]. For instance, switching the encapsulation method from dialysis to solvent evaporation is shown to increase the encapsulated levels of amphotericin B in MPEO-*block*-poly(*N*-hexyl stearate L-aspartamide) (MPEO-*b*-PHSA) micelles [71]. Similarly, an O/W emulsion method was proven to be more effective than a dialysis method for the encapsulation of doxorubicin in MPEO-*block*-poly(β-benzyl-L-aspartate) (MPEO-*b*-PBLA) micelles [40, 48]. In an attempt to optimize the characteristics of the micellar formulations of CyA (PM-CyA), in this study the effect of PCL molecular weight and different aspects of the micellization process on the characteristics of unloaded and CyA loaded micelles was investigated.

4.1.3.1. The effect of loading conditions on micellar characteristics and CyA encapsulation– The initial CyA level and the ionic strength of the aqueous phase were the factors that were assessed in this stage of the project. Increasing the initial CyA concentration from 2 to 3 mg/mL using the same aqueous phase and phase ratios of 1:2 increased the CyA loaded level from 0.740 to 0.825 mg/mg. This translated into a decrease in encapsulation efficiency (because of a higher starting concentration of CyA) and similar preparation micellar size for the two formulations. The observation may be attributed to the saturation of the MPEO-*b*-PCL micelles prepared under this condition with CyA.

Our experiments have also shown a significant increase in the encapsulation efficiency of CyA in MPEO-*b*-PCL micelles with substituting normal saline with distilled water. Premature precipitation of CyA during the micellization process in an acetone: normal saline solvent mixture in comparison to acetone: water environment might be the reason for lower levels of CyA encapsulation. Therefore initial concentration of 3 mg/mL for CyA and distilled water were used for the second stage of optimization procedure.

4.1.3.2. The effect of molecular weight of PCL on micellar characteristics and level of CyA encapsulation- Using acetone:water with the ratio of 1:2 and distilled water as the aqueous phase, unloaded MPEO-*b*-PCL micelles were prepared with PCL molecular weights of 5000 to 24000 g/mol (Table 3.2). Using 5000-24000 MPEO-*b*-PCL, the size of the unloaded micelles was significantly larger than the other two examined molecular weights, which is expected due to a larger hydrophobic core. There was no significant

difference in the size of unloaded 5000-5000 and 5000-13000 MPEO-*b*-PCL micelles. Smaller micelles were prepared with 5000-5000 MPEO-*b*-PCL after CyA loading (with initial level of 3 mg/mL CyA) than the other two molecular weights examined regardless of the solvent/co-solvent composition (Table 3.8), which is again in agreement with the expectation based on the molecular weight of the core forming block.

Increasing the molecular weight of the core forming block increased the mole per mole CyA/polymer loading level both with initial CyA levels of 2 (Table 3.3) and 3 mg (Figure 3.5) (α = 0.05, student's *t*-test). Increasing the molecular weight of the core forming block seems to increase the chances of hydrophobic interaction and compatibility between encapsulated drug and the micellar core, and in other words, increase the "room" for loading.

4.1.3.3. The effect of solvent/co-solvent composition– To achieve an optimum polymeric micellar carrier for the delivery of CyA, a systematic study determining the effect of solvent/co-solvent composition on carrier size, morphology and CyA encapsulation was conducted in this stage of the project. The acetone to water ratio was changed and its effect on the average diameter of self-assembled structures from 5000–13,000 MPEO-*b*-PCL was investigated. The volume fraction of the organic to aqueous phase was shown to be a crucial factor determining the average diameter of self-associated colloids. For 5000-13000 MPEO-*b*-PCL application of lower acetone: water ratios led to the formation of smaller particles (α = 0.05, unpaired student's *t*-test; Table 3.7). Addition of lower acetone to water ratios led to the assembly to smaller structures from 5000–5000 to

12,000–5000 MPEO-*b*-PCL, as well (Table 3.7). Compared to other block copolymers, 12,000–5000 MPEO-*b*-PCL micelles had a higher polydispersity and secondary peaks were present in the micellar population. This might be explained by a higher chance of inter-micellar interaction, because of a longer chain in the shell of individual micelles. Interaction of MPEO chains in adjacent micellar shells could cause clumping and eventually, aggregation of micelles, creating a second peak in the size spectrum. The diameter of nanostructures formed from assembly of 5000–24,000 MPEO-*b*-PCL was not significantly different between the 1:2 and 1:6 organic: aqueous phase ratios, however ($\alpha = 0.05$, unpaired student's *t*-test).

The effect of acetone to water volume fraction on the level of CyA loading in MPEO-*b*-PCL micelles and the diameter of loaded particles was assessed in the next stage (Table 3.8). For 5000–13,000 MPEO-*b*-PCL (similar to unloaded particles) the average diameter of CyA loaded micelles was significantly smaller when organic:aqueous phase ratio was 1:6 (unpaired student's *t*-test, $\alpha = 0.05$). Application of 1:6 organic to aqueous phase ratio also led to a higher polydispersity for the assembled structures (Table 3.8). The diameter of CyA loaded 5000–5000 and 12,000–5000 MPEO-*b*-PCL micelles were also significantly smaller when 1:6 acetone to water ratios were used in the encapsulation process. Similar to unloaded carrier, CyA loaded 12,000–5000 MPEO-*b*-PCL micelles showed higher polydispersity in the micellar population. The average diameter of loaded 5000–24,000 MPEO-*b*-PCL micelles was not significantly different for 1:2 and 1:6 acetone to water ratios (Table 3.8).

The results also showed organic to aqueous phase ratio to affect the final CyA loading in MPEO-*b*-PCL micelles (Tables 3.8). CyA reached a final aqueous concentration of 2.3 mg/mL in the presence of 5000–13,000 MPEO-*b*-PCL block copolymers and an initial organic to aqueous phase ratio of 1:6. A similar trend in CyA loading was observed for 5000–5000, 5000–24,000 and 12,000–5000 MPEO-*b*-PCL micelles. Addition of acetone to water at 1:6 phase ratio led to 1.7, 2.1, 1.5 and 4.3-fold increase in CyA encapsulated levels in 5000–5000, 5000–13,000, 5000–24,000 and 12,000–5000 MPEO-*b*-PCL micelles, respectively (Table 3.8, Figure 3.5). An increase in the PCL molecular weight from 5000 to 13,000 and 24,000 g/mol led to an increase the molar loading of CyA in polymeric micelles for the acetone:water ratio of 1:6 (Figure 3.5). Identical results were observed when an acetone: water ratio of 1:2 was applied ($\alpha = 0.05$, student's *t*-test). A comparison between 5000–5000 and 12,000–5000 MPEO-*b*-PCL micelles showed no significant difference in molar CyA loading between these two structures (irrespective of the organic:aqueous phase ratio) which may be a further implication for the association of CyA with the PCL block.

It has been shown that an increase in the concentration of MPEO-*b*-PCL can reduce critical water content of micellization (CWC) [54]. In 1999, Zhang et al. showed the importance of the water content on the morphology of crew-cut micelles prepared by a co-solvent evaporation method [299]. They suggested that in low water contents, the micelle formation process might be thermodynamically controlled; however, as the water content increases, kinetic aspects are expected to become more important. Vangeyte et al. [300] have suggested the same hypothesis by showing that the size of the MPEO-PCL

micelles increases when the polymer concentration in the organic solvent is decreased. Johnson and Prud'homme [301, 302] showed that a higher polymer concentration in the organic phase can decrease the aggregation time of micellization and lead to the formation of more compact nanoparticles.

The higher level of CyA loading in polymeric micelles prepared through the addition of one part acetone to six part water is most probably a result of high polymer concentrations in acetone added to water in this case. During the polymer assembly process, 30 mg of MePEO-*b*-PCL is dissolved in 0.5 mL of acetone and added to 3 mL of water in a drop-wise manner when 1:6 organic:aqueous phase ratio is used. For 1:2 organic: aqueous phase ratio 30 mg of MePEO-*b*-PCL is dissolved in 1.5 mL of acetone and added to 3 mL of water. Therefore, at an acetone to water ratio of 1:6, the concentration of polymeric solution added to water is threefold higher than the polymer concentration in acetone solutions added to water at 1:2 ratio. Therefore, it seems that a higher concentration of block copolymer in the organic solution is the key to a more compact micellar core for the MPEO-*b*-PCL nanoparticles prepared in this study, which could explain both smaller size and higher loading efficiency with the 1:6 ratio for acetone:water composition.

4.1.4. *In vitro* release of CyA from polymeric micelles

In formulation design, the *in vitro* rate of drug release from polymeric micelles can be assessed through various methods. The most popular method is dialysis of the polymeric micellar aqueous solutions versus an appropriate recipient phase. The molecular weight

cut-off of the dialysis membrane in such experiments is selected to ensure restriction of the micellar structures inside the sac, but permit free diffusion of the un-retained portion of drug to the recipient phase [55, 56]. Gel permeation chromatography after direct incubation of the polymeric micellar formulation with the recipient phase has also been used [72]. Unfortunately, for several reasons these methods may not always offer a realistic picture of drug release in a biological system.

At first we have used a conventional dialysis procedure using bovine serum albumin as the recipient phase in the dialysis procedure and compared the *in vitro* release of free CyA dissolved with the aid of ethanol (40 %) to that of CyA in Cremophor EL formulation (Sandimmune®) and two different micellar formulations: CyA-loaded in MPEO-*b*-PCL bearing either 5000 or 13000 g/mol PCL cores. Conventional micelles formed by the surfactant Cremophor EL were able to decrease the release rate of CyA compared to free drug. The difference between the release rate of this formulation and polymeric micellar formulations was even more significant. PEO-*b*-PCL micelles bearing 13000 PCL cores prevented the distribution of CyA to serum albumin to a greater extent and retained 94% of their drug content after 12 hours (Figure 3.1). However, the *in vitro* release test using BSA in the recipient phase was proven to be insufficient in revealing the subtle differences between the two different micellar formulations involved in this experiment.

The practical limitations of the traditional approach in providing a realistic picture for the *in vivo* stability of polymeric micellar formulations was well outlined by our results

shown in Figure 3.6, where in the 24 h period over which the dialysis was run, there were no differences apparent between the micellar formulations. As shown in this study, polymeric micelles of CyA prepared by different MPEO-*b*-PCL molecular weights or various levels of encapsulation demonstrated similar release patterns. However, again in this project, PM-CyA formulations prepared at different CyA loading levels were shown to be significantly different in their pharmacokinetic behavior. This might have different explanations: the required driving force (i.e. lack of sink conditions) for the release of poorly soluble compounds may not be reached under such conditions, and therefore an underestimation of release rate is possible. This drawback can be partially overcome by the addition of a plasma protein binder such as BSA to the buffer side of the dialysis bag, or frequent exchange of the recipient medium with fresh solutions [303], but this still may not resolve the problem. In several cases dialysis of the polymeric micellar formulation must be continued for days before differences are seen in the release rate especially between different polymeric micellar formulation, which raises a question of physicochemical stability of the formulation constituents and integrity [56, 80-82]. Another limitation of the conventional tests is the artificial environment into which the micelles are placed. *In vivo,* the formulation upon entering the systemic circulation finds itself in a complex biological "soup" (i.e. the blood) containing components such as red and white blood cells, proteins, enzymes and numerous other organic and inorganic chemicals. In the conventional experiments used to assess stability none of these situations are appropriately mimicked. Finally, in the conventional *in vitro* procedures, dilution of the formulation after administration in the biological system, which may bring

the final concentration of the polymeric micellar system below its critical micellar concentration (CMC), is not accounted for.

4.1.5. Determining the unbound fraction of CyA in blood *in vitro* as a measure of *in vivo* stability of PM-CyA

The *in vivo* stability of polymeric micelles is usually investigated comparing the pharmacokinetics and biodistribution of polymeric micellar and conventionally solubilized drug [46]. In this context, design of *in vitro* experiment that can assess the possible *in vivo* stability and release of hydrophobic drugs from micellar formulation is of great importance, since pharmacokinetic and/or biodistribution studies are very time consuming and expensive. Such a test permits rational selection of the most appropriate formulation to bring forth to preclinical or clinical *in vivo* pharmacokinetic evaluation.

In considering the limitations of the dialysis methods of determining stability of polymeric micellar formulations in an artificial environment, we thought it is appropriate to use the relatively simple *in vitro* erythrocyte binding method for determination of *fu* to see if it could predict the hematologic stability of a series of polymeric micellar formulations differing in micellar particle size and percent drug loading. If the formulation was more stable, it would be predicted that less drug would be released and that the unbound fraction measured in the plasma would be decreased. This all would occur in an environment (i.e. blood and plasma) that more closely resembles the *in vivo* situation. For drugs such as CyA which are known to bind to dialysis membranes, the erythrocyte binding method has been shown to be an invaluable procedure in determining

its *fu* [278]. In addition, this method has been used for the determination of the *fu* for drugs such as amiodarone [304], and halofantrine [305, 306], which are not known to bind extensively to blood cells. The *fu* of polymeric micelles at three different loading levels were compared in this stage of the project. Unlike the dialysis method, determination of *fu* from the various PM-CyA formulations resulted in differences (Table 3.9 and Figure 3.8). We were able to discriminate between those different micellar formulations such that it appeared as if increased loading resulted in more stable nanoparticles, from the perspective of CyA retention.

Each of the PM-CyA formulations had a significantly lower *fu* than Cremophor EL formulations; there was a consistent decrease in the plasma *fu* (Figure 3.8). This implies that the micellar formulation protected the drug from binding to blood cells and hence decreased the *fu* in plasma. Loading level, but not size, seemed to have a predictable effect on the *fu* (Figure 3.9). Several groups have reported the effect of the level of drug loading on the *in vitro* drug release rate from polymeric micelles [80, 81]. Similarly, an increase in loading levels for doxorubicin in polymeric micelles has been shown to decrease the release rate *in vitro* [56, 82]. It has been shown that the compatibility of the micellar core with the encapsulated drug, would increase not only the loading efficiency of the micelles for that particular drug, but also increases the *in vitro* and possibly, *in vivo* stability of the prepared micelles [27, 50, 68-70].

4.1.6. Pharmacokinetic and biodistribution of PM-CyA

Our pharmacokinetic experiments were done in two different stages: At first we compared the pharmacokinetic parameters of PM-CyA (I) with the commercially available formulation (results shown in Table 3.5; then a second round of experiments were designed to rank the different micellar formulations according to their *in vivo* performance, and to assess the correlation between this performance and the *fu* calculated in the *in vitro* experiments for the same formulations (Table 3.10). Due to insufficient loading level of CyA in PM-CyA (L) and PM-CyA (I), and the limitations on the maximum volume for i.v injections to rats, these two formulations were administered at a dose that was half the dose for Sandimmune® and PM-CyA (H). Since the pharmacokinetics of CyA has been shown to be linear in the administered dose range of this study (≤ 5mg/kg) in Sprague-Dawley rats [282], the blood concentrations were normalized for the lower doses for comparison purposes.

In the first set of experiments, PM-CyA (I) demonstrated some significant differences from the commercially available Cremophor formulation. The 6.1-fold higher AUC in whole blood is reflective of a high degree of *in vivo* stability of the polymeric micellar particles or a lower CL. This is a significant finding, because lipid based carriers have typically failed to show meaningful changes in the pharmacokinetics of encapsulated CyA [266, 267, 307]. In lipid based delivery systems, weak CyA binding to the lipid membrane appears to cause a premature leakage of the encapsulated drug from the carrier [266, 267, 296]. The change in the biological fate of CyA, imposed by its encapsulation in MPEO-*b*-PCL micelles, led to an increase in AUC as a result of a reduction in CL and

Vd for the encapsulated drug. This is in contrast to the results of pharmacokinetic studies by Kim et al. [268], who reported a decrease in AUC and an increase in the Vd and half-life, but no change in the CL of indomethacin loaded MPEO-*b*-PCL micelles in Sprague-Dawley rats. Stealth properties of the developed micellar carrier in the present study, induced by the nanoscopic dimension and hydrophilic shell of MPEO might have contributed to these observations. The higher AUC for PM-CyA shows higher blood concentrations for CyA, which along with the lower Vd and CL, indicates a limited distribution to peripheral tissue and residence of the encapsulated CyA in blood circulation. The data pointed to a potential for MPEO-*b*-PCL micelles as long circulating carriers for CyA delivery. A carrier that is expected to reduce CyA accumulation in sites of drug toxicity, i.e., kidney, and enhance the chance for the passive accumulation of the encapsulated drug in solid tumors through EPR effect at the same time.

With our observations in the second round of pharmacokinetics experiments, after normalizing the concentrations to administered dose (Figure 3.7), it was clear that the changes in *fu* were correlated to the change in the *in vivo* pharmacokinetic behaviors of the formulations. Cyclosporine A has a low hepatic extraction ratio in the rat [277], and as a consequence a decrease in unbound fraction, as was seen in the PM-CyA formulations, is expected to result in increased AUC, and decreased Vd and CL, with no change in $t_{1/2}$. As expected, the mean values of AUC, Vd, and CL were all ranked in order according to the change in *fu*, although statistically in some cases (e.g. Vdss and CL) there was some lumping of different formulations (Figure 3.8). For AUC_{0-24} and Vd_{λ}

the respective rank orders showed significance for each of the formulations (Figure 3.8) in a manner expected based on differences in *fu*.

It was of note that there were some approximately linear relationships between the *fu* of Sandimmune® and the two PM-CyA formulations with lower levels of loading with the pharmacokinetic parameters (Figure 3.9). Specifically, as the CyA *fu* increased, there were progressive decreases in AUC and increases in Vd and CL determined in whole blood. However, the PM-CyA (H) formulation did not appear to follow a linear relationship in CyA kinetics in line with those of the other formulations. Indeed overall the relationships between CyA kinetics and *fu* for these formulations were not linear, with the PM-CyA (H) formulation deviating from the others, which might be partially explained by the limited nature of the changes in Vd and CL.

The results of biodistribution studies showed, in general, CyA encapsulation in MPEO-*b*-PCL micelles to result in elevated CyA levels in blood, plasma and heart, but reduction in CyA uptake by kidney and spleen, in comparison to commercially available formulation, Sandimmune® (Figures 3.3 and 3.4, and Table 3.6). In this study, with the exception of heart, the increase in blood CyA concentrations seemed to coincide with a decrease in the tissue concentrations of the drug, which is in line with the reduced Vd after administration of the PM-CyA (I) formulation. Using Bailer's approach to statistical analysis of the AUC, significance was established for a decrease of splenic and renal uptake of CyA, and there were some discreet concentrations in liver that showed a significant decrease in CyA uptake for the PM-CyA. This shift in concentrations from

kidney to blood is of note, because one of the major dose-limiting side effects of CyA is nephrotoxicity. Therefore, the next step of this project was set to define whether this formulation dependent change in the biodistribution of CyA may translate to reduced CyA nephrotoxicity.

The Kp values were calculated based on the ratio of tissue to plasma concentrations to provide a more revealing picture of the distribution pattern of each formulation. Higher plasma concentrations should normally translate to higher tissue distribution as well. Therefore, the significance of a lower distribution to sensitive organs such as kidney and liver even with higher plasma concentrations achieved with PM-CyA would be better described by Kp values. The Kp values for CyA were lowered in kidney, spleen and liver by MPEO-*b*-PCL micelles especially at early time points, indicating the localization of the micellar carrier in the plasma compartment after i.v administration. In contrast, the Cremophor EL formulation showed high distribution of CyA in all organs. The maximum value of Kp observed in kidney, liver and spleen one hour after i.v administration of this formulation reflects the rapid distribution of CyA in those organs. An increase in the Kp value of PM-CyA in kidney, liver and heart after 12 h, which is a result of reduced CyA concentrations in plasma, may reflect the destabilization of the micellar formulation in plasma.

Again the biodistribution pattern of PM-CyA confirms the conclusions drawn from the pharmacokinetic studies. The lower concentrations of CyA in liver, kidney, and spleen is in complete agreement with the lower CL and Vd values calculated in pharmacokinetic

experiments, which again could be explained by the stealth properties of these nanocarriers that remain stable *in vivo* for a period of time to maximize the circulation time and the chance of accumulation inside the tumor. This change in the distribution pattern of the encapsulated drug is also different from the pattern of change by hyperlipidemia in the same animal model injected with Pluronic F-127 intraperiotoneally [308]. There is a similar increase in the AUC of CyA in poloxamer-induced hyperlipidemia in rats, which could be explained by the significant increase in the lipoprotein levels in this animal model. Enhanced lipoprotein level in plasma results in an increased binding of drug in plasma and a decrease in the unbound fraction in plasma. However, in the biodistribution experiments on hyperlipidemic rats, CyA levels were shown to be lower in spleen and heart, but higher in liver and kidneys, compared to normolipidemic animal model. While the higher drug levels in kidney might be a reflection of a higher plasma concentration, an increase in hepatic uptake might be related to a LDL-receptor mediated uptake in hyperlipidemic rats [308]. In contrast to this observation, polymeric micelles were shown to decrease CyA uptake by kidneys. This points to the direct effect of polymeric micelles in changing the pharmacokinetic and biodistribution of CyA, which differs from that induced by hyperlipidemia.

The trend towards accumulation of PM-CyA in heart is an interesting and unexpected observation. The higher CyA levels in heart might have been caused by preferential accumulation of the polymeric micellar carrier in heart or avoidance of efflux mechanisms by encapsulated CyA in this organ. This accumulation is especially of note, because heart is not the site of action for CyA and even though cardiotoxicity is not a

particular concern with this drug, unwanted accumulation of a targeted delivery system in a non-targeted tissue could be an important drawback. Especially for future directions of this project, where co-administration of P-gp inhibitor with a cytotoxic P-gp substrate will be considered. The accumulation of delivery system in heart in this case might enhance the cardiotoxicity of cytotoxic P-gp substrate. Further assessments are required to clarify the cause of this observation. Using an active targeting method (such as conjugation of monoclonal antibodies or ligand modified polymeric micelles) to enhance the accumulation of the delivery system in the targeted tissue seems to be the most effective solution.

4.1.7. Nephrotoxicity

Considering the results of the pharmacokinetic experiments, and the fact that the highest loading efficiency of PM-CyA(H) had provided the best *in vivo* performance, this formulation was used for the nephrotoxicity experiments. Taking all the results from the assessment of renal function after the treatment period into account, especially CLcr and histological findings, the PM-CyA formulation afforded protection of the kidneys against the nephrotoxic effects of CyA. This was despite a 2.1 fold higher CyA concentration in blood of animals receiving PM-CyA (H) (3.14), which makes this finding even more significant.

Assessment of renal function parameters revealed a significant difference in CLcr, CLur and plasma potassium levels between animals that received Sandimmune® and those that served as non-CyA administered controls (saline, Cremophor EL or unloaded MPEO-*b*-

PCL micelles) (Table 3.10 and Figure 3.11). This is consistent with the results of previous studies after multi-dose administration of CyA by different routes. For instance, a 33% increase in potassium levels in plasma after 14 day oral administration of 30 mg/kg/day CyA dissolved in olive oil to Wistar rats has been reported, which is slightly higher than the 21% increase in potassium level observed in the current study [309]. A 45 and 52% decrease in CLcr and CLur has also been reported with 20 mg/kg/day CyA administered subcutaneously to Wistar rats for 21 days, respectively [262].

Animals given the Sandimmune® formulation showed a significantly lower CLcr than those that received PM-CyA (Table 3.10, Figure 3.11), and the degree of change in CLcr before and after treatment in PM-CyA (H) group was very similar to control animals that received either saline, Cremophor EL or unloaded polymeric micelles (Figure 3.11D). Microscopic examination of stained kidney slices revealed mild tubular and glomerular changes in animals of the Sandimmune® formulation group that were qualitatively not as noticeable in the kidney of rats receiving PM-CyA (H) (Figure 3.13). The mean value of CLur was also lower in the Sandimmune® group than the PM-CyA (H) (Figure 3.11C), although the difference was not significant (P=0.051). No significant difference in plasma potassium levels between the Sandimmune® and PM-CyA (H) was detected (Figure 3.11B).

Creatinine clearance is considered to be a relatively specific indicator of glomerular filtration rate and renal function. In contrast, many factors are known to influence plasma/urine urea levels independent of changes in the glomerular filtration rate. For this

reason, CLur can not be relied on as a sole indicator of renal function [310]. Significant changes in CLur have been observed after short period administration of low doses of CyA. Shihab *et al* [311] reported a 71% increase in blood urea nitrogen (BUN) after 7 days of administration of 10 mg/kg/day CyA dissolved in olive oil to Sprague-Dawley rats subcutaneously.

The size of PM-CyA population developed in this study (between 71-97 nm range) is much larger than the gap in the glomerular capillaries of the kidney. Therefore, provided that there would be sufficient stability of the micellar structure such that encapsulated CyA were retained in the micelles, enhanced CyA blood levels and reduced CyA kidney accumulation would be expected. Indeed, the reduction in the nephrotoxicity of CyA seems to have been related to a reduced delivery of CyA to kidneys by the polymeric micelles after repeated dose administration. The results are consistent with previous findings on biodistribution of PM-CyA after single intravenous administration, where an increase in blood AUC and a decrease in volume of distribution, clearance and kidney AUC were observed for PM-CyA in comparison to Sandimmune® [312]. The greater plasma/kidney CyA concentrations induced by the polymeric micelles is afforded by three functional properties of the PEO-b-PCL micellar carrier in comparison to Cremophor EL micelles in the Sandimmune® formulation: 1) The greater thermodynamic and kinetic stability of the PEO-b-PCL micelles induced by the greater hydrophobicity of the PCL core and stronger interaction between the PCL chains in the micellar core, respectively. This ensures the intact integrity of the polymeric micellar structure (as opposed to Cremophor EL micelles) after dilution in blood circulation, which is a

prerequisite for controlled drug release and prolonged plasma residency for the encapsulated drug from the vehicle. 2) Reduced drug leakage in the presence of plasma proteins[22] and longer association of the encapsulated CyA with the polymeric micellar vehicle in comparison to Cremophor EL micelles, which allows a similar fate for the encapsulated drug and polymeric micellar carrier. 3) The stealth properties of the PEO shell as well as nanoscopic size distribution of the polymeric micelles, which limits their rapid elimination by the reticuloendothelial system and favor prolonged blood circulation of the polymeric micellar carrier in vivo. The combined effect of the three properties could account for the significantly higher plasma/kidney ratios of CyA loaded PEO-b-PCL micelles and reduction in CyA nephrotoxicity.

Indeed, the reduction in the nephrotoxicity of CyA seems to have been related to a reduced delivery of CyA to kidneys by the polymeric micelles after repeat dose administration (Figure 3.12). The results are consistent with previous findings on biodistribution of PM-CyA (I) after single intravenous administration, where an increase in blood AUC and a decrease in volume of distribution, clearance and kidney AUC were observed for PM-CyA (I) in comparison to Sandimmune®.

Other investigators have found that this approach can lead to an alteration in kidney uptake of drugs. For example, Zhang *et al* reported the application of MPEO-poly(D, L-lactide) micelles for physical encapsulation of PXT [51]. The results of biodistribution studies after IP and i.v administration of that formulation showed a 2.1-fold decrease in paclitaxel levels in kidney by polymeric micelles [65]. Encapsulation of paclitaxel in

poly(N-vinyl pyrrolidone)-*block*-PDLLA micelles led to a 2.6-fold decrease in accumulative paclitaxel levels in mice kidneys, as well [57]. Bogdanov *et al* reported the incorporation of cisplatin in MPEO-*b*-poly(L-lysine)-succinate, and demonstrated a 5-fold reduction in the accumulation of encapsulated drug in kidneys [148]. Nishiyama *et al* experiments on polyion complex micelles of cisplatin and MPEO-*block*-poly(glutamic acid) has shown a similar trend in healthy and tumor bearing animals [32]. This research group have also reported on a reduced nephrotoxicity for cisplatin loaded MPEO-*block*-poly(aspartic acid) micelles after a single intravenous administration [145]. The MPEO-*block*-poly(glutamic acid) formulation of cisplatin has also shown reduced nephrotoxicity for the incorporated drug characterized by a reduced plasma concentrations of BUN and creatinine compared to free cisplatin in healthy rats. The latter formulation has recently entered clinical trials in Japan under the name of NC-6004 [152].

Body weight gain in the age range of rats used in this study is normally rapid. A reduction in the rate of body weight is an indicator of a decrease in general health level of the animals. Body weight showed 1.8 % weight gain per day in animals receiving PM-CyA (H) (Figure 3.10) implying a lower systemic toxicity for PM-CyA (H) in comparison to Sandimmune® formulation. Nevertheless, the rate of weight gain in animals receiving PM-CyA (H) was lower than those receiving saline, Cremophor EL or unloaded MPEO-*b*-PCL micelles. This suggests that there was some measured effect of the high dose of CyA delivered by the PM-CyA (H) formulation, and that drug was released from the formulation, though not at a level sufficient to cause the same level of nephrotoxicity as Sandimmune® (Table 3.10). The equal weight gain of animals receiving

unloaded MPEO-*b*-PCL micelles to those receiving normal saline is a generalized indicator of the safety of MPEO-*b*-PCL block copolymers.

Other studies have documented decreases in body weight when given as repeated doses of CyA by other formulations and routes. For example, decreases in the rate of weight gain were noted after subcutaneous administration of 20 mg/kg/day CyA dissolved in olive oil to Wistar rats (150 – 200g) for 21 days [262, 263, 313]. In another study decreases in weight gain were observed in male Sprague-Dawley rats (225 – 250g) given subcutaneous injections of 15 mg/kg/day CyA dissolved in olive oil for 28 days, were found to weigh less than those receiving drug-free olive oil at the end of treatment period (218 vs. 256 g, respectively) [314]. A similar trend was obtained in animals receiving lower doses of 10 mg/kg/day of subcutaneous CyA after 7 or 28 days of administration although the difference between the CyA and olive oil group was not statistically significant [311]. In male spontaneous hypertensive rats (300 – 350 g) with given high doses of 50 mg CyA/kg/day orally dissolved in olive oil for 14 days, a notable weight loss was observed after treatment (266 g average final weight compared to 320 g average initial weight) [315]. The lower rate of weight gain in CyA treated animals observed in these studies is consistent with a CyA-dependent and Cremophor EL independent systemic toxicity in CyA treated rats.

The results have established the ability of MPEO-*b*-PCL as a delivery system capable of directing a nephrotoxic drug such as CyA from kidney, resulting in a reduced nephrotoxicity. Although other liposomal carriers have been developed to reduce

nephrotoxicity and/or increase pharmacological effects of CyA, prior attempts to alter CyA pharmacokinetics by encapsulation of drug in liposomes have not been very successful. For instance, Vadiei *et al* [316] have reported a similar AUC and blood levels for liposomal CyA and Sandimmune® administered intravenously. They also reported higher levels of CyA in liver and spleen. In other studies on pharmacokinetics and biodistribution of liposomal CyA, other than liver accumulation, no significant difference in organ distribution of liposomal CyA and Sandimmune® were observed [266, 267]. Smeesters *et al* [293] reported lower plasma creatinine levels after 14 day intravenous administration of 25 mg/kg/day of CyA associated with phosphatidylcholine/cholesterol liposomes compared to Sandimmune®, but the CyA plasma levels were the same for both groups after the treatment period. Liposome-associated CyA in Freise *et al* study also caused lower plasma creatinine levels after intravenous injection of 1.75 mg/kg/day of CyA for 7 days compared to Sandimmune®, which could have been explained by a lower AUC for the liposomal CyA in blood [317]. This is in contrast to MPEO-*b*-PCL micelles that reduce CyA delivery and toxicity in kidneys while maintaining high blood AUC, which affords promise of an improved therapeutic outcome for CyA administration.

4.1.8. Tumor accumulation

Many studies have demonstrated the efficiency of the polymeric micellar-based nanocarriers in changing the biodistribution pattern of the encapsulated drug by passive targeting, and therefore increasing the chance of accumulation of the drug in a solid tumor in animal models. In micelle forming drug-polymer conjugates, such accumulation is expected due to the stable bond between the therapeutic agent and delivery system. For

instance, in a biodistribution study in solid tumor (C26) bearing mice a tumor/heart concentration ratio of 12, 8.1, and 0.9 was demonstrated for MPEO-*b*-P(Asp)-DOX with MPEO chains of 12000 and 5000 g/mol, and free DOX, respectively, 24 h after i.v injection [20]. In case of drugs physically entrapped in polymeric micelles, however, this achievement is more challenging. Many studies on different micellar formulations have failed to show a favorable change in the pharmacokinetic profile of the encapsulated drug and/or its AUC in different solid tumor models. Even a formulation of MPEO-*b*-PDLLA micelles for physical encapsulation of PXT known as PAXCEED that has reached the clinical trials showed a 5.5 fold decrease in the AUC of polymeric micellar PXT in blood after its i.v administration [65]. The results of biodistribution experiments in healthy rats using radio-labeled PXT demonstrated a rapid loss of drug from the micellar carrier. On the other hand, many other micellar nanocarriers have achieved significant increase in antitumor activity of the encapsulated drug by increasing the AUC of the drug in the tumor via passive targeting [129, 131, 140, 143, 148]. Micelle-forming block copolymers of MPEO-*b*-poly(4-phenyl-1-butanoate) L-aspartamide) (MPEO-*b*-PPBA) for PXT delivery, known as NK105, are probably one of the most successful examples for this achievement. NK105 has shown 86-fold increase in its AUC in plasma, 86-fold decrease in CL and 15–fold decrease in Vdss compared to Taxol® after i.v injection. This has resulted in a 25-fold increase in drug AUC in tumor and stronger anti-tumor activity in C26 tumor bearing mice model, in turn [144].

The results of our preliminary *in vitro* and *in vivo* studies in healthy rodents pointed to a greater promise for PEO-*b*-PCL micellar formulation in tumor targeting and

accumulation. *In vitro* release study and the *fu* results indicated the stability of the micellar formulation, even in presence of biological components. Pharmacokinetic and biodistribution studies showed stealth properties for PM-CyA that increased the AUC of the encapsulated drug in blood and diminished distribution to peripheral tissue, especially for the PM-CyA (H) formulation. Therefore, with the pattern of change in pharmacokinetic and biodistribution of PM-CyA in healthy animals, significant increase in CyA accumulation in a tumor bearing animal model was expected. In fact, 6 hours after the i.v administration, CyA levels were 2.5-fold higher for the micellar formulation compared to Sandimmune® (Figure 3.21). Even though this experiment was only a pilot stage for a complete biodistribution study, the result supports the hypotheses of this project.

4.1.9. Assessing the *in vitro* efficacy of CyA formulations in sensitizing resistant breast tumor cells to DOX

One of the major concerns with the nanocarrier based drug delivery systems is the efficacy of the encapsulated drug. It has been shown that different nanocarriers (including liposomes and polymeric micelles) are capable of changing the pharmacokinetic profile of the encapsulated drug, and therefore, have a promising potential in controlling the toxic effects of the drug on one hand, and increasing the tumor accumulation on the other hand. However, the question is that after the accumulation of the nanocarrier in the tumor, is the effectiveness of the drug limited because of the reduced exposure to the site of action. In this step, stability of the nanocarrier, which is vital to the "targeting" aspect of the delivery system, may work against the efficacy of the drug. The classic example

for such problematic stability is DOX chemically conjugated to MPEO-*b*-P(Asp), which has shown to accumulate in tumor, but not effective due to limited DOX release from its polymeric micellar conjugate [26]. In the present study, the *in vitro* cytotoxicity of DOX against sensitive and resistant breast cancer cells (MDA- MB435/LCC6) after co-administration with Sandimmune® and PM-CyA (H) was compared as a measure of *in vitro* CyA efficacy after a 48 hour incubation period. The MDR phenotype of MDA-MB435/LCC6 cell line is prepared through transfection of the wild type MDA-MB435/LCC6 cells with P-gp gene, i.e., *mdr-1* in the laboratory of Dr Clarck, University of Washington. Therefore, P-gp expression was the only MDR mechanism in effect this cell line making this cell the perfect model for assessing the reversal of P-gp mediated drug resistance.

The resistance of the MDR cell line was indicated by a 17-fold higher IC_{50} for DOX in the resistant cell line (Tables 3.11 and 3.12, and Figures 3.15 and 3.18). Increase in sensitivity factor (or fold reversal) reflects the extent to which the modulator reverses resistance relative to the unmodulated tumor cell. The addition of unloaded micelles (as the vehicle of the micellar formulation) to the cell culture media did not change the IC_{50} of DOX significantly in wild type and MDR cell line. These results point to the non-toxic nature of this biocompatible block copolymer. Besides, no change in the IC_{50} of DOX in the MDR cells after addition of unloaded block copolymers was seen. This observation points to no additional effect on P-gp modulation for 5000-13000 MPEO-*b*-PCL block copolymers. This is in contrast to Pluronic block copolymers that have shown to reverse P-gp mediated drug resistance in the human colon Adenocarcinoma cell line (caco-2)

[318]. However, Cremophor EL, the vehicle used in the Sandimmune® formulation, decreased the IC_{50} of DOX in both wild and resistant cell lines (sensitizing factor of 3.14 and 6.72, respectively; Tables 3.11 and 3.12, and Figures 3.15 and 3.18). Cell growth inhibitory effects of Cremophor EL in different malignant cell lines have been reported in previous studies [319, 320]. Formation of free radicals by peroxidation of polyunsaturated fatty acids and/or a direct perturbing effect on the cell membrane have been hypothesized to be responsible mechanisms for the inhibition of cell growth by Cremophor EL [321]. Several *in vitro* studies have also shown a modulatory effect on P-gp for Cremophor EL [322, 323].

We have seen a decrease in the IC_{50} of DOX in the presence of Sandimmune® compared to free CyA with identical CyA concentrations of 10 μg/mL (Table 3.13 and Figure 3.20) in the resistant cell line. The observation can be attributed to the effect of Cremophor EL present in the formulation of Sandimmune® on cell growth and/or P-gp inhibition. However, the IC_{50} of DOX in the presence of Sandimmune® and free CyA at 5 mg/mL CyA concentration was not significantly different. Perhaps at this concentration the level of Cremophor EL present in the Sandimmune® formulation was not sufficient for cytotoxicity and/or MDR modulation (Table 3.13 and Figure 3.20).

The *in vitro* efficacy of CyA to reverse P-gp mediated MDR has been shown in different cell lines [324, 325]. A significant increase in the sensitivity factor in the presence of CyA formulations have also been observed in our study. For free CyA, increasing the concentration of CyA from 5 to 10 μg /mL did not increase the efficacy of CyA in

reversing MDR in the resistant cell line further (Table 3.13 and Figure 3.20). On the other hand, an identical increase in the concentration of CyA as part of Sandimmune® increased the sensitivity factor from 32.31 to 48.45. This increase can partially be due to the Cremophor EL present in the Sandimmune® formulation, which seems to be the only contribution to the sensitizing effect of CyA at the higher concentrations.

At the concentration of 5 μg/mL, PM-CyA (H) showed a lower efficiency (increase in sensitivity factor = 24.23) compared to Sandimmune® and free CyA sensitivity factors (32.31 for Sandimmune® and free CyA both; Table 3.12 and Figures 3.19 and 3.20). However, at the higher examined CyA concentration (10 μg /mL), there was no significant difference between free CyA and PM-CyA (H) effect in sensitizing the resistant cell line to the cytotoxic effects of DOX, which shows that the micellar nanocarrier has not decrease the MDR modulatory effect of the encapsulated CyA. At this concentration, Sandimmune® showed a higher efficiency in sensitizing the resistant cell line to cytotoxic effect of DOX compared to PM-CyA (H) and free CyA (Table 3.12 and Figures 3.19 and 3.20). Since free CyA and PM-CyA (H) show no significant difference in their sensitizing efficiency, and considering the Cremophor EL effect on the IC_{50} of DOX on this cell line, this higher efficiency of Sandimmune® could be explained by presence of Cremophor EL in the formulation.

4.2 Conclusions

The results of this study showed polymeric micelles of MPEO-*b*-PCL to be capable of efficient encapsulation of CyA by a co-solvent evaporation method achieving 100 fold

increase in the aqueous solubility of CyA. The solubilized level of CyA by its MPEO-*b*-PCL micellar vehicles was comparable to injectable concentration of CyA as part of its Cremophor EL formulation and is considered clinically relevant (Sandimmune® is administered at a concentration of 0.5-2.5 mg/mL intravenously [46]. MPEO-*b*-PCL polymeric micelles were shown to be superior to Cremophor EL micelles in controlling the rate of CyA release *in vitro*.

Additional studies showed manipulation of the self-assembly conditions through reduction of organic to aqueous phase ratio in the co-solvent evaporation method to improve the efficiency of CyA encapsulation in polymeric nanocarriers. The same factor led to the formation of CyA-loaded MPEO-*b*-PCL micelles that were more stable in the presence of blood components avoiding CyA partition out of micelles and binding to plasma proteins. CyA-loaded MPEO-*b*-PCL micelles were able to change the pharmacokinetic pattern of the encapsulated drug increasing its AUC in blood and plasma, and reducing its CL and Vd compared to Cremophor EL formulation. Correlation of pharmacokinetic parameters with the unbound fraction of different CyA formulations estimated by the protein binding experiments confirmed the potential of this *in vitro* test test in estimating the *in vivo* performance of polymeric micellar nanocarriers in changing the pharmacokinetics of the encapsulated drug.

In line with changes in the pharmacokinetic parameters, of encapsulated CyA by its polymeric micellar carrier, the biodistribution pattern of CyA was also modified significantly. Rapid distribution of CyA in kidney and liver, which may be associated

with unfavorable effects of CyA in those organs, was reduced by its incorporation in MPEO-*b*-PCL micelles. This change in CyA's *in vivo* disposition was shown to translate into reduced CyA nephrotoxicity (evidenced by no significant change in the creatinine clearance) by its polymeric micellar formulation after multiple dosing. The reduction in nephrotoxic side effects of CyA was seen despite higher CyA blood levels provided by its polymeric micellar formulation.

Our pilot studies on the biodistribution pattern of PM-CyA in tumor bearing animals showed an increase in the tumor accumulation of CyA and a decrease in its distribution to the sensitive, non-target tissues, such as kidney. Encapsulation of CyA in polymeric micelles did not diminish the efficacy of CyA in sensitizing a human breast cancer resistant cell line to the cytotoxic effects of DOX *in vitro* at higher CyA concentrations. This was evidenced as no significant difference in the IC_{50} of DOX in presence of free CyA or PM-CyA (H) at a CyA concentration of 10 μg /mL was observed.

4.3. Future perspectives

We have shown that the PM-CyA can reduce the toxicity of CyA and possibly act as a sustained release formulation in blood circulation for CyA. Future studies can determine whether this formulation is an effective immunosuppressant in healthy or diseased animal models for autoimmune disorders or transplantation. The developed PM-CyA formulations have a potential application as a tumor targeted P-gp inhibitor that may increase the efficacy while reducing the toxicity of anticancer drugs in co-administration.

The immunosuppressive function of CyA may jeopardize its chance of success as a P-gp inhibitor in overcoming drug resistance in cancer patients that are already immunocomprimised. Therefore, application of second or third generation P-gp inhibitors that are more potent, more specific for P-gp and not immunosuppressive may prove to be a better choice in this case. For instance, CyA analogues (from second and third generations of MDR modulators, such as PSC833) with a higher P-gp inhibition potency and no immunosuppression effect have been extensively studied during last few years. Due to the chemical similarities among these analogues and CyA, the results of this study are expected to be reproducible with any of these analogues. Optimization of preparation process and *in vivo* performance of the polymeric micellar formulations of PSC833 could be a future direction for this project.

An important drawback of using MDR modulators to overcome resistance is the pharmacokinetic interaction between the MDR modulator and the antineoplastic drug that can cause a significant decrease in the elimination of antineoplastic drug (due to inhibition of P-gp dependent excretory mechanisms and cytochrom P450 dependent metabolic processes), enhanced toxic effects for the cytotoxic drug, and therefore an unwanted decrease in the tolerable dose of the anticancer drug. Determination of the maximum tolerable dose (MTD) of a model anticancer drug (such as DOX) in a healthy animal model with and without co-administration of different formulations of CyA can determine the potentials of these nanocarriers to minimize this dose limiting pharmacokinetic interaction.

Conduction of pharmacokinetic, biodistribution, toxicity, and efficacy studies on the anticancer drugs that are substrates of P-gp in co-administration with different CyA formulations can clarify the effect of polymeric micellar formulations on the overall therapeutic benefit of tumor targeted P-gp inhibitor in overcoming drug resistance. Since our biodistribution study in a healthy animal model has shown an increased CyA level in heart with PM-CyA, and the fact that cardiotoxicity of DOX is considered the major side effect for this cytotoxic agent, loading DOX and CyA in this developed MPEO-*b*-PCL nanocarrier might not be suitable. To avoid the risk of cardiotoxicity, we could either pursue this part of project with a different anticancer drug (that is not cardiotoxic), or deliver DOX with a different micellar nanocarrier that is not accumulated in the heart, separately from PM-CyA.

Stability of the micellar structures is one of the challenges in the scale-up and commercialization of micellar formulations. Aggregation of the nanocarriers and loss of encapsulated drug have been reported with storage of the micellar solutions or after reconstitution of freeze dried or frozen samples. In this project, all the micellar formulations were prepared freshly just before the experiments to avoid these complications. A comprehensive study on different stabilizing methods (such as lyophylization) and ingredients (such as lyoprotectants), and determination of stability of each formulation by periodic analysis of micellar characteristics could shed light on proper strategies that would be useful for different micellar formulations.

References

1. Adams, M.L., A. Lavasanifar, and G.S. Kwon, *Amphiphilic block copolymers for drug delivery.* Journal of Pharmaceutical Sciences, 2003. **92**(7): p. 1343-55.
2. Allen, C., A. Eisenberg, and D. Maysinger, *Copolymer drug carriers: Conjugates, micelles and microspheres.* S.T.P. Pharma Sciences, 1999. **9**(1): p. 139-151.
3. Allen, C., D. Maysinger, and A. Eisenberg, *Nano-engineering block copolymer aggregates for drug delivery.* Colloids & Surfaces B: Biointerfaces, 1999. **16**(1-4): p. 3-27.
4. Jones, M. and J. Leroux, *Polymeric micelles - a new generation of colloidal drug carriers.* European Journal of Pharmaceutics & Biopharmaceutics, 1999. **48**(2): p. 101-11.
5. Kabanov, A.V., et al., *Water-soluble block polycations as carriers for oligonucleotide delivery.* Bioconjugate Chemistry, 1995. **6**(6): p. 639-43.
6. Kakizawa, Y. and K. Kataoka, *Block copolymer micelles for delivery of gene and related compounds.* Adv Drug Deliv Rev, 2002. **54**(2): p. 203-22.
7. Kataoka, K., A. Harada, and Y. Nagasaki, *Block copolymer micelles for drug delivery: Design, characterization and biological significance.* Advanced Drug Delivery Reviews, 2001. **47**(1): p. 113-131.
8. Kataoka, K., et al., *Block copolymer micelles as vehicles for drug delivery.* Journal of Controlled Release, 1993. **24**(1-3): p. 119-132.
9. Kwon, G.S., *Block copolymer micelles as drug delivery systems.* Advanced Drug Delivery Reviews, 2002. **54**(2): p. 167.
10. Kwon, G.S., *Diblock copolymer nanoparticles for drug delivery.* Crit Rev Ther Drug Carrier Syst, 1998. **15**(5): p. 481-512.
11. Kwon, G.S., *Polymeric Micelles for Delivery of Poorly Water-Soluble Compounds.* Critical Reviews in Therapeutic Drug Carrier Systems, 2003. **20**(5): p. 357-403.
12. Kwon, G.S. and T. Okano, *Soluble self-assembled block copolymers for drug delivery.* Pharm Res, 1999. **16**(5): p. 597-600.
13. Lavasanifar, A., J. Samuel, and G.S. Kwon, *Poly(ethylene oxide)-block-poly(L-amino acid) micelles for drug delivery.* Adv Drug Deliv Rev, 2002. **54**(2): p. 169-90.
14. Le Garrec, D., M. Ranger, and J.C. Leroux, *Micelles in anticancer drug delivery.* American Journal of Drud Delivery, 2004. **2**(1): p. 15-42.
15. Torchilin, V.P., *PEG-based micelles as carriers of contrast agents for different imaging modalities.* Advanced Drug Delivery Reviews, 2002. **54**(2): p. 235-52.
16. Torchilin, V.P., *Structure and design of polymeric surfactant-based drug delivery systems.* Journal of Controlled Release, 2001. **73**(2-3): p. 137-172.
17. Torchilin, V.P., *Targeted polymeric micelles for delivery of poorly soluble drugs.* Cellular & Molecular Life Sciences, 2004. **61**(19-20): p. 2549-59.
18. Torchilin, V.P., et al., *Immunomicelles: targeted pharmaceutical carriers for poorly soluble drugs.* Proceedings of the National Academy of Sciences of the United States of America, 2003. **100**(10): p. 6039-44.

19. Yokoyama, M., et al., *In vivo antitumor activity of polymeric micelle anticancer drug against murine C 26 tumor.* Journal of Controlled Release, 1994. **28**(1-3): p. 336-337.
20. Kwon, G.S., et al., *Enhanced tumor accumulation and prolonged circulation times of Micelle- forming poly(ethylene oxide-aspartate) block copolymer-adriamycin conjugates.* Journal of Controlled Release, 1994. **28**(1-3): p. 334-335.
21. Yokoyama, M., et al., *Influencing factors on in vitro micelle stability of adriamycin-block copolymer conjugates.* Journal of Controlled Release, 1994. **28**(1-3): p. 59-65.
22. Kwon, G.S., et al., *Biodistribution of micelle-forming polymer-drug conjugates.* Pharmaceutical Research, 1993. **10**(7): p. 970-974.
23. Yokoyama, M., et al., *Analysis of micelle formation of an adriamycin-conjugated poly(ethylene glycol)-poly(aspartic acid) block copolymer by gel permeation chromatography.* Pharmaceutical Research, 1993. **10**(6): p. 895-899.
24. Yokoyama, M., et al., *Preparation of adriamycin-conjugated poly(ethylene glycol)-poly(aspartic acid) block copolymer: A new type of polymeric anticancer agent.* Makromol. Chem., 1987. **8**: p. 431 - 435.
25. Yokoyama, M., et al., *Polymer micelles as novel drug carrier: Adriamycin-conjugated poly(ethylene glycol)-poly(aspartic acid) block copolymer.* Journal of Controlled Release, 1990. **11**(1-3): p. 269-278.
26. Yokoyama, M., et al., *Characterization and anticancer activity of the micelle-forming polymeric anticancer drug Adriamycin-conjugated poly(ethylene glycol)-poly(aspartic acid) block copolymer.* Cancer Research, 1990. **50**(6): p. 1693-1700.
27. Yokoyama, M., et al., *Improved synthesis of adriamycin-conjugated poly(ethylene oxide)-poly(aspartic acid) block copolymer and formation of unimodal micellar structure with controlled amount of physically entrapped adriamycin.* Journal of Controlled Release, 1994. **32**: p. 269-277.
28. Yoo, H.S., E.A. Lee, and T.G. Park, *Doxorubicin-conjugated biodegradable polymeric micelles having acid-cleavable linkages.* J Control Release, 2002. **82**(1): p. 17-27.
29. Yoo, H.S., et al., *In vitro and in vivo anti-tumor activities of nanoparticles based on doxorubicin-PLGA conjugates.* Journal of Controlled Release, 2000. **68**(3): p. 419-31.
30. Yoo, H.S. and T.G. Park, *Biodegradable polymeric micelles composed of doxorubicin conjugated PLGA-PEG block copolymer.* Journal of Controlled Release, 2001. **70**(1-2): p. 63-70.
31. Nishiyama, N., et al., *Preparation and characterization of self-assembled polymer-metal complex micelle from cis-dichlorodiammineplatinium (II) and poly(ethylene glycole)-poly(aspartic acid) block copolymer in an aqueous medium.* Langmuir, 1999. **15**: p. 377-383.
32. Nishiyama, N., et al., *Novel cisplatin-incorporated polymeric micelles can eradicate solid tumors in mice.* Cancer Research., 2003. **63**(24): p. 8977-83.
33. Yuan, X., et al., *Stabilization of lysozyme-incorporated polyion complex micelles by the omega-end derivatization of poly(ethylene glycol)-poly(alpha,beta-aspartic*

acid) block copolymers with hydrophobic groups. Langmuir, 2005. **21**(7): p. 2668-74.

34. Wakebayashi, D., et al., *Polyion complex micelles of pDNA with acetal-poly(ethylene glycol)-poly(2-(dimethylamino)ethyl methacrylate) block copolymer as the gene carrier system: physicochemical properties of micelles relevant to gene transfection efficacy.* Biomacromolecules, 2004. **5**(6): p. 2128-36.
35. Wakebayashi, D., et al., *Lactose-conjugated polyion complex micelles incorporating plasmid DNA as a targetable gene vector system: their preparation and gene transfecting efficiency against cultured HepG2 cells.* J Control Release, 2004. **95**(3): p. 653-64.
36. Itaka, K., et al., *Polyion complex micelles from plasmid DNA and poly(ethylene glycol)-poly(L-lysine) block copolymer as serum-tolerable polyplex system: physicochemical properties of micelles relevant to gene transfection efficiency.* Biomaterials, 2003. **24**(24): p. 4495-506.
37. Rapoport, N.Y., et al., *Micellar delivery of doxorubicin and its paramagnetic analog, ruboxyl, to HL-60 cells: effect of micelle structure and ultrasound on the intracellular drug uptake.* Journal of Controlled Release, 1999. **58**(2): p. 153-62.
38. Kabanov, A.V., et al., *The neuroleptic activity of haloperidol increases after its solubilization in surfactant micelles. Micelles as microcontainers for drug targeting.* FEBS Lett, 1989. **258**(2): p. 343-5.
39. Batrakova, E.V., et al., *Pluronic P85 increases permeability of a broad spectrum of drugs in polarized BBMEC and Caco-2 cell monolayers.* Pharmaceutical Research, 1999. **16**(9): p. 1366-72.
40. Kwon, G.S., et al., *Physical entrapment of adriamycin in AB block copolymer micelles.* Pharmaceutical Research, 1995. **12**(2): p. 192-195.
41. Kim, S.C., et al., *In vivo evaluation of polymeric micellar paclitaxel formulation: toxicity and efficacy.* J Control Release, 2001. **72**(1-3): p. 191-202.
42. Yu, B.G., et al., *Polymeric micelles for drug delivery: solubilization and haemolytic activity of amphotericin B.* Journal of Controlled Release, 1998. **53**(1-3): p. 131-6.
43. Lavasanifar, A., J. Samuel, and G.S. Kwon, *Micelles of poly(ethylene oxide)-block-poly(N-alkyl stearate L-aspartamide): synthetic analogues of lipoproteins for drug delivery.* J Biomed Mater Res, 2000. **52**(4): p. 831-5.
44. Allen, C., et al., *PCL-b-PEO micelles as a delivery vehicle for FK506: Assessment of a functional recovery of crushed peripheral nerve.* Drug Delivery: Journal of Delivery & Targeting of Therapeutic Agents, 2000. **7**(3): p. 139-145.
45. Allen, C., et al., *Polycaprolactone-b-poly(ethylene oxide) copolymer micelles as a delivery vehicle for dihydrotestosterone.* Journal of Controlled Release, 2000. **63**(3): p. 275-86.
46. Aliabadi, H.M. and A. Lavasanifar, *Polymeric micelles for drug delivery.* Expert Opinion on Drug Delivery, 2006. **3**(1): p. 139-162.
47. La, S.B., T. Okano, and K. Kataoka, *Preparation and characterization of the micelle-forming polymeric drug indomethacin-incorporated poly(ethylene oxide)-poly(beta-benzyl L-aspartate) block copolymer micelles.* Journal of Pharmaceutical Sciences, 1996. **85**(1): p. 85-90.

48. Kataoka, K., et al., *Doxorubicin-loaded poly(ethylene glycol)-poly(beta-benzyl-L-aspartate) copolymer micelles: Their pharmaceutical characteristics and biological significance.* Journal of Controlled Release, 2000. **64**(1-3): p. 143-153.
49. Kwon, G., et al., *Block copolymer micelles for drug delivery: Loading and release of doxorubicin.* Journal of Controlled Release, 1997. **48**(2-3): p. 195-201.
50. Lavasanifar, A., J. Samuel, and G.S. Kwon, *The effect of fatty acid substitution on the in vitro release of amphotericin B from micelles composed of poly(ethylene oxide)-block-poly(N-hexyl stearate-L-aspartamide).* J Control Release, 2002. **79**(1-3): p. 165-72.
51. Zhang, X., J.K. Jackson, and H.M. Burt, *Development of amphiphilic diblock copolymers as micellar carriers of taxol.* International Journal of Pharmaceutics, 1996. **132**(1-2): p. 195-206.
52. Zhang, X., et al., *An investigation of the antitumour activity and biodistribution of polymeric micellar paclitaxel.* Cancer Chemother Pharmacol, 1997. **40**(1): p. 81-6.
53. Shuai, X., et al., *Core-cross-linked polymeric micelles as paclitaxel carriers.* Bioconjugate Chemistry, 2004. **15**(3): p. 441-8.
54. Jette, K.K., et al., *Preparation and drug loading of poly(ethylene glycol)-block-poly(epsilon- caprolactone) micelles through the evaporation of a cosolvent azeotrope.* Pharm Res, 2004. **21**(7): p. 1184-1191.
55. Liu, L., et al., *Biodegradable polylactide/poly(ethylene glycol)/polylactide triblock copolymer micelles as anticancer drug carriers.* Journal of Applied Polymer Science, 2001. **80**: p. 1976-1982.
56. Shuai, X., et al., *Micellar carriers based on block copolymers of poly(epsilon-caprolactone) and poly(ethylene glycol) for doxorubicin delivery.* Journal of Controlled Release, 2004. **98**(3): p. 415-26.
57. Le Garrec, D., et al., *Poly(N-vinylpyrrolidone)-block-poly(D,L-lactide) as a new polymeric solubilizer for hydrophobic anticancer drugs: in vitro and in vivo evaluation.* J Control Release, 2004. **99**(1): p. 83-101.
58. Fournier, E., et al., *A novel one-step drug-loading procedure for water-soluble amphiphilic nanocarriers.* Pharm Res, 2004. **21**(6): p. 962-8.
59. Gelderblom, H., et al., *Cremophor EL: The drawbacks and advantages of vehicle selection for drug formulation.* Eur J Cancer, 2001. **37**: p. 1590-1598.
60. Theis, J.G., et al., *Anaphylactoid reactions in children receiving high-dose intravenous cyclosporine for reversal of tumor resistance: the causative role of improper dissolution of Cremophor EL.* J Clin Oncol, 1995. **13**(10): p. 2508-16.
61. Thiel, G., M. Hermle, and F.P. Brunner, *Acutely impaired renal function during intravenous administration of cyclosporine A: a cremophore side-effect.* Clinical Nephrology, 1986. **25 Suppl 1**: p. S40-2.
62. Tibell, A., M. Larsson, and A. Alvestrand, *Dissolving intravenous cyclosporin A in a fat emulsion carrier prevents acute renal side effects in the rat.* Transpl Int, 1993. **6**(2): p. 69-72.
63. Cheon Lee, S., et al., *Polymeric micelles of poly(2-ethyl-2-oxazoline)-block-poly(epsilon-caprolactone) copolymer as a carrier for paclitaxel.* Journal of Controlled Release, 2003. **89**(3): p. 437-46.

64. Ellis, A.G., N.A. Crinis, and L.K. Webster, *Inhibition of etoposide elimination in the isolated perfused rat liver by Cremophor EL and Tween 80.* Cancer Chemother Pharmacol, 1996. **38**(1): p. 81-7.
65. Zhang, X., et al., *Anti-tumor efficacy and biodistribution of intravenous polymeric micellar paclitaxel.* Anticancer Drugs, 1997. **8**(7): p. 696-701.
66. Leung, S.Y., et al., *Polymeric micellar paclitaxel phosphorylates Bcl-2 and induces apoptotic regression of androgen-independent LNCaP prostate tumors.* Prostate, 2000. **44**(2): p. 156-63.
67. Piskin, E., et al., *Novel PDLLA/PEG copolymer micelles as drug carriers.* Journal of Biomaterials Science, Polymer Edition, 1995. **7**(4): p. 359-73.
68. Yokoyama, M., et al., *Incorporation of water-insoluble anticancer drug into polymeric micelles and control of their particle size.* J Control Release, 1998. **55**(2-3): p. 219-29.
69. Matsumura, Y., et al., *Reduction of the side effects of an antitumor agent, KRN5500, by incorporation of the drug into polymeric micelles.* Jpn J Cancer Res, 1999. **90**(1): p. 122-8.
70. Mizumura, Y., et al., *Incorporation of the anticancer agent KRN5500 into polymeric micelles diminishes the pulmonary toxicity.* Jpn J Cancer Res, 2002. **93**(11): p. 1237-43.
71. Lavasanifar, A., J. Samuel, and G.S. Kwon, *Micelles self-assembled from poly(ethylene oxide)-block-poly(N-hexyl stearate L-aspartamide) by a solvent evaporation method: effect on the solubilization and haemolytic activity of amphotericin B.* J Control Release, 2001. **77**(1-2): p. 155-60.
72. Li, Y. and G.S. Kwon, *Methotrexate esters of poly(ethylene oxide)-block-poly(2-hydroxyethyl-L-aspartamide). Part I: Effects of the level of methotrexate conjugation on the stability of micelles and on drug release.* Pharm Res, 2000. **17**(5): p. 607-11.
73. Nishiyama, N., et al., *Differential gene expression profile between PC-14 cells treated with free cisplatin and cisplatin-incorporated polymeric micelles.* Bioconjugate Chemistry., 2003. **14**(2): p. 449-57.
74. Matsuya, T., et al., *A core-shell-type fluorescent nanosphere possessing reactive poly(ethylene glycol) tethered chains on the surface for zeptomole detection of protein in time-resolved fluorometric immunoassay.* Anal Chem, 2003. **75**(22): p. 6124-32.
75. Lee, J., E.C. Cho, and K. Cho, *Incorporation and release behavior of hydrophobic drug in functionalized poly(D,L-lactide)-block-poly(ethylene oxide) micelles.* J Control Release, 2004. **94**(2-3): p. 323-35.
76. Rapoport, N., *Stabilization and activation of Pluronic micelles for tumor-targeted drug delivery.* Colloids & Surfaces B: Biointerfaces, 1999. **16**(1-4): p. 93-111.
77. Jeong, Y.I., et al., *Adriamycin release from flower-type polymeric micelle based on star-block copolymer composed of poly(gamma-benzyl L-glutamate) as the hydrophobic part and poly(ethylene oxide) as the hydrophilic part.* International Journal of Pharmaceutics, 1999. **188**(1): p. 49-58.
78. Yokoyama, M., et al., *Selective delivery of adiramycin to a solid tumor using a polymeric micelle carrier system.* Journal of Drug Targeting, 1999. **7**(3): p. 171-186.

79. Lavasanifar, A., et al., *Block copolymer micelles for the encapsulation and delivery of amphotericin B.* Pharmaceutical Research, 2002. **19**(4): p. 418-422.
80. Nah, J.W., et al., *Clonazepam release from poly(DL-lactide-co-glycolide) nanoparticles prepared by dialysis method.* Arch Pharm Res, 1998. **21**(4): p. 418-22.
81. Jeong, Y.I., et al., *Clonazepam release from core-shell type nanoparticles in vitro.* J Control Release, 1998. **51**(2-3): p. 169-78.
82. Tsukioka, Y., et al., *Pharmaceutical and biomedical differences between micellar doxorubicin (NK911) and liposomal doxorubicin (Doxil).* Jpn J Cancer Res, 2002. **93**(10): p. 1145-53.
83. Maeda, H. and Y. Matsumura, *Tumoritropic and lymphotropic principles of macromolecular drugs.* Critical Reviews in Therapeutic Drug Carrier Systems, 1989. **6**(3): p. 193-210.
84. Matsumura, Y. and H. Maeda, *A new concept for macromolecular therapeutics in cancer chemotherapy: mechanism of tumoritropic accumulation of proteins and the antitumor agent smancs.* Cancer Res, 1986. **46**(12 Pt 1): p. 6387-92.
85. Maeda, H., *The enhanced permeability and retention (EPR) effect in tumor vasculature: the key role of tumor-selective macromolecular drug targeting.* Advances in Enzyme Regulation, 2001. **41**: p. 189-207.
86. Maeda, H., et al., *Tumor vascular permeability and the EPR effect in macromolecular therapeutics: A review.* Journal of Controlled Release, 2000. **65**(1-2): p. 271-284.
87. Hashizume, H., et al., *Openings between defective endothelial cells explain tumor vessel leakiness.* American Journal of Pathology, 2000. **156**(4): p. 1363-80.
88. Heldin, C.H., et al., *High interstitial fluid pressure - an obstacle in cancer therapy.* Nat Rev Cancer, 2004. **4**(10): p. 806-13.
89. Edens, H.A., et al., *Neutrophil transepithelial migration: evidence for sequential, contact-dependent signaling events and enhanced paracellular permeability independent of transjunctional migration.* Journal of Immunology, 2002. **169**(1): p. 476-86.
90. Schiffelers, R.M., G. Storm, and I.A. Bakker-Woudenberg, *Host factors influencing the preferential localization of sterically stabilized liposomes in Klebsiella pneumoniae-infected rat lung tissue.* Pharmaceutical Research, 2001. **18**(6): p. 780-7.
91. Harris, A.L., *Hypoxia--a key regulatory factor in tumour growth.* Nat Rev Cancer, 2002. **2**(1): p. 38-47.
92. Wang, G.L., et al., *Hypoxia-inducible factor 1 is a basic-helix-loop-helix-PAS heterodimer regulated by cellular O2 tension.* Proc Natl Acad Sci U S A, 1995. **92**(12): p. 5510-4.
93. Jubb, A.M., et al., *Predicting benefit from anti-angiogenic agents in malignancy.* Nat Rev Cancer, 2006. **6**(8): p. 626-35.
94. Senger, D.R., et al., *Tumor cells secrete a vascular permeability factor that promotes accumulation of ascites fluid.* Science, 1983. **219**(4587): p. 983-5.
95. Ferrara, N., *Vascular endothelial growth factor: basic science and clinical progress.* Endocr Rev, 2004. **25**(4): p. 581-611.

96. Rafii, S., et al., *Vascular and haematopoietic stem cells: novel targets for anti-angiogenesis therapy?* Nat Rev Cancer, 2002. **2**(11): p. 826-35.
97. Maeda, H., Y. Matsumura, and H. Kato, *Purification and identification of [hydroxyprolyl3]bradykinin in ascitic fluid from a patient with gastric cancer.* Journal of Biological Chemistry, 1988. **263**(31): p. 16051-4.
98. Matsumura, Y., et al., *Involvement of the kinin-generating cascade in enhanced vascular permeability in tumor tissue.* Japanese Journal of Cancer Research, 1988. **79**(12): p. 1327-34.
99. Matsumura, Y., et al., *Kinin-generating cascade in advanced cancer patients and in vitro study.* Japanese Journal of Cancer Research, 1991. **82**(6): p. 732-41.
100. Wu, J., T. Akaike, and H. Maeda, *Modulation of enhanced vascular permeability in tumors by a bradykinin antagonist, a cyclooxygenase inhibitor, and a nitric oxide scavenger.* Cancer Research, 1998. **58**(1): p. 159-65.
101. Doi, K., et al., *Excessive production of nitric oxide in rat solid tumor and its implication in rapid tumor growth.* Cancer, 1996. **77**(8 Suppl): p. 1598-604.
102. Maeda, H., et al., *Enhanced vascular permeability in solid tumor is mediated by nitric oxide and inhibited by both new nitric oxide scavenger and nitric oxide synthase inhibitor.* Japanese Journal of Cancer Research, 1994. **85**(4): p. 331-4.
103. Reichman, H.R., C.L. Farrell, and R.F. Del Maestro, *Effects of steroids and nonsteroid anti-inflammatory agents on vascular permeability in a rat glioma model.* Journal of Neurosurgery, 1986. **65**(2): p. 233-7.
104. Wu, J., et al., *Enhanced vascular permeability in solid tumor involving peroxynitrite and matrix metalloproteinases.* Japanese Journal of Cancer Research, 2001. **92**(4): p. 439-51.
105. Bergers, G. and L.E. Benjamin, *Tumorigenesis and the angiogenic switch.* Nat Rev Cancer, 2003. **3**(6): p. 401-10.
106. Fukumura, D., S. Kashiwagi, and R.K. Jain, *The role of nitric oxide in tumour progression.* Nat Rev Cancer, 2006. **6**(7): p. 521-34.
107. Overall, C.M. and O. Kleifeld, *Tumour microenvironment - opinion: validating matrix metalloproteinases as drug targets and anti-targets for cancer therapy.* Nat Rev Cancer, 2006. **6**(3): p. 227-39.
108. Jain, R.K., *Transport of molecules across tumor vasculature.* Cancer & Metastasis Reviews, 1987. **6**(4): p. 559-93.
109. Noguchi, Y., et al., *Early phase tumor accumulation of macromolecules: a great difference in clearance rate between tumor and normal tissues.* Japanese Journal of Cancer Research, 1998. **89**(3): p. 307-14.
110. Maki, S., T. Konno, and H. Maeda, *Image enhancement in computerized tomography for sensitive diagnosis of liver cancer and semiquantitation of tumor selective drug targeting with oily contrast medium.* Cancer, 1985. **56**(4): p. 751-7.
111. Konno, T., et al., *Selective targeting of anti-cancer drug and simultaneous image enhancement in solid tumors by arterially administered lipid contrast medium.* Cancer, 1984. **54**(11): p. 2367-74.
112. Chau, Y., et al., *Investigation of targeting mechanism of new dextran-peptide-methotrexate conjugates using biodistribution study in matrix-metalloproteinase-overexpressing tumor xenograft model.* Journal of Pharmaceutical Sciences, 2006. **95**(3): p. 542-51.

113. Xiong, X.B., et al., *Enhanced intracellular delivery and improved antitumor efficacy of doxorubicin by sterically stabilized liposomes modified with a synthetic RGD mimetic.* Journal of Controlled Release, 2005. **107**(2): p. 262-75.
114. Shenoy, D., et al., *Poly(ethylene oxide)-modified poly(beta-amino ester) nanoparticles as a pH-sensitive system for tumor-targeted delivery of hydrophobic drugs: part 2. In vivo distribution and tumor localization studies.* Pharmaceutical Research, 2005. **22**(12): p. 2107-14.
115. Jun, Y.J., et al., *Selective tumor targeting by enhanced permeability and retention effect. Synthesis and antitumor activity of polyphosphazene-platinum (II) conjugates.* Journal of Inorganic Biochemistry, 2005. **99**(8): p. 1593-601.
116. Greish, K., et al., *Copoly(styrene-maleic acid)-pirarubicin micelles: high tumor-targeting efficiency with little toxicity.* Bioconjugate Chemistry, 2005. **16**(1): p. 230-6.
117. Gao, Z.G., et al., *Doxorubicin loaded pH-sensitive micelle targeting acidic extracellular pH of human ovarian A2780 tumor in mice.* Journal of Drug Targeting, 2005. **13**(7): p. 391-7.
118. Maeda, H., *SMANCS and polymer-conjugated macromolecular drugs: advantages in cancer chemotherapy.* Advanced Drug Delivery Reviews, 2001. **46**(1-3): p. 169-85.
119. Muggia, F.M., *Doxorubicin-polymer conjugates: further demonstration of the concept of enhanced permeability and retention.[comment].* Clinical Cancer Research, 1999. **5**(1): p. 7-8.
120. Allen, T.M. and C. Hansen, *Pharmacokinetics of stealth versus conventional liposomes: effect of dose.* Biochim Biophys Acta, 1991. **1068**(2): p. 133-41.
121. Allen, T.M., et al., *Liposomes containing synthetic lipid derivatives of poly(ethylene glycol) show prolonged circulation half-lives in vivo.* Biochim Biophys Acta, 1991. **1066**(1): p. 29-36.
122. Allen, T.M., C.B. Hansen, and D.E. Lopes de Menezes, *Pharmacokinetics of long circulating liposomes.* Adv Drug Deliv Rev, 1995. **16**(2-3): p. 267-284.
123. Allen, T.M., et al., *Pharmacokinetics and anti-tumor activity of vincristine encapsulated in sterically stabilized liposomes.* Int J Cancer, 1995. **62**(2): p. 199-204.
124. Gabizon, A., H. Shmeeda, and Y. Barenholz, *Pharmacokinetics of pegylated liposomal Doxorubicin: review of animal and human studies.* Clin Pharmacokinet, 2003. **42**(5): p. 419-36.
125. Harris, J.M., N.E. Martin, and M. Modi, *Pegylation: a novel process for modifying pharmacokinetics.* Clin Pharmacokinet, 2001. **40**(7): p. 539-51.
126. Moghimi, S.M. and J. Szebeni, *Stealth liposomes and long circulating nanoparticles: critical issues in pharmacokinetics, opsonization and protein-binding properties.* Prog Lipid Res, 2003. **42**(6): p. 463-78.
127. Gao, Z., et al., *PEG-PE/phosphatidylcholine mixed immunomicelles specifically deliver encapsulated taxol to tumor cells of different origin and promote their efficient killing.* J Drug Target, 2003. **11**(2): p. 87-92.
128. Park, E.K., et al., *Folate-conjugated methoxy poly(ethylene glycol)/poly(epsilon-caprolactone) amphiphilic block copolymeric micelles for tumor-targeted drug delivery.* J Control Release, 2005. **109**(1-3): p. 158-68.

129. Yoo, H.S. and T.G. Park, *Folate receptor targeted biodegradable polymeric doxorubicin micelles.* Journal of Controlled Release, 2004. **96**(2): p. 273-83.
130. Pitt, W.G., G.A. Husseini, and B.J. Staples, *Ultrasonic drug delivery--a general review.* Expert Opin Drug Deliv, 2004. **1**(1): p. 37-56.
131. Rapoport, N.Y., et al., *Ultrasound-triggered drug targeting of tumors in vitro and in vivo.* Ultrasonics, 2004. **42**(1-9): p. 943-50.
132. Le Garrec, D., et al., *Optimizing pH-responsive polymeric micelles for drug delivery in a cancer photodynamic therapy model.* Journal of Drug Targeting, 2002. **10**(5): p. 429-37.
133. Lee, E.S., et al., *Poly(L-histidine)-PEG block copolymer micelles and pH-induced destabilization.* Journal of Controlled Release, 2003. **90**(3): p. 363-74.
134. Taillefer, J., et al., *In-vitro and in-vivo evaluation of pH-responsive polymeric micelles in a photodynamic cancer therapy model.* J Pharm Pharmacol, 2001. **53**(2): p. 155-66.
135. Chung, J.E., M. Yokoyama, and T. Okano, *Inner core segment design for drug delivery control of thermo-responsive polymeric micelles.* Journal of Controlled Release, 2000. **65**(1-2): p. 93-103.
136. Liu, S.Q., Y.W. Tong, and Y.Y. Yang, *Incorporation and in vitro release of doxorubicin in thermally sensitive micelles made from poly(N-isopropylacrylamide-co-N,N-dimethylacrylamide)-b-poly(D,L-lactide-co-glycolide) with varying compositions.* Biomaterials, 2005. **26**(24): p. 5064-74.
137. Bae, Y., et al., *Multifunctional polymeric micelles with folate-mediated cancer cell targeting and pH-triggered drug releasing properties for active intracellular drug delivery.* Mol Biosyst, 2005. **1**(3): p. 242-50.
138. Sawant, R.M., et al., *"SMART" drug delivery systems: double-targeted pH-responsive pharmaceutical nanocarriers.* Bioconjug Chem, 2006. **17**(4): p. 943-9.
139. Sethuraman, V.A. and Y.H. Bae, *TAT peptide-based micelle system for potential active targeting of anti-cancer agents to acidic solid tumors.* J Control Release, 2007. **118**(2): p. 216-24.
140. Nakanishi, T., et al., *Development of the polymer micelle carrier system for doxorubicin.* Journal of Controlled Release, 2001. **74**(1-3): p. 295-302.
141. Matsumura, Y., et al., *Phase I clinical trial and pharmacokinetic evaluation of NK911, a micelle-encapsulated doxorubicin.* Br J Cancer, 2004. **91**(10): p. 1775-81.
142. Yokoyama, M., et al., *Toxicity and antitumor activity against solid tumors of micelle-forming polymeric anticancer drug and its extremely long circulation in blood.* Cancer Res, 1991. **51**(12): p. 3229-36.
143. Alakhov, V., et al., *Block copolymer-based formulation of doxorubicin. From cell screen to clinical trials.* Colloids & Surfaces B: Biointerfaces, 1999. **16**(1-4): p. 113-134.
144. Hamaguchi, T., et al., *NK105, a paclitaxel-incorporating micellar nanoparticle formulation, can extend in vivo antitumour activity and reduce the neurotoxicity of paclitaxel.* Br J Cancer, 2005. **92**(7): p. 1240-6.
145. Nishiyama, N., et al., *Cisplatin-loaded polymer-metal complex micelle with time-modulated decaying property as a novel drug delivery system.* Pharm Res, 2001. **18**(7): p. 1035-41.

146. Mizumura, Y., et al., *Cisplatin-incorporated polymeric micelles eliminate nephrotoxicity, while maintaining antitumor activity.* Japanese Journal of Cancer Research, 2001. **92**(3): p. 328-336.
147. Cabral, H., et al., *Preparation and biological properties of dichloro(1,2-diaminocyclohexane)platinum(II) (DACHPt)-loaded polymeric micelles.* J Control Release, 2005. **101**(1-3): p. 223-32.
148. Bogdanov, A.A., Jr., et al., *An adduct of cis-diamminedichloroplatinum(II) and poly(ethylene glycol)poly(L-lysine)-succinate: synthesis and cytotoxic properties.* Bioconjugate Chemistry, 1996. **7**(1): p. 144-9.
149. Shi, B., et al., *Stealth MePEG-PCL micelles: Effects of polymer composition on micelles physiochemical characteristics, in vitro drug release, in vivo pharmacokinetics in rats and biodistribution in S180 tumor bearing mice.* Colloid and Polymer Science, 2005. **283**(9): p. 954-967.
150. Danson, S., et al., *Phase I dose escalation and pharmacokinetic study of pluronic polymer-bound doxorubicin (SP1049C) in patients with advanced cancer.* Br J Cancer, 2004. **90**(11): p. 2085-91.
151. Kim, T.Y., et al., *Phase I and pharmacokinetic study of Genexol-PM, a cremophor-free, polymeric micelle-formulated paclitaxel, in patients with advanced malignancies.* Clin Cancer Res, 2004. **10**(11): p. 3708-16.
152. Uchino, H., et al., *Cisplatin-incorporating polymeric micelles (NC-6004) can reduce nephrotoxicity and neurotoxicity of cisplatin in rats.* British Journal of Cancer, 2005. **93**(6): p. 678-87.
153. Zhang, N. and S. Guo, *Studies on a kind of new biodegradable biomaterial, polycaprolactone and developments in medicinal area.* Journal of Biomedical Engineering, 2003. **20**(4): p. 746-749.
154. Ory, S., et al., *The effect of a biodegradable contraceptive capsule (Capronor) containing levonorgestrel on gonadotropine, estrogen and progestrone levels.* American Journal of Obstetrics and Gynecology, 1983. **145**(5): p. 600-605.
155. Rutledge, B., et al., *Treatment of Osteomyelitis with local antibiotics delivered via bioabsorbable polymer.* Clinical Orthopedics and Related Research, 2003. **441**: p. 280-287.
156. Isotalo, T., et al., *Tissue biocompatibility of a new caprolactone-coated self-reinforced self-expandable poly-L-lactic acid bioabsorbable urethral stent.* Journal of Endourology, 1999. **13**(7): p. 525-530.
157. Liu, J., F. Zeng, and C. Allen, *In vivo fate of unimers and micelles of a poly(ethylene glycol)-block-poly(caprolactone) copolymer in mice following intravenous administration.* Eur J Pharm Biopharm, 2007. **65**(3): p. 309-19.
158. Park, Y.J., et al., *Radioisotope carrying polyethylene oxide-polycaprolactone copolymer micelles for targetable bone imaging.* Biomaterials, 2002. **23**(3): p. 873-9.
159. Shin, I.G., et al., *Methoxy poly(ethylene glycol)/epsilon-caprolactone amphiphilic block copolymeric micelle containing indomethacin. I. Preparation and characterization.* Journal of Controlled Release, 1998. **51**(1): p. 1-11.
160. Ge, H., et al., *Preparation, characterization, and drug release behaviors of drug nimodipine-loaded poly(epsilon-caprolactone)-poly(ethylene oxide)-poly(epsilon-*

caprolactone) amphiphilic triblock copolymer micelles. Journal of Pharmaceutical Sciences, 2002. **91**(6): p. 1463-73.
161. Boumendjel, A., et al., *Anticancer multidrug resistance mediated by MRP1: recent advances in the discovery of reversal agents.* Med Res Rev, 2005. **25**(4): p. 453-72.
162. Tsuruo, T., et al., *Molecular targeting therapy of cancer: drug resistance, apoptosis and survival signal.* Cancer Sci, 2003. **94**(1): p. 15-21.
163. Donnenberg, V.S. and A.D. Donnenberg, *Multiple drug resistance in cancer revisited: the cancer stem cell hypothesis.* J Clin Pharmacol, 2005. **45**(8): p. 872-7.
164. Krishna, R. and L.D. Mayer, *Multidrug resistance (MDR) in cancer. Mechanisms, reversal using modulators of MDR and the role of MDR modulators in influencing the pharmacokinetics of anticancer drugs.* European Journal of Pharmaceutical Sciences, 2000. **11**(4): p. 265-83.
165. Gottesman, M.M., *Mechanisms of Cancer Drug Resistance.* Annual Reviews of Medicine, 2002. **53**: p. 615-27.
166. Thomas, H. and H.M. Coley, *Overcoming multidrug resistance in cancer: an update on the clinical strategy of inhibiting p-glycoprotein.* Cancer Control, 2003. **10**(2): p. 159-65.
167. Krishnamachary, N. and M.S. Center, *The MRP gene associated with a non-P-glycoprotein multidrug resistance encodes a 190-kDa membrane bound glycoprotein.* Cancer Res, 1993. **53**(16): p. 3658-61.
168. Almquist, K.C., et al., *Characterization of the M(r) 190,000 multidrug resistance protein (MRP) in drug-selected and transfected human tumor cell.* Cancer Res, 1995. **55**(1): p. 102-10.
169. Dean, M., T. Fojo, and S. Bates, *Tumour stem cells and drug resistance.* Nat Rev Cancer, 2005. **5**(4): p. 275-84.
170. Meister, A., *Glutathione deficiency produced by inhibition of its synthesis, and its reversal; applications in research and therapy.* Pharmacol Ther, 1991. **51**(2): p. 155-94.
171. Meister, A., *Glutathione, ascorbate, and cellular protection.* Cancer Res, 1994. **54**(7 Suppl): p. 1969s-1975s.
172. Tewey, K.M., et al., *Intercalative antitumor drugs interfere with the breakage-reunion reaction of mammalian DNA topoisomerase II.* J Biol Chem, 1984. **259**(14): p. 9182-7.
173. Matsuo, K., et al., *Reduction of drug accumulation and DNA topoisomerase II activity in acquired teniposide-resistant human cancer KB cell lines.* Cancer Res, 1990. **50**(18): p. 5819-24.
174. Tan, K.B., et al., *Altered expression and transcription of the topoisomerase II gene in nitrogen mustard-resistant human cells.* Biochem Pharmacol, 1988. **37**(22): p. 4413-6.
175. Lowe, S.W., et al., *p53-dependent apoptosis modulates the cytotoxicity of anticancer agents.* Cell, 1993. **74**(6): p. 957-67.
176. Fisher, T.C., et al., *bcl-2 modulation of apoptosis induced by anticancer drugs: resistance to thymidylate stress is independent of classical resistance pathways.* Cancer Res, 1993. **53**(14): p. 3321-6.

177. Johnstone, R.W., A.A. Ruefli, and M.J. Smyth, *Multiple physiological functions for multidrug transporter P-glycoprotein?* Trends Biochem Sci, 2000. **25**(1): p. 1-6.
178. Matheny, C.J., et al., *Pharmacokinetic and pharmacodynamic implications of P-glycoprotein modulation.* Pharmacotherapy, 2001. **21**(7): p. 778-96.
179. Higgins, C.F., et al., *Structure of the multidrug resistance P-glycoprotein.* Semin Cancer Biol, 1997. **8**(3): p. 135-42.
180. Bellamy, W.T., *P-glycoproteins and multidrug resistance.* Annu Rev Pharmacol Toxicol, 1996. **36**: p. 161-83.
181. Loo, T.W. and D.M. Clarke, *Inhibition of oxidative cross-linking between engineered cysteine residues at positions 332 in predicted transmembrane segments (TM) 6 and 975 in predicted TM12 of human P-glycoprotein by drug substrates.* J Biol Chem, 1996. **271**(44): p. 27482-7.
182. Bliss, J.M. and R.P. Silver, *Evidence that KpsT, the ATP-binding component of an ATP-binding cassette transporter, is exposed to the periplasm and associates with polymer during translocation of the polysialic acid capsule of Escherichia coli K1.* J Bacteriol, 1997. **179**(4): p. 1400-3.
183. Homolya, L., et al., *Fluorescent cellular indicators are extruded by the multidrug resistance protein.* J Biol Chem, 1993. **268**(29): p. 21493-6.
184. Cordon-Cardo, C., et al., *Expression of the multidrug resistance gene product (P-glycoprotein) in human normal and tumor tissues.* J Histochem Cytochem, 1990. **38**(9): p. 1277-87.
185. Ambudkar, S.V., et al., *Biochemical, cellular, and pharmacological aspects of the multidrug transporter.* Annu Rev Pharmacol Toxicol, 1999. **39**: p. 361-98.
186. Hsing, S., Z. Gatmaitan, and I.M. Arias, *The function of Gp170, the multidrug-resistance gene product, in the brush border of rat intestinal mucosa.* Gastroenterology, 1992. **102**(3): p. 879-85.
187. Watkins, P.B., *Drug metabolism by cytochromes P450 in the liver and small bowel.* Gastroenterol Clin North Am, 1992. **21**(3): p. 511-26.
188. Kusuhara, H., H. Suzuki, and Y. Sugiyama, *The role of P-glycoprotein and canalicular multispecific organic anion transporter in the hepatobiliary excretion of drugs.* J Pharm Sci, 1998. **87**(9): p. 1025-40.
189. Garcia del Moral, R., et al., *Relationship between P-glycoprotein expression and cyclosporin A in kidney. An immunohistological and cell culture study.* Am J Pathol, 1995. **146**(2): p. 398-408.
190. Okamura, N., et al., *Digoxin-cyclosporin A interaction: modulation of the multidrug transporter P-glycoprotein in the kidney.* J Pharmacol Exp Ther, 1993. **266**(3): p. 1614-9.
191. Joo, F., *Endothelial cells of the brain and other organ systems: some similarities and differences.* Prog Neurobiol, 1996. **48**(3): p. 255-73.
192. van Asperen, J., et al., *The functional role of P-glycoprotein in the blood-brain barrier.* J Pharm Sci, 1997. **86**(8): p. 881-4.
193. Drion, N., et al., *Role of P-glycoprotein in the blood-brain transport of colchicine and vinblastine.* J Neurochem, 1996. **67**(4): p. 1688-93.

194. Beaulieu, E., et al., *P-glycoprotein is strongly expressed in the luminal membranes of the endothelium of blood vessels in the brain.* Biochem J, 1997. **326 (Pt 2)**: p. 539-44.
195. Srinivas, R.V., et al., *Human immunodeficiency virus protease inhibitors serve as substrates for multidrug transporter proteins MDR1 and MRP1 but retain antiviral efficacy in cell lines expressing these transporters.* Antimicrob Agents Chemother, 1998. **42**(12): p. 3157-62.
196. Klimecki, W.T., C.W. Taylor, and W.S. Dalton, *Inhibition of cell-mediated cytolysis and P-glycoprotein function in natural killer cells by verapamil isomers and cyclosporine A analogs.* J Clin Immunol, 1995. **15**(3): p. 152-8.
197. Gupta, S. and S. Gollapudi, *P-glycoprotein (MDR 1 gene product) in cells of the immune system: its possible physiologic role and alteration in aging and human immunodeficiency virus-1 (HIV-1) infection.* J Clin Immunol, 1993. **13**(5): p. 289-301.
198. Fardel, O., V. Lecureur, and A. Guillouzo, *The P-glycoprotein multidrug transporter.* Gen Pharmacol, 1996. **27**(8): p. 1283-91.
199. Tsuruo, T., et al., *Overcoming of vincristine resistance in P388 leukemia in vivo and in vitro through enhanced cytotoxicity of vincristine and vinblastine by verapamil.* Cancer Res, 1981. **41**(5): p. 1967-72.
200. Roepe, P.D., *Analysis of the steady-state and initial rate of doxorubicin efflux from a series of multidrug-resistant cells expressing different levels of P-glycoprotein.* Biochemistry, 1992. **31**(50): p. 12555-64.
201. Foxwell, B.M., et al., *Identification of the multidrug resistance-related P-glycoprotein as a cyclosporine binding protein.* Molecular Pharmacology, 1989. **36**(4): p. 543-6.
202. Atadja, P., et al., *PSC-833, a frontier in modulation of P-glycoprotein mediated multidrug resistance.* Cancer Metastasis Rev, 1998. **17**(2): p. 163-8.
203. Kessel, D. and C. Wilberding, *Promotion of daunorubicin uptake and toxicity by the calcium antagonist tiapamil and its analogs.* Cancer Treat Rep, 1985. **69**(6): p. 673-6.
204. Dantzig, A.H., et al., *Reversal of P-glycoprotein-mediated multidrug resistance by a potent cyclopropyldibenzosuberane modulator, LY335979.* Cancer Research, 1996. **56**(18): p. 4171-9.
205. Hyafil, F., et al., *In vitro and in vivo reversal of multidrug resistance by GF120918, an acridonecarboxamide derivative.* Cancer Res, 1993. **53**(19): p. 4595-602.
206. Dale, I.L., et al., *Reversal of P-glycoprotein-mediated multidrug resistance by XR9051, a novel diketopiperazine derivative.* British Journal of Cancer, 1998. **78**(7): p. 885-92.
207. Newman, M.J., et al., *Discovery and characterization of OC144-093, a novel inhibitor of P-glycoprotein-mediated multidrug resistance.* Cancer Res, 2000. **60**(11): p. 2964-72.
208. Germann, U.A., et al., *VX-853: A novel bispecific chemosentisizer which reverses P-glycoprotein and MRP-mediated multidrug resistance.* Proc. of American Assosation for Cancer Research, 1996. **37**: p. 335.

209. Bradshaw, D.M. and R.J. Arceci, *Clinical relevance of transmembrane drug efflux as a mechanism of multidrug resistance. [erratum appears in J Clin Oncol 1999 Apr;17(4):1330.].* Journal of Clinical Oncology, 1998. **16**(11): p. 3674-90.
210. Mayer, L.D. and J.A. Shabbits, *The role for liposomal drug delivery in molecular and pharmacological strategies to overcome multidrug resistance.* Cancer & Metastasis Reviews, 2001. **20**(1-2): p. 87-93.
211. Oudard, S., J.P. Marie, and E. Pujade Lauraine, *[MDR (Multiple Drug Resistant) type of resistance to chemotherapy in clinical practice].* Bull Cancer, 1996. **83**(8): p. 609-18.
212. Sikic, B.I., *Pharmacologic approaches to reversing multidrug resistance.* Semin Hematol, 1997. **34**(4 Suppl 5): p. 40-7.
213. Ferry, D.R., H. Traunecker, and D.J. Kerr, *Clinical trials of P-glycoprotein reversal in solid tumours.* Eur J Cancer, 1996. **32A**(6): p. 1070-81.
214. Speeg, K.V., et al., *Effect of cyclosporine on colchicine secretion by a liver canalicular transporter studied in vivo.* Hepatology, 1992. **15**(5): p. 899-903.
215. Speeg, K.V. and A.L. Maldonado, *Effect of the nonimmunosuppressive cyclosporin analog SDZ PSC-833 on colchicine and doxorubicin biliary secretion by the rat in vivo.* Cancer Chemother Pharmacol, 1994. **34**(2): p. 133-6.
216. Kaye, S.B., *Multidrug resistance: clinical relevance in solid tumours and strategies for circumvention.* Curr Opin Oncol, 1998. **10 Suppl 1**: p. S15-9.
217. Advani, R., et al., *A phase I trial of doxorubicin, paclitaxel, and valspodar (PSC 833), a modulator of multidrug resistance.* Clin Cancer Res, 2001. **7**(5): p. 1221-9.
218. Fracasso, P.M., et al., *Phase I study of paclitaxel in combination with a multidrug resistance modulator, PSC 833 (Valspodar), in refractory malignancies.* J Clin Oncol, 2000. **18**(5): p. 1124-34.
219. Fracasso, P.M., et al., *Phase II study of paclitaxel and valspodar (PSC 833) in refractory ovarian carcinoma: a gynecologic oncology group study.* J Clin Oncol, 2001. **19**(12): p. 2975-82.
220. Seelig, A. and E. Landwojtowicz, *Structure-activity relationship of P-glycoprotein substrates and modifiers.* European Journal of Pharmaceutical Sciences, 2000. **12**(1): p. 31-40.
221. Watanabe, T., et al., *Comparative study on reversal efficacy of SDZ PSC 833, cyclosporin A and verapamil on multidrug resistance in vitro and in vivo.* Acta Oncol, 1995. **34**(2): p. 235-41.
222. List, A.F., et al., *Benefit of cyclosporine modulation of drug resistance in patients with poor-risk acute myeloid leukemia: a Southwest Oncology Group study.* Blood, 2001. **98**(12): p. 3212-20.
223. Warner, E., et al., *Phase II study of dexverapamil plus anthracycline in patients with metastatic breast cancer who have progressed on the same anthracycline regimen.* Clinical Cancer Research, 1998. **4**(6): p. 1451-7.
224. Boesch, D., et al., *In vivo circumvention of P-glycoprotein-mediated multidrug resistance of tumor cells with SDZ PSC 833.* Cancer Res, 1991. **51**(16): p. 4226-33.
225. Boesch, D., et al., *Restoration of daunomycin retention in multidrug-resistant P388 cells by submicromolar concentrations of SDZ PSC 833, a*

nonimmunosuppressive cyclosporin derivative. Exp Cell Res, 1991. **196**(1): p. 26-32.
226. Ling, V., *Multidrug resistance: molecular mechanisms and clinical relevance.* Cancer Chemother Pharmacol, 1997. **40 Suppl**: p. S3-8.
227. Lum, B.L., et al., *Clinical trials of modulation of multidrug resistance. Pharmacokinetic and pharmacodynamic considerations.* Cancer, 1993. **72**(11 Suppl): p. 3502-14.
228. Kapturczak, M.H., H.U. Meier-Kriesche, and B. Kaplan, *Pharmacology of calcineurin antagonists.* Transplant Proc, 2004. **36**(2 Suppl): p. 25S-32S.
229. Kahan, B.D., *Cyclosporine.* N Engl J Med, 1989. **321**(25): p. 1725-38.
230. Kavukcu, S., et al., *Effect of seasonal changes on the cyclosporine A blood levels in renal transplant recipients during childhood.* Nephron, 1999. **81**(3): p. 366-7.
231. Fahr, A., *Cyclosporin clinical pharmacokinetics.* Clinical Pharmacokinetics, 1993. **24**(6): p. 472-95.
232. Mueller, E.A., et al., *Improved dose linearity of cyclosporine pharmacokinetics from a microemulsion formulation.* Pharm Res, 1994. **11**(2): p. 301-4.
233. Kovarik, J.M., et al., *Reduced inter- and intraindividual variability in cyclosporine pharmacokinetics from a microemulsion formulation.* J Pharm Sci, 1994. **83**(3): p. 444-6.
234. Lensmeyer, G.L., et al., *Concentrations of cyclosporin A and its metabolites in human tissues postmortem.* J Anal Toxicol, 1991. **15**(3): p. 110-5.
235. Shimada, T., et al., *Interindividual variations in human liver cytochrome P-450 enzymes involved in the oxidation of drugs, carcinogens and toxic chemicals: studies with liver microsomes of 30 Japanese and 30 Caucasians.* J Pharmacol Exp Ther, 1994. **270**(1): p. 414-23.
236. Christians, U., et al., *Cyclosporine metabolite pattern in blood from patients with acute GVHD after BMT.* Bone Marrow Transplant, 1993. **12**(1): p. 27-33.
237. Radeke, H.H., et al., *The synergistic immunosuppressive potential of cyclosporin metabolite combinations.* Int J Immunopharmacol, 1992. **14**(4): p. 595-604.
238. Maurer, G. and M. Lemaire, *Biotransformation and distribution in blood of cyclosporine and its metabolites.* Transplant Proc, 1986. **18**(6 Suppl 5): p. 25-34.
239. Urien, S., et al., *Assessment of cyclosporine A interactions with human plasma lipoproteins in vitro and in vivo in the rat.* Journal of Pharmacology & Experimental Therapeutics, 1990. **253**(1): p. 305-9.
240. Akhlaghi, F. and A.K. Trull, *Distribution of cyclosporin in organ transplant recipients.* Clinical Pharmacokinetics, 2002. **41**(9): p. 615-37.
241. Legg, B. and M. Rowland, *Cyclosporin: measurement of fraction unbound in plasma.* J Pharm Pharmacol, 1987. **39**(8): p. 599-603.
242. Bram, R.J., et al., *Identification of the immunophilins capable of mediating inhibition of signal transduction by cyclosporin A and FK506: roles of calcineurin binding and cellular location.* Mol Cell Biol, 1993. **13**(8): p. 4760-9.
243. Cardenas, M.E., et al., *Immunophilins interact with calcineurin in the absence of exogenous immunosuppressive ligands.* EMBO Journal, 1994. **13**(24): p. 5944-57.
244. Rao, A., C. Luo, and P.G. Hogan, *Transcription factors of the NFAT family: regulation and function.* Annu Rev Immunol, 1997. **15**: p. 707-47.

245. Khanna, A.K. and J.D. Hosenpud, *Cyclosporine induces the expression of the cyclin inhibitor p21.* Transplantation, 1999. **67**(9): p. 1262-8.
246. Karin, M., *The regulation of AP-1 activity by mitogen-activated protein kinases.* J Biol Chem, 1995. **270**(28): p. 16483-6.
247. Janeway Jr., C.A., et al., *Immunobiology: The immune system in health and disease*. 6th ed. 2005, New York: Garland Science Publishing.
248. Twentyman, P.R., N.E. Fox, and D.J. White, *Cyclosporin A and its analogues as modifiers of adriamycin and vincristine resistance in a multi-drug resistant human lung cancer cell line.* Br J Cancer, 1987. **56**(1): p. 55-7.
249. Goldberg, H., et al., *Reduced cyclosporin accumulation in multidrug-resistant cells.* Biochem Biophys Res Commun, 1988. **152**(2): p. 552-8.
250. Delle Monache, M.D., et al., *Effect of pharmacological modulation of liver P-glycoproteins on cyclosporin A biliary excretion and cholestasis: a study in isolated perfused rat liver.* Dig Dis Sci, 1999. **44**(11): p. 2196-204.
251. Stein, W.D., *Kinetics of the multidrug transporter (P-glycoprotein) and its reversal.* Physiol Rev, 1997. **77**(2): p. 545-90.
252. Litman, T., et al., *From MDR to MXR: new understanding of multidrug resistance systems, their properties and clinical significance.* Cell Mol Life Sci, 2001. **58**(7): p. 931-59.
253. Aouali, N., et al., *Immunosuppressors and reversion of multidrug-resistance.* Crit Rev Oncol Hematol, 2005. **56**(1): p. 61-70.
254. Calne, R.Y., et al., *Cyclosporin A in patients receiving renal allografts from cadaver donors.* Lancet, 1978. **2**(8104-5): p. 1323-7.
255. Mihatsch, M.J., et al., *Morphological patterns in cyclosporine-treated renal transplant recipients.* Transplantation Proceedings, 1985. **17**(4 Suppl 1): p. 101-16.
256. Sweny, P., et al., *Nephrotoxicity of cyclosporine A.* Lancet, 1981. **1**: p. 663.
257. Chapman, J.R., et al., *Reversibility of cyclosporine nephrotoxicity after three months treatment.* Lancet, 1985. **1**: p. 128-130.
258. Stores, E., et al., *Cyclosporine increases nitric oxide activity in vivo.* Hypertension, 1997. **29**(2): p. 570 - 575.
259. Tariq, M., et al., *N-acetylcysteine attenuates cyclosporin-induced nephrotoxicity in rats.* Nephrology Dialysis Transplantation, 1999. **14**(4): p. 923-9.
260. Mun, K.C., *Effect of epigallocatechin gallate on renal function in cyclosporine-induced nephrotoxicity.* Transplant Proc, 2004. **36**(7): p. 2133 - 2134.
261. Satyanarayana, P.S., D. Singh, and K. Chopra, *Quercetin, a bioflavonoid, protects against oxidative stress-related renal dysfunction by cyclosporine in rats.* Methods Find Exp Clin Pharmacol, 2001. **23**(4): p. 175-81.
262. Satyanarayana, P.S. and K. Chopra, *Oxidative stress-mediated renal dysfunction by cyclosporine A in rats: attenuation by trimetazidine.* Ren Fail, 2002. **24**(3): p. 259-74.
263. Satyanarayana, P.S. and K. Chopra, *Selective Angiotensin II type 1 receptor blockade ameliorates cyclosporine nephrotoxicity.* Pharmacological Research, 2002. **45**(5): p. 413 - 420.

264. Colombo, T., M. Zucchetti, and M. D'Incalci, *Cyclosporin A markedly changes the distribution of doxorubicin in mice and rats.* J Pharmacol Exp Ther, 1994. **269**(1): p. 22-7.
265. Kim, W.J., et al., *Multidrug resistance-associated protein-mediated multidrug resistance modulated by cyclosporin A in a human bladder cancer cell line.* Jpn J Cancer Res, 1995. **86**(10): p. 969-77.
266. Fahr, A., M. Holz, and G. Fricker, *Liposomal formulations of cyclosporin A: influence of lipid type and dose on pharmacokinetics.* Pharmaceutical Research, 1995. **12**(8): p. 1189-98.
267. Choice, E., *Liposomal cyclosporine. Comparison of drug and lipid carrier pharmacokinetics and biodistribution.* Transplantation, 1995. **60**(9): p. 1006-11.
268. Kim, S.Y., et al., *Indomethacin-loaded methoxy poly(ethylene glycol)/ poly(epsilon-caprolactone) diblock copolymeric nanosphere: pharmacokinetic characteristics of indomethacin in the normal Sprague-Dawley rats.* Biomaterials, 2001. **22**(14): p. 2049-56.
269. Arote, R., et al., *A biodegradable poly(ester amine) based on polycaprolactone and polyethylenimine as a gene carrier.* Biomaterials, 2007. **28**(4): p. 735-44.
270. Vaquette, C., et al., *In vitro biocompatibility of different polyester membranes.* Biomed Mater Eng, 2006. **16**(4 Suppl): p. S131-6.
271. Varela, M.C., et al., *Cyclosporine-loaded polycaprolactone nanoparticles: immunosuppression and nephrotoxicity in rats.* Eur J Pharm Sci, 2001. **12**(4): p. 471-8.
272. Yuan, M., et al., *polymerization of lactides and lactones.10. Synthesis, characteization, and application of amino terminated poly(ethylene glycol)-co-poly(e-caprolactone) block copolymer.* Macromolecules, 2000. **33**: p. 1613-1617.
273. Shin, I.G., et al., *Methoxy poly(ethylene glycol)/epsilon-caprolactone amphiphilic block copolymeric micelle containing indomethacin. I. Preparation and characterization.* J Control Release, 1998. **51**(1): p. 1-11.
274. Aliabadi, H.M., et al., *Micelles of methoxy poly(ethylene oxide)-b-poly(-caprolactone) as vehicles for the solublization and controlled delivery of cyclosporine A.* Journal of Controlled Release, 2005. **104**(2): p. 301-311.
275. Aliabadi, H.M., et al., *Encapsulation of hydrophobic drugs in polymeric micelles through co-solvent evaporation: The effect of solvent composition on micellar properties and drug loading.* International Journal of Pharmaceutics, 2007. **329**: p. 158 - 165.
276. Chimalakonda, A.P., R.B. Shah, and R. Mehvar, *High-performance liquid chromatographic analysis of cyclosporin A in rat blood and liver using a commercially available internal standard.* J Chromatogr B Analyt Technol Biomed Life Sci, 2002. **772**(1): p. 107-14.
277. Brocks, D.R., S. Ala, and H.M. Aliabadi, *The effect of increased lipoprotein levels on the pharmacokinetics of cyclosporine A in the laboratory rat.* Biopharmaceutics & Drug Disposition, 2006. **27**(1): p. 7-16.
278. Schuhmacher, J., K. Buhner, and A. Witt-Laido, *Determination of the free fraction and relative free fraction of drugs strongly bound to plasma proteins.* Journal of Pharmaceutical Sciences, 2000. **89**(8): p. 1008-21.

279. Brocks, D.R., *Drug disposition in three dimensions: an update on stereoselectivity in pharmacokinetics.* Biopharm Drug Dispos, 2006. **27**(8): p. 387-406.
280. Brocks, D.R. and R. Mehvar, *Stereoselectivity in the pharmacodynamics and pharmacokinetics of the chiral antimalarial drugs.* Clin Pharmacokinet, 2003. **42**(15): p. 1359-82.
281. Ma, Z., et al., *High-performance liquid chromatography analysis of curcumin in rat plasma: application to pharmacokinetics of polymeric micellar formulation of curcumin.* Biomed Chromatogr, 2007. **21**(5): p. 546-52.
282. Tanaka, C., R. Kawai, and M. Rowland, *Dose-dependent pharmacokinetics of cyclosporin A in rats: events in tissues.* Drug Metabolism & Disposition, 2000. **28**(5): p. 582-9.
283. Krishan, A. and L. Mayer, *In Vitro Evaluation of Doxorubicin cytotoxicity and cellular uptake in the presence and absence of multidrug resistance modulators.* Pharmacy and Pharmacology communications, 1999. **5**: p. 511-517.
284. Lopes de Menezes, D.E., Y. Hu, and L.D. Mayer, *Combined treatment of Bcl-2 antisense oligodeoxynucleotides (G3139), p-glycoprotein inhibitor (PSC833), and sterically stabilized liposomal doxorubicin suppresses growth of drug-resistant growth of drug-resistant breast cancer in severely combined immunodeficient mice.* Journal of Experimental Therapeutics & Oncology, 2003. **3**(2): p. 72-82.
285. Krishna, R., G. de Jong, and L.D. Mayer, *Pulsed exposure of SDZ PSC 833 to multidrug resistant P388/ADR and MCF7/ADR cells in the absence of anticancer drugs can fully restore sensitivity to doxorubicin.* Anticancer Res, 1997. **17**(5A): p. 3329-34.
286. Bailer, A.J., *Testing for the Equality of Area Under the Curves When Using Destructive Measurement Techniques.* Journal of Pharmacokinetics and Biopharmaceutics, 1988. **16**(3): p. 303-309.
287. Mehvar, R., M.A. Robinson, and J.M. Reynolds, *Molecular Weight Dependent Tissue Accumulation of Dextrans: In vivo Studies in Rats.* Journal of Pharmaceutical Sciences, 1994. **83**(10): p. 1495-1499.
288. Yuan, J., *Estimation of Variance for AUC in Animal Studies.* Journal of Pharmaceutical Sciences, 1993. **82**(7): p. 761-763.
289. Miller, R.G., *Simultaneous Statistical Inference*. McGraw-Hill Series in Probability and Statistic. 1966, USA: McGraw-Hill. 272.
290. Mahmud, A. and A. Lavasanifar, *The effect of block copolymer structure on the internalization of polymeric micelles by human breast cancer cells.* Colloids Surf B Biointerfaces, 2005. **45**(2): p. 82-9.
291. Faulds, D., K.L. Goa, and P. Benfield, *Cyclosporin. A review of its pharmacodynamic and pharmacokinetic properties, and therapeutic use in immunoregulatory disorders.[erratum appears in Drugs 1993 Sep;46(3):377].* Drugs, 1993. **45**(6): p. 953-1040.
292. List, A.F., et al., *Phase I/II trial of cyclosporine as a chemotherapy-resistance modifier in acute leukemia.[see comment].* Journal of Clinical Oncology, 1993. **11**(9): p. 1652-60.
293. Smeesters, C., et al., *Efficacy of incorporating cyclosporine into liposomes to reduce its nephrotoxicity.* Canadian Journal of Surgery, 1988. **31**(1): p. 34-36.

294. Smeesters, C., et al., *Reduced nephrotoxicity of cyclosporine A after incorporation into liposomes.* Transplantation Proceedings, 1988. **20**(3 SUPPL. 3): p. 831-832.
295. Fahr, A. and J. Seelig, *Liposomal formulations of Cyclosporin A: a biophysical approach to pharmacokinetics and pharmacodynamics.* Critical Reviews in Therapeutic Drug Carrier Systems, 2001. **18**(2): p. 141-72.
296. Ouyang, C., et al., *Liposomal cyclosporine. Characterization of drug incorporation and interbilayer exchange.* Transplantation, 1995. **60**(9): p. 999-1006.
297. Liggins, R.T. and H.M. Burt, *Polyether-polyester diblock copolymers for the preparation of paclitaxel loaded polymeric micelle formulations.* Adv Drug Deliv Rev, 2002. **54**(2): p. 191-202.
298. Kim, S.Y., et al., *Methoxy poly(ethylene glycol) and epsilon-caprolactone amphiphilic block copolymeric micelle containing indomethacin. II. Micelle formation and drug release behaviours.* Journal of Controlled Release, 1998. **51**(1): p. 13-22.
299. Zhang, L. and A. Eisenberg, *Thermodynamic vs. kinetic aspects in the formation and morphological transitions of crew-cut aggregates produced by self-assembly of polystyrene-b-poly(acrylic acid) block copolymers in dilute solution.* Macromolecules, 1999. **32**: p. 2239 - 2249.
300. Vangeyte, P., S. Gautier, and R. Jerome, *About the methods of preparation of poly(ethylene oxide)-b-poly(□-caprolactone) nanoparticles inwater analysis by dynamic light scattering.* Colloids Surf. A: Physiochem. Eng. Aspects, 2004. **242**: p. 203 - 211.
301. Johnson, B.K. and R.K. Prud'homme, *Mechanism for rapid self-assembly of block copolymer nanoparticles.* Phys Rev Lett, 2003. **91**(11): p. 118302.
302. Johnson, B.K. and R.K. Prud'homme, *Flash nanoprecipitation of organic actives and block copolymers using a confined impinging jets mixer.* Aust. J. Chem., 2003. **56**: p. 1021 - 1024.
303. Forrest, M.L., et al., *In vitro release of the mTOR inhibitor rapamycin from poly(ethylene glycol)-b-poly(epsilon-caprolactone) micelles.* J Control Release, 2006. **110**(2): p. 370-7.
304. Shayeganpour, A., A.S. Jun, and D.R. Brocks, *Pharmacokinetics of Amiodarone in hyperlipidemic and simulated high fat-meal rat models.* Biopharm Drug Dispos, 2005. **26**(6): p. 249-57.
305. Brocks, D.R., *Stereoselective halofantrine and desbutylhalofantrine disposition in the rat: cardiac and plasma concentrations and plasma protein binding.* Biopharm Drug Dispos, 2002. **23**(1): p. 9-15.
306. Brocks, D.R. and K.M. Wasan, *The influence of lipids on stereoselective pharmacokinetics of halofantrine: Important implications in food-effect studies involving drugs that bind to lipoproteins.* J Pharm Sci, 2002. **91**(8): p. 1817-26.
307. Lee, M.K., et al., *Pharmacokinetics and organ distribution of cyclosporin A incorporated in liposomes and mixed micelles.* International Journal of Pharmaceutics, 1999. **191**(2): p. 87-93.

308. Aliabadi, H.M., et al., *Insights into the effects of hyperlipoproteinemia on cyclosporine A biodistribution and relationship to renal function.* Aaps J, 2006. **8**(4): p. E672-81.
309. Ishikawa, A., K. Suzuki, and K. Fujita, *Mechanisms of cyclosporine-induced nephrotoxicity.* Transplant Proc, 1999. **31**(1-2): p. 1127-8.
310. First, M.R., *Renal function.* Clinical Chemistry: Theory, Anlaysis, Correlation, ed. K. L.A. and P. A.J. 2003, St. Louis, Missouri: Mosby Inc. p. 483.
311. Shihab, F.S., et al., *Mycophenolate mofetil ameliorates arteriolopathy and decreases transforming growth factor-beta1 in chronic cyclosporine nephrotoxicity.* Am J Transplant, 2003. **3**(12): p. 1550-9.
312. Aliabadi, H.M., D.R. Brocks, and A. Lavasanifar, *Polymeric micelles for the solublization and delivery of cyclosporine A: Pharmacokinetics and biodistribution.* Biomaterials, 2005. **26**(35): p. 7251-7259.
313. Anjaneyulu, M., N. Tirkey, and K. Chopra, *Attenuation of cyclosporine-induced renal dysfunction by catechin: possible antioxidant mechanism.* Renal Failure, 2003. **25**(5): p. 691-707.
314. Yang, C.W., et al., *Synergistic effects of mycophenolate mofetil and losartan in a model of chronic cyclosporine nephropathy.* Transplantation, 2003. **75**(3): p. 309-15.
315. Hosogai, N., et al., *Phosphodiesterase type 5 inhibition ameliorates nephrotoxicity induced by cyclosporin A in spontaneous hypertensive rats.* European Journal of Pharmacology, 2003. **477**(2): p. 171-8.
316. Vadiei, K., et al., *Tissue distribution and in vivo immunosuppressive activity of liposomal cyclosporine.* Drug Metabolism & Disposition, 1991. **19**(6): p. 1147-1151.
317. Freise, C.E., et al., *The increased efficacy and decreased nephrotoxicity of a cyclosporine liposome.* Transplantation, 1994. **57**(6): p. 928-932.
318. Zastre, J., et al., *Enhanced cellular accumulation of a P-glycoprotein substrate, rhodamine-123, by caco-2 cells using low molecular weight methoxypolyethylene glycol-block-polycaprolactone diblock copolymers.* Eur J Pharm Biopharm, 2002. **54**(3): p. 299-309.
319. Csoka, K., et al., *Differential activity of Cremophor EL and paclitaxel in patients' tumor cells and human carcinoma cell lines in vitro.* Cancer, 1997. **79**(6): p. 1225-33.
320. Nygren, P., et al., *The cytotoxic activity of Taxol in primary cultures of tumour cells from patients is partly mediated by Cremophor EL.* Br J Cancer, 1995. **71**(3): p. 478-81.
321. Burton, A.F., *Oncolytic effects of fatty acids in mice and rats.* Am J Clin Nutr, 1991. **53**(4 Suppl): p. 1082S-1086S.
322. Schuurhuis, G.J., et al., *The polyoxyethylene castor oil Cremophor EL modifies multidrug resistance.* Br J Cancer, 1990. **62**(4): p. 591-4.
323. Woodcock, D.M., et al., *Reversal of multidrug resistance by surfactants.* 1992.
324. Cowie, F.J., et al., *Multidrug resistance modulation in rhabdomyosarcoma and neuroblastoma cell lines.* Int J Oncol, 1998. **12**(5): p. 1143-9.

033
3/3

325. Van Rensburg, C.E., et al., *The riminophenazine agents clofazimine and B669 reverse acquired multidrug resistance in a human lung cancer cell line.* Cancer Lett, 1994. **85**(1): p. 59-63.